The Dual Olfactory Pathway in the Honeybee Brain:

Sensory Supply and Electrophysiological Properties

Der duale olfaktorische Weg im Gehirn der Honigbiene:

Sensorischer Eingang und elektrophysiologische Eigenschaften

Doctoral thesis for a doctoral degree
at the Graduate School of Life Sciences,
Julius-Maximilians-Universität Würzburg,
Section Integrative Biology

submitted by

Jan Kropf

from

Münchberg

Würzburg 2014

Submitted on: ……..……..

Office stamp

Members of the *Promotionskomitee*:

Chairperson: Prof. Dr. Alexander Buchberger

Primary Supervisor: Prof. Dr. Wolfgang Rössler

Supervisor (Second): Dr. Robert Kittel (Pl)

Supervisor (Third): Prof. Dr. Sylvia Anton

Date of Public Defence: 18.12.2014

Date of Receipt of Certificates:

Affidavit

I hereby confirm that my thesis entitled "The Dual Olfactory Pathway in the Honeybee Brain: Sensory Supply and Electrophysiological Properties" is the result of my own work. I did not receive any help or support from commercial consultants. All sources and / or materials applied are listed and specified in the thesis.

Furthermore, I confirm that this thesis has not yet been submitted as part of another examination process neither in identical nor in similar form.

Würzburg, 20.10.2014 Signature

Eidesstattliche Erklärung

Hiermit erkläre ich an Eides statt, die Dissertation "Der duale olfaktorische Weg im Gehirn der Honigbiene: Sensorischer Eingang und elektrophysiologische Eigenschaften" eigenständig, d.h. insbesondere selbständig und ohne Hilfe eines kommerziellen Promotionsberaters, angefertigt und keine anderen als die von mir angegebenen Quellen und Hilfsmittel verwendet zu haben.

Ich erkläre außerdem, dass die Dissertation weder in gleicher noch in ähnlicher Form bereits in einem anderen Prüfungsverfahren vorgelegen hat.

Würzburg, 20.10.2014 Unterschrift

"Dissertation Based on Several Published Manuscripts"

Statement of individual author contributions and of legal second publication rights

(if required use more than one sheet)

Publication (complete reference):					
Olfactory subsystems in the honeybee: sensory supply and sex specificity Kropf, Jan; Kelber, Christina; Bieringer, Kathrin; Rössler, Wolfgang Cell and Tissue Research Volume 3 Pages 583-595 2014					
Participated in	**Author Initials,** Responsibility decreasing from left to right				
Study Design	WR	CK	JK		
Data Collection	KB	JK			
Data Analysis and Interpretation	JK	CK	WR	KB	
Manuscript Writing	JK	WR	CK		

Explanations (if applicable):

open choice manuscript

Publication (complete reference):					
Olfactory coding along a dual pathway in the honey bee: potential contribution of intrinsic neuronal properties of projection neurons and Kenyon cells Kropf, Jan; Rössler, Wolfgang Manuscript					
Participated in	**Author Initials,** Responsibility decreasing from left to right				
Study Design	JK	WR			
Data Collection	JK				
Data Analysis and Interpretation	JK	WR			
Manuscript Writing	JK	WR			

Explanations (if applicable):

Manuscript is close to publication

I confirm that I have obtained permission from both the publishers and the co-authors for legal second publication.

I also confirm my primary supervisor's acceptance.

Jan Kropf 20.10.2014 Würzburg

_____

Doctoral Researcher's Name Date Place Signature

Table of contents

Summary

The olfactory sense is of utmost importance for honeybees, *Apis mellifera*. Honeybees use olfaction for communication within the hive, for the identification of nest mates and non-nest mates, the localization of food sources, and in case of drones (males), for the detection of the queen and mating. Honeybees, therefore, can serve as excellent model systems for an integrative analysis of an elaborated olfactory system.

To efficiently filter odorants out of the air with their antennae, honeybees possess a multitude of sensilla that contain the olfactory sensory neurons (OSN). Three types of olfactory sensilla are known from honeybee worker antennae: *Sensilla trichoidea*, *Sensilla basiconica* and *Sensilla placodea*. In the sensilla, odorant receptors that are located in the dendritic arborizations of the OSNs transduce the odorant information into electrical information. Approximately 60.000 OSN axons project in two parallel bundles along the antenna into the brain. Before they enter the primary olfactory brain center, the antennal lobe (AL), they diverge into four distinct tracts (T1-T4). OSNs relay onto ~3.000-4.000 local interneurons (LN) and ~900 projection neurons (PN), the output neurons of the AL. The axons of the OSNs together with neurites from LNs and PNs form spheroidal neuropil units, the so-called glomeruli. OSN axons from the four AL input tracts (T1-T4) project into four glomerular clusters. LNs interconnect the AL glomeruli, whereas PNs relay the information to the next brain centers, the mushroom body (MB) - associated with sensory integration, learning and memory - and the lateral horn (LH). In honeybees, PNs project to the MBs and the LH via two separate tracts, the medial and the lateral antennal-lobe tract (m/lALT) which run in parallel in opposing directions. The mALT runs first to the MB and then to the LH, the lALT runs first to the LH and then to the MB. This dual olfactory pathway represents a feature unique to Hymenoptera. Interestingly, both tracts were shown to process information about similar sets of odorants by extracting different features. Individual mALT PNs are more odor specific than lALT PNs. On the other hand, lALT PNs have higher spontaneous and higher odor response action potential (AP) frequencies than mALT PNs. In the MBs, PNs form synapses with ~184.000 Kenyon cells (KC), which are the MB intrinsic neurons. KCs, in contrast to PNs, show almost no spontaneous activity and employ a spatially and temporally sparse code for odor coding.

In manuscript I of my thesis, I investigated whether the differences in specificity of odor responses between m- and lALT are due to differences in the synaptic input. Therefore, I investigated the axonal projection patterns of OSNs housed in *S. basiconica* in honeybee workers and compared them with *S. trichoidea* and *S. placodea* using selective anterograde

labeling with fluorescent tracers and confocal- microscopy analyses of axonal projections in AL glomeruli. Axons of *S. basiconica*-associated OSNs preferentially projected into the T3 input-tract cluster in the AL, whereas the two other types of sensilla did not show a preference for a specific glomerular cluster. T3- associated glomeruli had previously been shown to be innervated by mALT PNs. Interestingly, *S. basiconica* as well as a number of T3 glomeruli lack in drones. Therefore I set out to determine whether this was associated with the reduction of glomeruli innervated by mALT PNs. Retrograde tracing of mALT PNs in drones and counting of innervated glomeruli showed that the number of mALT-associated glomeruli was strongly reduced in drones compared to workers. The preferential projections of *S. basiconica*-associated OSNs into T3 glomeruli in female workers together with the reduction of mALT-associated glomeruli in drones support the presence of a female-specific olfactory subsystem that is partly innervated by OSNs from *S. basiconica* and is associated with mALT projection neurons. As mALT PNs were shown to be more odor specific, I suppose that already the OSNs in this subsystem are more odor specific than lALT associated OSNs. I conclude that this female-specific subsystem allows the worker honeybees to respond adequately to the enormous variety of odorants they experience during their lifetime.

In manuscript II, I investigated the ion channel composition of mALT and lALT PNs and KCs *in situ*. This approach represents the first study dealing with the honeybee PN and KC ion channel composition under standard conditions in an intact brain preparation. With these recordings I set out to investigate the potential impact of intrinsic neuronal properties on the differences between m- and lALT PNs and on the sparse odor coding properties of KCs. In PNs, I identified a set of Na^+ currents and diverse K^+ currents depending on voltage and Na^+ or Ca^{2+} that support relatively high spontaneous and odor response AP frequencies. This set of currents did not significantly differ between mALT and lALT PNs, but targets for potential modulation of currents leading to differences in AP frequencies were found between both types of PNs. In contrast to PNs, KCs have very prominent K^+ currents, which are likely to contribute to the sparse response fashion observed in KCs. Furthermore, Ca^{2+} dependent K^+ currents were found, which may be of importance for coincidence detection, learning and memory formation. Finally, I conclude that the differences in odor specificity between m- and lALT PNs are due to their synaptic input from different sets of OSNs and potential processing by LNs. The differences in spontaneous activity between the two tracts may be caused by different neuronal modulation or, in addition, also by interaction with LNs. The temporally sparse representation of odors in KCs is very likely based on the intrinsic KC properties, whereas general excitability and spatial sparseness are likely to be regulated through GABAergic feedback neurons.

Zusammenfassung

Der Geruchssinn ist für die Honigbiene, *Apis mellifera*, von größter Bedeutung. Honigbienen kommunizieren olfaktorisch, sie können Nestgenossinnen und koloniefremde Honigbienen aufgrund des Geruchs unterscheiden, sie suchen und erkennen Nahrungsquellen olfaktorisch, und Drohnen (männliche Honigbienen) finden die Königin mit Hilfe des Geruchssinns. Deshalb dient die Honigbiene als exzellentes Modell für die Untersuchung hochentwickelter olfaktorischer Systeme.

Honigbienen filtern Duftmoleküle mit ihren Antennen aus der Luft. Auf diesen Antennen sitzen Sensillen, die die olfaktorischen sensorischen Neurone (OSN) beinhalten. Drei verschiedene olfaktorische Sensillen existieren bei Arbeiterinnen: *Sensilla trichoidea*, *Sensilla basiconica* und *Sensilla placodea*. In diesen Sensillen sind olfaktorische Rezeptorproteine auf den Dendriten der OSN lokalisiert. Diese Duftrezeptoren wandeln die Duftinformationen in elektrische Informationen um. Die Axone von ca. 60.000 OSN ziehen in zwei Bündeln entlang der Antenne in das Gehirn. Bevor sie das erste olfaktorische Gehirnzentrum, den Antennallobus (AL), erreichen, spalten sie sich in vier distinkte Trakte (T1-T4) auf. Im AL verschalten sie auf 3.000-4.000 lokale Interneurone (LN) und auf etwa 900 Ausgangsneurone des AL, die Projektionsneurone (PN). Die axonalen Endigungen der OSN bilden mit Neuriten der PN und LN kugelförmige Strukturen, die so genannten Glomeruli. Die OSN aus den vier Trakten T1-T4 ziehen in vier zugehörige glomeruläre Cluster. LN verschalten die Information unter den AL Glomeruli, PN leiten olfaktorische Informationen zu den nächsten Gehirnstrukturen, den Pilzkörpern und dem lateralen Horn, weiter. Die Pilzkörper werden als Zentrum für sensorische Integration, Lernen und Gedächtnis gesehen. Die PN, die den AL mit dem Pilzkörper und dem lateralen Horn verbinden, verlaufen in Honigbienen parallel über zwei Bahnen, den medialen und den lateralen Antennallobustrakt (mALT/lALT), aber in entgegengesetzter Richtung. Dieser duale olfaktorische Signalweg wurde in dieser Ausprägung bisher nur in Hymenopteren gefunden. Interessanterweise prozessieren beide Trakte Informationen über die gleichen Düfte. Dabei sind mALT PN duftspezifischer und lALT PN haben höhere spontane Aktionspotentialfrequenzen sowie höhere Aktionspotentialfrequenzen in Antwort auf einen Duftreiz. Im Pilzkörper verschalten PN auf Kenyon Zellen (KC), die intrinsischen Neurone des Pilzkörpers. KC sind im Gegensatz zu PN fast nicht spontan aktiv und kodieren Informationen auf räumlicher und zeitlicher Ebene mit geringer Aktivität. Man spricht von einem so genannten "sparse code".

Im ersten Manuskript meiner Doktorarbeit habe ich untersucht, ob die Unterschiede in der Spezifität der Duftantworten zwischen mALT und lALT PN zumindest zum Teil auf Unterschieden im sensorischen Eingang beruhen. Ich habe die axonalen Projektionen der OSN der *S. basiconica* in Honigbienen untersucht und mit den Projektionen von OSN in *S. trichoidea* und *S. placodea* verglichen. Dazu wurden die OSN in den *S. basiconica* anterograd mit Fluoreszenzmarkern gefärbt und mit mittels konfokaler Mikroskopie untersucht und quantifiziert. Die Axone von OSN aus *S. basiconica* ziehen präferentiell in das T3 Glomerulus Cluster, die Axone der anderen beiden Sensillentypen zeigen keine Präferenz für ein spezielles Cluster. Es wurde bereits gezeigt, dass die Glomeruli des T3 Clusters von mALT PN innerviert werden. Interessanterweise fehlen *S. basiconica* und Teile der T3 Glomeruli in Drohnen. Deshalb habe ich untersucht, ob die T3 Reduzierung in Drohnen mit einer Reduzierung der mALT Glomeruli einhergeht. Retrograde Färbungen der mALT PN in Drohnen zeigten, daß die Zahl der mALT Glomeruli in Drohnen gegenüber Arbeiterinnen deutlich reduziert ist. Die Präferenz der OSN der *S. basiconica* für das T3 Cluster und die reduzierte Anzahl von mALT Glomeruli in Drohnen weisen auf ein arbeiterinnenspezifisches olfaktorisches Subsystem hin, welches aus *S. basiconica*, T3 Glomeruli und einer Gruppe von mALT PN besteht. Da die mALT PN duftspezifischer als lALT PN sind, vermute ich, dass auch die OSN, die auf mALT PN verschalten, duftspezifischer antworten als OSN die auf lALT PN verschalten. Daraus schließe ich, daß dieses Subsystem den Arbeiterinnen ermöglicht, passend auf die enorme Breite an Duftstoffen zu reagieren, die diese im Laufe ihres arbeitsteiligen Lebens wahrnehmen müssen.

Im zweiten Manuskript meiner Doktorarbeit habe ich die Ionenkanalzusammensetzung der mALT PN, der lALT PN und der KC *in situ* untersucht. Mein Ansatz stellt die erste Studie dar, die die Ionenkanäle von Neuronen in der Honigbiene unter Standardbedingungen an einer intakten Gehirnpräparation untersucht. Mit diesen Messungen versuche ich die potentiellen bioelektrischen Grundlagen für Unterschiede in der Informationskodierung in mALT PN, lALT PN und Kenyon Zellen zu ergründen. In PN konnte ich eine Gruppe von Na^+ Ionenkanälen und Na^+ abhängigen, Ca^{2+} abhängigen sowie spannungsabhängigen K^+ Ionenkanälen identifizieren, die die Grundlagen für hohe, spontane Aktionspotentialfrequenzen und hohe Duftantwortfrequenzen schaffen. Diese Ströme unterschieden sich nicht grundsätzlich zwischen m- und lALT PN. Jedoch wurden potentielle Ziele für neuronale Modulation gefunden, welche zu unterschiedlichen Aktionspotentialfrequenzen zwischen PN der beiden Trakte führen könnten. Im Gegensatz zu den PN wurden in Kenyon Zellen in der Relation sehr starke K^+ Ionenströme gemessen. Diese dienen sehr wahrscheinlich der schnellen Terminierung

von Duftantworten, also dem Erzeugen des zeitlichen "sparse code". Außerdem wurden Ca^{2+} abhängige K^+ Kanäle gefunden, die für Koinzidenzdetektion, Lernen und Gedächtnis von Bedeutung sein können.

In der Gesamtsicht folgere ich aus meinen Ergebnissen, dass die Unterschiede in der Duftspezifizität zwischen m- und lALT PN überwiegend auf deren sensorischen Eingängen von unterschiedlichen Populationen von OSN und der Verarbeitung über lokale Interneuronen im AL beruht. Die Unterschiede in der Spontanaktivität zwischen mALT und lALT basieren sehr wahrscheinlich auf neuronaler Modulation und/oder Interaktion mit LN. Die zeitliche Komponente des "sparse code" in KC entsteht höchstwahrscheinlich durch die intrinsischen elektrischen Eigenschaften der KC, wohingegen die generelle Erregbarkeit und der räumliche "sparse code" mit großer Wahrscheinlichkeit auf der Regulation durch GABAerge Neurone beruht.

General introduction

The olfactory world

"Odors have a power of persuasion stronger than that of words, appearances, emotions, or will. The persuasive power of an odor cannot be fended off, it enters into us like breath into our lungs, it fills us up, imbues us totally. There is no remedy for it."

Patrick Süskind, *Perfume: The Story of a Murderer*

These words about odors, taken from a speech from a fictional fanatic murderer, give an impression of how much impact an odor can have on the emotions of a human being. The emotions happiness, disgust, and anxiety were shown to be easily described by olfactory elicitors, whereas sadness and anger are more often described by visual cues (Croy et al. 2011). When presented to another subject, the olfactory cues a human body produces after experiencing a certain emotion can elicit facial expressions and even behavior appropriate to the emotion of the person who experienced the emotion first (de Groot et al. 2012). To be able to respond appropriately to such olfactory stimuli, the olfactory system has to be able to identify the stimuli, to process certain stimuli innately according to their valence or to learn the valence of the odor. Just recently, the number of different olfactory stimuli a human being can discriminate was estimated to be above one trillion (Bushdid et al. 2014), which is much more than the approximately 2.3 million different colors humans can distinguish (Pointer and Attridge 1997). Some olfactory stimuli have been shown to be innately aversive for humans (Hussain et al. 2013), whereas the valence of many odors can be influenced by either learned experience or by the context in which they are presented (Pollatos et al. 2007, Prescott 2012). Although the existence of human sex pheromones is highly unlikely (Petrulis 2013), non-pheromonal olfactory cues can influence the attractiveness of faces (Demattè et al. 2007) and thus might influence partner choice even in humans. Despite such a huge variety of usage of olfaction, vision and hearing are often considered much more important in humans. This evaluation becomes even more evident by considering the degree of disability attributed after losing sensory perception after an accident: the loss of a single eye leads to a degree of disability of 50%, the loss of hearing on one ear to a degree of 30% and the total loss of olfaction only to a degree of 10% (Grimm 2006).

Whether these numbers correctly reflect the importance of the different senses for all humans cannot be determined in an easy way, as the extent to which individuals from different cultures rely on olfaction may differ (Majid and Burenhult 2014). Primates, in general, are thought to

be mainly visually guided (Matsui et al. 2010) compared to many other animal species. This becomes already evident by looking at the reduced pheromone-based communication in primates. The main organ responsible for pheromone communication in mammals is the vomeronasal organ (VNO). Adult old world monkeys including humans do not have a functional VNO (Bhatnagar and Meisami 1998) and new world monkeys seem to have an impaired VNO (Smith et al. 2011).

In contrast to the neglected use of olfaction in humans, a lot of impressive olfactory performances that seem almost supernatural to humans are well known in non-primate animals: dogs are famous for their tracking behavior of prey and are even used to identify odorants emerging from explosive materials at airports (Kranz et al. 2014). Most humans are familiar with the superb, but highly annoying olfactory-guided host-seeking behavior of mosquitoes (Reddy et al. 2011), and male moths are famous for their sophisticated pheromone-source localization abilities (see for example Vickers and Baker 1994). Last but not least honeybees display an enormous variety of olfactory guided behaviors (reviewed for example by Slessor et al. 2005).

Regardless of the importance of olfaction for their lifestyle, all animals using olfaction have to deal with similar problems. The odorant space includes a huge variety of different molecules (Haddad et al. 2008), which leads to an almost infinite number of potential stimuli. These odor molecules can differ in many different qualitative aspects including, for example, chain length, functional groups and even isomerization status. Compared to this multidimensional variability in odorant quality, the quality of visual and auditory signals only vary in one dimension, which are wavelength and, respectively frequency. Additionally, odorants are almost never present in a pure form but always as mixtures with other odorant molecules. One major breakthrough concerning the olfactory puzzle was the identification of a family of G-protein coupled receptors as mammalian olfactory receptors (OR) (Buck and Axel 1991). This discovery was awarded with the Nobel Prize in 2004. The OR gene family is highly diverse and about 400 ORs are present in the human genome (Malnic et al. 2004), and approximately 1200 can be found in the mouse genome (Godfrey et al. 2004). At a first glance, these numbers suggest only a limited number of molecules, which can be identified by the olfactory system. Yet different molecules were shown to bind to the same receptor with different binding affinities. Assuming that almost every molecule is recognized by several receptors with distinct binding probabilities, a combinatorial odor code allowing almost infinite odor recognition properties emerges (Malnic et al. 1999).

The olfactory system of insects and vertebrates

Some conceptual features of olfactory chemoreception are strikingly similar in vertebrates and insects (Ache and Young 2005). This is hardly surprising as both groups need to deal with the same problems. Generally, in both vertebrates and insects, air-born molecules need to pass through a fluid-filled compartment before they can bind to a receptor. This compartment consists mainly of a variety of proteins and the most abundant ones are odorant binding proteins (OBPs) (reviewed by Ache and Young 2005). The function of OBPs is still not finally resolved, yet the common idea suggests that they bind odorants and then act as carriers for hydrophobic molecules (Pelosi et al. 2006). One key feature of olfactory systems is that each olfactory sensory neuron (OSN) expresses one type of odorant receptor (OR). This has been shown for both mice (Malnic et al. 1999; Serizawa et al. 2000) and *Drosophila* (Couto et al. 2005). Although insect ORs are proteins with seven transmembrane domains, their N-terminus is located intracellularly. This is in contrast to vertebrates where the N-terminus is located extracellularly (Benton 2006). Another difference to vertebrate ORs is that insect ORs have been shown to be always coexpressed with a second OR (Larsson et al. 2004). This OR was termed OR83b in *Drosophila*, yet it is conserved over a wide range of species and was named differently in these (Krieger et al. 2003). Recently, a unifying nomenclature approach termed this coreceptor Orco (**o**lfactory **r**eceptor **co**-receptor) for all insect species (Vosshall and Hansson 2011). The function of the Orco has been under debate since its discovery. So far, it was clearly shown to be important for the transport of the OR-Orco complex to the dendritic parts of the neuron (Larsson et al. 2004). Furthermore, heteromeric complexes of an OR with Orco were shown to have an increased functionality compared to the single receptors (Neuhaus et al. 2005). In the first studies dealing with the exact function of Orco, two different views emerged. One group could show that the complex of an OR and Orco forms a ligand-gated ion channel (Sato et al. 2008), whereas the other identified the OR/Orco complex as a both ligand-gated and cyclic-nucleotide-activated cation channel (Wicher et al. 2008). The exact function of the OR/Orco complex is still under debate, yet recent reviews described it as a metabotropically regulated ionotropic receptor (Stengl and Funk 2013; Wicher 2013).

Regardless of the exact mechanism, OR/Orco complexes recognize odors and transmit the chemical stimulus into electrical information which is sent along the OSNs into the brain. In both insects and vertebrates, OSNs form synapses with the following neurons in typical spheroidal structures termed glomeruli (general review: reviewed in Hildebrandt and Shepherd 1997; for example rat: Pinching and Powell 1971; hawkmoth: Rössler et al. 1998; 1999a; b). All OSNs projecting to the same glomerulus express the same OR gene (mouse: Mombaerts et

al. 1996, *Drosophila*: Vosshall et al. 2000). Therefore, olfactory glomeruli represent functional units of the AL/olfactory bulb (OB). Various imaging studies using Ca^{2+} sensitive dyes or intrinsic imaging of the AL/OB have been performed in the recent past and mainly show that few glomeruli are activated during stimulation with a single odorant (for example in different insects: Joerges et al. 1997; Lin et al. 2006; Silbering and Galizia 2007; Zube et al. 2008; for example in vertebrates: Tabor et al. 2004; Patterson et al. 2013). These results suggest a unifying spatial combinatorial coding hypothesis in glomerular arrays within primary olfactory centers.

In the glomeruli, OSNs relay their information on projection neurons (PN) and local interneurons (LN) in insects. LNs are highly diverse, for example in *Drosophila*, they have been shown to be either excitatory, inhibitory or even to couple neurons electrically (Shang et al. 2007; Yaksi and Wilson 2010). In cockroaches spiking and non-spiking LNs were found (Husch et al. 2009), and in Hymenoptera GABA as well as histamine were found as inhibitory transmitters of LNs (Dacks et al. 2010). Additionally to the diversity of physiological and anatomical subtypes, LNs of several insects also have multiple neuropeptides (reviewed by Schachtner et al. 2005; for example: *Heliothis virescens*: Berg et al. 2007; *Drosophila*: Carlsson et al. 2010; *Tribolium castaneum*: Binzer et al. 2014; *Aedes aegypti*: Siju et al. 2014). The exact functions of the single neuropeptides are mostly unknown, yet their sheer number already indicates that neuropeptidergic signaling is of high importance in the insect AL. The enormous variety of LNs leaves much room for speculation about their diverse functions in AL processing, and is likely to be a major research topic in the future. PNs can be divided into two major types: uniglomerular and multiglomerular PNs. Uniglomerular PNs have been studied with various methods (intracellular recordings, extracellular recordings, patch-clamp recordings, Ca^{2+} imaging, and multi-unit recordings) so far and were shown to relay odor information to the next brain structure, the mushroom bodies (MB) (for example see Heinbockel et al. 1999; Szyzska et al. 2005; Chaffiol et al. 2012; Brill et al. 2013). Only few data is available on multiglomerular PNs and, so far, no clear function was attributed to them.

The anatomy of the mouse OB is partly similar (Hildebrandt and Shepherd 1997). Mitral cells and tufted cells relay the olfactory information via the olfactory tract to higher brain centers, i.e. the olfactory cortex. Granular cells interconnect mitral cells as well as tufted cells and form inhibitory synapses which promote lateral inhibition. Additionally, periglomerular cells mediate lateral inhibition within one glomerulus (reviewed by Ache and Young 2005 and Diaz et al. 2013). Despite the differences between vertebrates and insects, several similarities at the first and second odor processing level are striking. As worm like common ancestors of

vertebrates and insects most likely did not possess primary olfactory centers with glomerular organization, these similarities in olfactory circuits are likely to represent an impressive case of convergent evolution (Strausfeld and Hildebrand 1999). In any case, this asks for an approach investigating phenomena and their mechanisms in diverse species in order to discover common principles. This approach, for example, has been performed over recent years within a Germany wide DFG priority program on “The integrative analysis of olfaction” in a variety of animal species. The general features of olfactory systems are summarized in fig. 1.

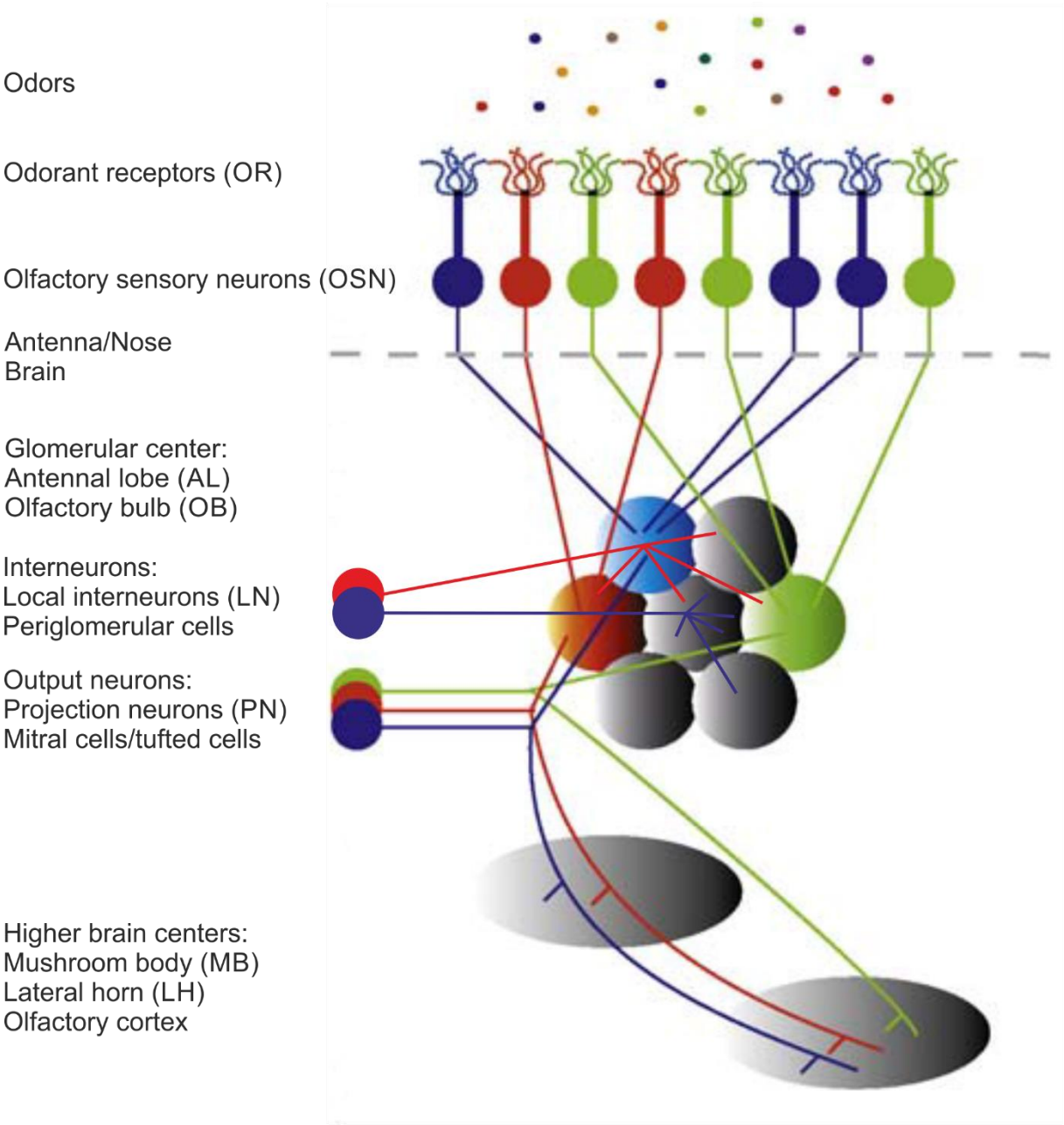

Fig. 1 Schematic drawing showing a comparison of olfactory pathways of insects and vertebrates. Odor molecules are recognized by odorant receptors (*OR*). Axons of olfactory sensory neuron (*OSN*) expressing the same OR project into the same glomerulus in the glomerular center (insects: antennal lobe (*AL*), vertebrates: olfactory bulb (*OB*)). Interneurons (local interneurons (*LN*) in insects and periglomerular cells in vertebrates) interconnect in the primary glomerular centers. Vertebrate granular cells were not included in this scheme. Output neurons (insects: projection neurons (*PN*) vertebrates: mitral cells, tufted cells) project to higher brain centers (insects: mushroom body (*MB*), lateral horn (*LH*), vertebrates: olfactory cortex). Adapted from Ramdya and Benton 2010.

The olfactory world of the honeybee

Honeybees (*Apis mellifera*) live in colonies consisting of one queen, on average 10.000-40.000 female worker bees and, depending on the time of year, a few hundred male drones (Page 2012). Honeybees are typical eusocial insects fulfilling all necessary criteria: cooperative brood care, overlapping generations and division of labor (Wilson and Hölldobler 2005). The evolutionary success of the impressive social systems in insects is largely based on diverse olfactory capabilities that are performed over the individual life spans (reviewed by Galizia and Rössler 2010).

One odorant often associated with honeybees is the alarm pheromone with its typical banana-like smell originating from the principal active component isoamyl acetate (Boch et al. 1962). This pheromone is emitted by honeybees when they sting and recruits other workers to perform hive-defending tasks (reviewed by Breed et al. 2004). However, honeybees use pheromones to a similar extent for 'peaceful' tasks: the Nasanov pheromone, for example, induces swarming behavior and drastically reduces the aggressiveness of honeybees (Williams et al. 1981). The queen emits the so-called queen retinue pheromone (or queen mandibular pheromone, QMP), which consists of at least 9 components. The pheromone emitted by the queen signals her presence and inhibits worker reproduction (reviewed by Slessor et al. 2005). Additionally, one component of the queen retinue pheromone, 9-ODA, is used as a sex pheromone and attracts drones during the mating flight (Gary 1962). Furthermore, a whole range of fatty acid esters is employed by larvae, workers and queens to act as either primer or releaser pheromones that can be sensed by olfaction (Muenz et al. 2012) and thereby regulate a variety of tasks (for a comprehensive review, see Slessor et al. 2005). Besides communication and regulation of division of labor honeybees need their olfactory system also for the identification of nest mates. The guards sitting at the entrance of the hive smell the cuticular hydrocarbon profile of bees entering the hive. If the profile does not match to the hive's profile, the intruder is attacked (Downs and Ratnieks 2000).

Olfaction also plays a crucial role during the foraging behavior of honeybees. Foragers use scent marks to navigate to food sources (Arenas et al. 2007), where they take up nectar or pollen. Along with the nectar/pollen, also odor molecules corresponding to the food source are taken up. During recruitment of other honeybees to the food source with the waggle dance, dancers emit four specific substances into the hive, which were shown to elicit foraging behavior in other honeybees (Thom et al. 2007). Followers of the recruiting dancers also smell the odor typical for the food source and thus have an additional cue, which allows them to navigate to the food source (Diaz et al. 2007). Additionally, the forager which originally found the food

source established an olfactory associative memory with the smell of the source (reviewed by Giurfa 2007). Then, the pure smell of flowers blown into the hive can already recruit experienced foragers: they will fly to the food source, where they experienced this odor (Reinhard et al. 2004). This demonstrates the importance of olfactory associative learning in honeybees. The learning abilities of honeybees are immense and have studied intensively over the past years (reviewed by Giurfa 2007). The standardized paradigm used in the laboratory to investigate for example influence of pharmacological agents on learning and memory is the proboscis extension response (PER, described in detail by Matsumoto et al. 2012). The relevance of this essay becomes evident as flower odors transmitted to the hive by foragers elicit memory formation in followers that can even be tested with the PER (Farina et al. 2005). The majority of the olfactory tasks mentioned above needs to be fulfilled by honeybee workers. In contrast, honeybee drones mainly need to find the queen as fast as possible, which already predicts potential differences of their olfactory systems. Nevertheless, the combination of all these impressive olfactory tasks makes it obvious that honeybees require a sophisticated olfactory system.

The anatomy of the olfactory system of the honeybee

The peripheral olfactory organs of honeybees are their antennae. These antennae are used to filter odor molecules out of the air. They contain small sensory organs, the so-called sensilla, which partly increase the surface of the antenna and thus maximize odor molecule reception. On honeybee antennae, olfactory, hygro-sensitive, mechano-sensitive and thermo-sensitive sensilla have been found (Esslen and Kaissling 1976). Three different types of olfactory sensilla are present on honeybee antennae: *Sensilla trichoidea*, *Sensilla basiconica* and *Sensilla placodea*. *S. placodea* contain 7-23 OSNs (Kelber et al. 2006) and were shown to respond to a broad spectrum of odorants (Getz and Akers 1993) and thus were proven to be olfactory. Both *S. trichoidea* and *S. basiconica* are hair-like sensilla, which were classified as olfactory due to pores found in electron-microscopic studies (Slifer and Slekhorn 1961). Both of them are thin-walled sensilla, yet *S. basiconica* are thicker and shorter and have a blunt profile. Interestingly, honeybee drones were shown to lack *S. basiconica* implying that these sensilla are responsible for honeybee-worker specific tasks (Lacher 1964; Esslen and Kaissling 1976; Nishino et al. 2009).

To activate a neuron, odorant molecules need to be filtered out of the air and to travel through the pores of the sensilla. Odorant molecules pass the sensillum lymph and afterwards bind to

ORs situated at the membrane of OSN dendrites. How exactly odorants pass through the lymph is unknown, yet nine odorant binding proteins were found in the honeybee antenna and are thought to participate in this transfer (Foret and Maleszka 2006). Honeybees have approximately 163 ORs (Robertson and Wanner 2006), which is a high number compared to ~60 in *Drosophila* (Vosshall et al. 2000), yet a low number compared to 300-400 in the fire ant, *Solenopsis invicta* (Wurm et al. 2011). As in all other insects studied so far, honeybees also express an Orco additionally to the ORs (Krieger et al. 2003).

One antenna contains approximately 65.000 OSNs. As the majority of sensilla are olfactory in nature, about 60.000 OSNs are supposedly situated in one antenna (Esslen and Kaissling 1976). These OSNs run in two bundles along the antenna into the brain of the honeybee. In the brain, they diverge in 4 tracts into the first olfactory relay center in the brain, the AL. The four tracts terminate in four glomerular clusters containing about 163 glomeruli in total (Kirschner et al. 2006). This number fits well with the number of ORs identified by Robertson and Wanner (2006) and supports the one OR, one OSN, one glomerulus dogma. Similar to sensillum repertoire, honeybee drones have less glomeruli than workers (see for example Nishino et al. 2009). This hints that OSNs from *S. basiconica* terminate in the AL glomeruli that appear to be missing in drones compared to workers.

Inside of each glomerulus, OSNs form synapses with LNs and PNs. The honeybee AL contains about 3.000-4.000 LNs, which can be broadly divided into homogenous LNs branching similarly in almost all glomeruli and heterogeneous LNs innervating one glomerulus densely and a few other glomeruli sparsely (Fonta et al. 1993). About 800 LNs are GABAergic in nature (Schäfer and Bicker 1986) and ~35 LNs were shown to use histamine as a neurotransmitter (Bornhauser and Meyer 1997). The neurotransmitters of the remaining LNs are not known to date. Additionally, LNs were shown to contain a variety of neuropeptides (reviewed by Galizia and Kreissl 2012).

The output neurons of the honeybee AL, the PNs, connect the AL with the MB and the lateral horn (LH) (for a review, see Galizia and Rössler 2010). Two different types of PNs exist, namely uniglomerular PNs (described for example by Bicker et al. 1993) and multiglomerular PNs (Fonta et al. 1993). In the honeybee approximately 900 uniglomerular PNs project to the MB via two distinct tracts receiving input from two separate sets of glomeruli (Abel et al. 2001). One of the two tracts passes the vertical lobe medially and innervates first the MB and then the LH. The other runs laterally to the vertical lobe and innervates firstly the LH and then the MB (described in detail by Kirschner et al. 2006). According to their position, these two tracts were named medial and lateral antenno-cerebral tract (Kirschner et al. 2006). A recent unifying

nomenclature approach termed the two tracts medial and lateral antennal-lobe tract (m- and lALT) (Ito et al. 2014). These two tracts represent a dual olfactory pathway, which is a unique feature of Hymenoptera (Galizia and Rössler 2010; Rössler and Zube 2011). The mALT was shown to be cholinergic, whereas the transmitter of the lALT is not known to date (Kreissl and Bicker 1989). Multiglomerular PNs do not project to the MB but run directly via the mediolateral antennal-lobe tract (mlALT) to the LH (Fonta et al. 1993). Exact pre- and postsynaptic profiles, electrophysiological recordings or the transmitter composition are not available for multiglomerular PNs to date, therefore their function remains to be investigated.

In the MBs, m- and lALT PNs form distinct synaptic complexes, so called microglomeruli (Homberg et al. 1989; Groh et al. 2004; Groh and Rössler 2011), with about 184.000 intrinsic MB neurons, the Kenyon cells (KCs). The MB are well known as centers for learning and memory in insects (see for example Hammer and Menzel 1995; Heisenberg 2003; Keene and Waddell 2007). This could also be confirmed for long-term memory formation in the honeybee, in which the synaptic density, but not the volume of the MBs changes after long-term memory formation (Hourcade et al. 2010). The output of the MBs is mediated by extrinsic MB neurons (EN), which receive synaptic input from the KCs in the vertical lobe of the MB (Rybak and Menzel 1993). A comprehensive summary of most neurons involved in the olfactory pathway is depicted in fig. 2.

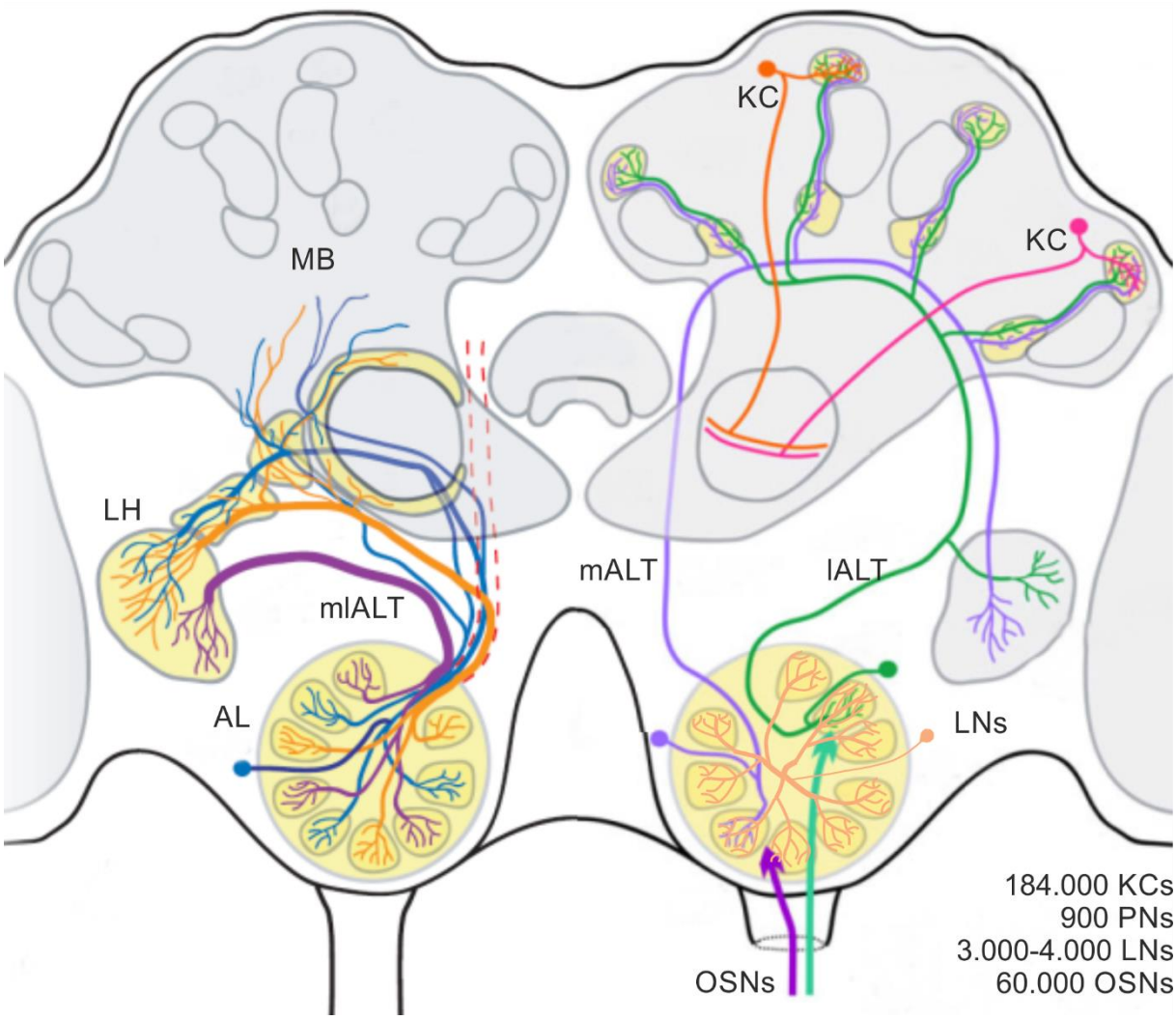

Fig. 2 The olfactory pathway of the honeybee. About 60.000 olfactory sensory neurons (*OSNs*) project into the antennal lobe (*AL*). In the glomeruli their axons terminate on the dendrites of approximately 900 projection neurons (*PNs*) (Galizia and Rössler 2010) and 3.000-4.000 local interneurons (*LNs*) (Galizia and Kreissl 2012). PNs of the mediolateral antennal-lobe tract (*mlALT*) directly project from the AL to the lateral horn (*LH*). PNs belonging to the medial or the lateral antennal-lobe tract (*mALT*/*lALT*) innervate both the mushroom body (*MB*) and the LH. In the MB, PN axons terminate on the dendrites of ~184.000 Kenyon cells (*KC*) (Witthoeft 1967; Strausfeld 2002). Combined and adapted from Kirschner et al. 2006; Galizia and Rössler 2010; Rössler and Brill 2013.

Coding of information in the olfactory pathway of the honeybee

The anatomy of the olfactory system of the honeybee has been intensively studied, yet precise functional data is not available for all neuronal components of the olfactory pathway. Antennal potentials can be recorded with electroantennography (EAG) recordings rather easily (see for example Muenz et al. 2012). But as EAG recordings sum up all activity from antennal neurons, they are merely a measure for the quality and the time of the antennal response to a certain

olfactory stimulus. Single sensillum recording is a method well established in a several insects (see for example *Drosophila melanogaster*, Ibba et al. 2010 and *Spodoptera littoralis*, Pézier et al. 2007), and is well suited to identify responses of single or a few OSNs to odor stimulation. As a matter of fact, honeybee *S. placodea* are rather small, situated under the cuticle, and contain between 7 and 23 OSNs (Kelber et al. 2006). Therefore, electrophysiological recordings are fairly difficult. Nevertheless, *S. placodea* were shown to respond to a broad range of odorants (Getz and Akers 1993; Akers and Getz 1993), although the responses of individual neurons could not be resolved. The spontaneous action potential (AP) frequencies as well as the response frequencies were above the frequencies observed in cockroaches (Getz and Akers 1993), yet the recorded cockroach sensilla contain only up to four OSNs. Therefore, the higher frequencies in honeybee single sensillum recordings are most likely due to the recording of more neurons at the same time. Similar to cockroaches, honeybee OSNs also exhibit low spontaneous AP frequencies and phasic tonic odor responses. Both in recordings of *S. trichoidea* and *S. basiconica* only spontaneous activity and no odor responses were observed (Lacher, 1964). This is likely due to the fact that individual neurons could not be recorded and the majority of OSNs in one sensillum did not respond to an odor stimulus and thus masked single responses.

The next classes of neurons in the olfactory pathway, PNs and LNs, were studied with a variety of methods including intracellular, extracellular electrophysiology, and Ca^{2+} imaging recordings. LNs were shown to respond to a variety of odorants in also varying response patterns (Galizia and Kimmerle 2004; Krofczik et al. 2008; Meyer et al. 2013). However, this did not allow to cluster them into distinct subtypes. The responses of uniglomerular PNs were studied more frequently, and some distinct parameters could be observed. Ca^{2+} imaging of the sensory input and PN responses showed that both the m- and the lALT respond to a similar sets of odorants (Carcaud et al. 2012; Galizia et al. 2012; Brill et al. 2013). Multi-unit recordings of a large sets of PNs conformed these parallel processing properties by PNs of both tracts and showed that lALT PNs respond faster and less specific to odorants compared to more narrow odorant tuning and slower temporal response profiles in mALT PNs (Brill et al. 2013; Rössler and Brill 2013). Additionally, lALT PNs have higher response rates and spontaneous frequencies (Brill et al. 2013). Generally, PNs of both tracts normally respond in a phasic tonic fashion. With increasing stimulus concentration, PNs also show AP-bursts with follow-up inhibition responses and rarely purely inhibitory responses (Müller et al. 2002; Krofczik et al. 2008; Brill et al. 2013). In contrast to these complex odor response patterns of PNs, KCs encode odors in spatially and temporally sparse fashion. This means that only a few of the 184.000 KCs

respond with only a few APs to odorant stimulation (Szyszka et al. 2005). Besides this sparse temporal response patterns, most KCs are mainly silent when they do not receive strong synaptic input, resulting in spatial sparseness of KC responses (Szyszka et al. 2005). ENs receiving synaptic input directly from KCs respond to odor stimulation with relatively high spiking frequencies, slightly higher than PN response frequencies (Strube-Bloss et al. 2011; 2012; Brill et al. 2013). Compared to PNs, ENs show less diverse odor responses and mostly respond in a strict phasic-tonic fashion (Strube-Bloss et al. 2011; 2012).

Differences in coding of olfactory information between different neuronal populations

Olfactory information needs to pass through the different neuronal building blocks of the olfactory pathway. The key players of this system have been shown to differ in anatomy and physiology as described above, yet the origin and the functional implications of these differences remain uninvestigated to date. By looking only at the numbers of OSNs, PNs, KCs and ENs, some necessary neuronal properties become obvious. About 60.000 OSNs terminate on 900 PNs, which diverge onto 184.000 KCs. These 184.000 KCs then converge on 400 ENs (reviewed by Galizia and Rössler 2010). To ensure reliable information transfer within these neurons, it is necessary that neurons, which are outnumbered by their preceding neurons, need to have higher spiking frequencies and/or specific coding properties to overcome this bottleneck. Indeed, this principle can be seen in the honeybee olfactory system. OSNs have lower spiking frequencies than PNs, KCs are almost silent and ENs again have relatively high spiking frequencies. Whether the differences in AP frequencies between these neurons are only based on their synaptic connections or are also due to intrinsic neuronal properties needs to be investigated.

Yet, principle differences between coding of information between distinct neuronal classes is expected. In contrast, also m- and lALT PNs display different coding properties for information (Brill et al. 2013; Rössler and Brill 2013), which leads to the question dealing with the mechanism involved in this.

1. Are the differences in specificity of odor responses due to differences in the synaptic input? As the overall set of odorants recognized between m- and lALT does not fundamentally differ, this implies that OSNs projecting to the mALT glomeruli may be more odor specific, yet still cover the whole range of odor molecules used in the recordings (Carcaud et al. 2012; Brill et

al. 2013). Glomeruli belonging to the lALT likely receive input from more generalist OSNs or show a difference in the specificity of OSN projections into glomeruli.

I therefore assume that the OSNs arborizing in the mALT glomeruli differ from OSNs arborizing in the lALT glomeruli.

2. What is the basis of the differences in spontaneous and maximal frequencies between m- and lALT PNs? In contrast to the odor specificity these differences are less likely to be caused by difference in the OSNs projecting to the glomeruli of the two tracts. I assume that the difference are rather due to either inhibition of the mALT via LNs, to different neuronal modulation of the two tracts or to different intrinsic properties of the neurons of the two tracts.

3. How can KCs encode olfactory information in such a sparse way, which promotes coincidence detection? As PNs have relatively high AP frequencies, KCs must receive regular synaptic input. Nevertheless, they encode odors in a sparse fashion and odor responses do not seem to last over the entire stimulation duration (Szyszka et al. 2005). These brief responses demand a negative feedback circuit in KCs, either by GABAergic neurons or by intrinsic, strongly hyperpolarizing ion channels that activate right after neuron activation.

Thesis outline

The questions and hypothesis explained above can be formulated in two most important questions:

1. What are the differences in the connectivity of sensory input that may promote differences in the m- and lALT PNs?
2. How different are the intrinsic neuronal properties of the distinct neuronal classes (l/mALT PNs, KCs), and how do these properties affect neuronal coding?

These two principal questions inspired two major experimental approaches for this thesis:

1. In a first step, I set out to investigate the synaptic targets of OSNs from *S. basiconica* and their relation to sex specific differences. Therefore, the projection patterns of individual *S. basiconica* were investigated in honeybee (female) workers and compared with missing aspects in (male) drones. As drones lack *S. basiconica*, it can be predicted that some parts of the AL glomeruli are missing as well. This approach was expected to give hints regarding the potential origin of differences in odor specificity and parallel processing capabilities of the honeybee dual olfactory system.

This approach and the results are detailed in publication I:
Olfactory subsystems in the honeybee: sensory supply and sex specificity.

2. The second approach comprises investigations on the electrical properties, in particular ion channel compositions in mALT/lALT PNs and in KCs. We expect that differences between m- and lALT PNs are not likely to be prominent, yet they may explain differences between AP frequencies in the two populations. Conversely, KCs should exhibit a completely different set of ion channels compared to PNs.

This approach and its results are detailed in manuscript II:
Complex and sparse coding along the honeybee's olfactory pathway: potential contribution of ionic currents in medial and lateral projection neurons and Kenyon cells

Manuscript I

Olfactory subsystems in the honeybee: sensory supply and sex specificity

Jan Kropf, Christina Kelber, Kathrin Bieringer, Wolfgang Rössler
Cell and Tissue Research (2014) 357: 583-595

The antennae of honeybee (*Apis mellifera*) workers and drones differ in various aspects. One striking difference is the presence of *Sensilla basiconica* in (female) workers and their absence in (male) drones. We investigate the axonal projection patterns of olfactory receptor neurons (ORNs) housed in *S. basiconica* in honeybee workers by using selective anterograde labeling with fluorescent tracers and confocal- microscopy analysis of axonal projections in antennal lobe glomeruli. Axons of *S. basiconica*-associated ORNs preferentially projected into a specific glomerular cluster in the antennal lobe, namely the sensory input-tract three (T3) cluster. T3-associated glomeruli had previously been shown to be innervated by uniglomerular projection (output) neurons of the medial antennal lobe tract (mALT). As the number of T3 glomeruli is reduced in drones, we wished to determine whether this was associated with the reduction of glomeruli innervated by medial-tract projection neurons. We retrogradely traced mALT projection neurons in drones and counted the innervated glomeruli. The number of mALT-associated glomeruli was strongly reduced in drones compared with workers. The preferential projections of *S. basiconica*-associated ORNs in T3 glomeruli together with the reduction of mALT-associated glomeruli support the presence of a female (worker)-specific olfactory subsystem that is partly innervated by ORNs from *S. basiconica* and is associated with the T3 cluster of glomeruli and mALT PNs. We propose that this olfactory subsystem supports parallel olfactory processing related to worker-specific olfactory tasks such as the coding of colony odors, colony pheromones and/or odorants associated with foraging on floral resources.

Manuscript II

Complex and sparse coding along the honeybee's olfactory pathway: potential contribution of ionic currents of medial and lateral projection neurons and Kenyon cells

Jan Kropf, Wolfgang Rössler

In the olfactory system of the honeybee an intriguing pattern of convergence and divergence between the individual neuronal types within the olfactory pathway exists: approximately 60.000 olfactory sensory neurons (OSN) convey olfactory information on 900 projection neurons (PN) in the antennal lobe. In order to transmit all information from the OSNs reliably, PNs need to employ relatively high spiking frequencies. PNs then project via a dual olfactory pathway to the mushroom bodies (MB) .This pathway comprises two tracts, the medial (mALT) and the lateral antennal lobe tract (lALT). Although both tracts receive input from different OSNs, they were shown to transmit information from a similar set of odors, yet with slight differences. LALT PNs respond faster but mALT PNs are more odor specific (Brill et al. 2013). In the MBs, PNs form synaptic complexes with ~184.000 Kenyon cells (KC), the MB intrinsic neurons. Generally, insect MBs are regarded as the centers for sensory integration and learning and memory. As KCs drastically outnumber PNs, they are likely to employ much lower spiking frequencies than PNs. Indeed, they were shown to respond in a very phasic and sparse fashion to odor stimulation using Ca^{2+}-imaging (Szyszka et al. 2005). In the present study, we aim to identify the neuronal properties leading to the differences between m- and lALT PNs and KCs. In PNs, we could identify a set of Na^+ currents and diverse K^+ currents depending on voltage and Na^+ or Ca^{2+}relatively similar to currents observed in locust DUM (dorsal unpaired median) neurons that support spiking activity (Wicher et al. 2006). Conversely in KCs, we found very prominent K^+ currents, which are likely to contribute to the sparse response fashion observed in KCs.

Cell Tissue Res (2014) 357:583–595
DOI 10.1007/s00441-014-1892-y

REGULAR ARTICLE

Manuscript I: Olfactory subsystems in the honeybee: sensory supply and sex specificity

Jan Kropf & Christina Kelber & Kathrin Bieringer & Wolfgang Rössler

Received: 7 February 2014 / Accepted: 8 April 2014 / Published online: 13 May 2014

Abstract The antennae of honeybee (*Apis mellifera*) workers and drones differ in various aspects. One striking difference is the presence of *Sensilla basiconica* in (female) workers and their absence in (male) drones. We investigate the axonal projection patterns of olfactory receptor neurons (ORNs) housed in *S. basiconica* in honeybee workers by using selective anterograde labeling with fluorescent tracers and confocal- microscopy analysis of axonal projections in antennal lobe glomeruli. Axons of *S. basiconica*-associated ORNs preferentially projected into a specific glomerular cluster in the antennal lobe, namely the sensory input-tract three (T3) cluster. T3- associated glomeruli had previously been shown to be inner- vated by uniglomerular projection (output) neurons of the medial antennal lobe tract (mALT). As the number of T3 glomeruli is reduced in drones, we wished to determine wheth- er this was associated with the reduction of glomeruli innervat- ed by medial-tract projection neurons. We retrogradely traced mALT projection neurons in drones and counted the innervated glomeruli. The number of mALT-associated glomeruli was strongly reduced in drones compared with workers. The pref- erential projections of *S. basiconica*-associated ORNs in T3 glomeruli together with the reduction of mALT-associated glomeruli support the presence of a female (worker)-specific olfactory subsystem that is partly innervated by ORNs from *S. basiconica* and is associated with the T3 cluster of glomeruli and mALT projection neurons. We propose that this olfactory subsystem supports parallel olfactory processing related to worker-specific olfactory tasks such as the coding of colony odors, colony pheromones and/or odorants associated with foraging on floral resources.

Keywords *Sensilla basiconica* · Antennal lobe · Glomeruli · Projection neuron · Honeybee drone

This work was supported by the DFG Priority Program SPP 1392 "Integrative Analysis of Olfaction" (RO 1177/5-2 to W.R.). C.K. is funded by the Deutsche Forschungsgesellschaft (DFG KE 1701/1).

Electronic supplementary material The online version of this article (doi:10.1007/s00441-014-1892-y) contains supplementary material, which is available to authorized users.

J. Kropf (*) : C. Kelber : K. Bieringer : W. Rössler Department of Behavioral Physiology and Sociobiology,

Biozentrum, University of Würzburg, Am Hubland, 97074 Würzburg, Germany
e-mail: jan.kropf@uni-wuerzburg.de
C. Kelber
Ecological Networks, Technical University of Darmstadt, Schnittspahnstrasse 3, 64287 Darmstadt, Germany

Introduction

Olfaction is an ancient sensory modality and plays a crucial role in most animals for approaching or avoiding various odor sources and for judging their quality in a variety of behavioral contexts. Whereas odorant reception at the molecular level exhibits distinct differences between vertebrates and insects, the basic wiring pattern of receptor neurons with second-order neurons within the primary olfactory centers, the vertebrate olfactory bulb and the insect antennal lobe (AL) shows several striking similarities. These have been the subject of intense research over recent years (for reviews, see Hildebrand and Shepherd 1997; Ache and Young 2005; Touhara and Vosshall 2009; Martin et al. 2011). Insect antennae are covered with various types of sensory sensilla; most of them being specialized for chemoreception but also for hygro-, mechano- and thermoreception (Esslen and Kaissling 1976; Maronde 1991; Ai et al. 2007). Olfactory sensilla house the olfactory receptor neurons (ORNs) that extend axons into spheroidal structures termed glomeruli to form synaptic connections with local interneurons and projection neurons (PNs). Glomeruli represent the functional unitsof the AL (e.g., Anton and Homberg 1999). In the honeybee, *Sensilla placodea*, *Sensilla trichoidea* and *Sensilla basiconica* have been classified as olfactory sensilla, either according to their odor-response profiles in single-sensillum recordings (*S. placodea*) or based on specific anatomical features (*S. trichoidea, S. basiconica*; Lacher 1964; Esslen and Kaissling 1976; Akers and Getz 1993; Getz and Akers 1993). ORN axons from olfactory sensilla project via four distinct AL sensory-input tracts to four clusters of glomeruli in the AL termed the T1-T4 cluster (Mobbs 1982; Galizia et al. 1999; Abel et al. 2001; Kirschner et al. 2006). Axons from ORNs in *S. placodea* project to all four clusters of glomeruli T1-T4 (Brockmann and Brückner 1995; Kelber et al. 2006) and single-sensillum recordings from *S. placodea* have revealed responses to a broad range of odorants (Getz and Akers 1993). This might be either caused by the broad tuning of ORNs or attributable to the finding that *S. placodea* house many individual ORNs (between 7 and 23; Kelber et al. 2006), each covering a certain spectrum of molecular receptive ranges. In insects, PNs convey the olfactory information to the mushroom bodies (MBs), higher sensory association centers and sites associated with learning and memory (Gerber et al. 2004; Davis 2005; Giurfa 2007; Hourcade et al. 2010; Cervantes-Sandoval et al. 2013). Uniglomerular PNs in the honeybee and other Hymenoptera have been shown to project to the MBs and lateral horn (LH) via two parallel tracts: the medial and the lateral AL tracts (mALT and lALT) forming a dual olfactory pathway (Abel et al. 2001; Kirschner et al. 2006; Galizia and Rössler 2010; Rössler and Brill 2013; tract terminology according to Ito et al.

2014). Comparative anatomical studies indicate that a dual olfactory pathway probably emerged in the basal Hymenoptera (Dacks and Nighorn 2011; Rössler and Zube 2011; Rössler and Brill 2013). However, the selective pressure that promoted the evolution of a dual olfactory pathway within this group of insects remains to be further investigated (Rössler and Brill 2013). Female honeybee workers show complex social behavior that is largely influenced by pheromonal communication (Slessor et al. 2005; Le Conte and Hefetz 2008). This is different in male drones, which mainly perform reproductive tasks, do not forage actively for food and might not need to distinguish minor changes in colony pheromone concentrations. On the other hand, drones are highly sensitive to the queen sex-pheromone (Gary 1962). Therefore, differences in the olfactory system reflecting these behavioral specializations are likely to exist between honeybee workers and drones. One striking sex-specific difference is the absence of *S. basiconica* on drone antennae (Esslen and Kaissling 1976; Nishino et al. 2009). Furthermore, drone ALs contain a smaller number of glomeruli compared with both female castes (workers and queens) but comprise several enlarged macroglomeruli (Arnold et al. 1985; Sandoz 2006; Groh and Rössler 2008; Nishino et al. 2009). The largest macroglomerulus has been shown to respond to the major component of the queen mandibular pheromone (Sandoz 2006; Wanner et al. 2007). The reduction of AL glomeruli is mostly associated with the T3 cluster (Nishino et al. 2009), which has been demonstrated to be mainly innervated by medial tract PNs in honeybee workers (Kirschner et al. 2006). Comparative studies in other Hymenoptera indicate that the lack of *S. basiconica* in males is a characteristic trait across both social and solitary Hymenoptera (Ågren 1977, 1978; Wcislo 1995; Ågren and Hallberg 1996; Nakanishi et al. 2009, 2010; Mysore et al. 2010; Nishikawa et al. 2012; Streinzer et al. 2013). In the leaf-cutting ant Atta vollenweideri, *S. basiconica* have been found exclusively to innervate a specific (T6) cluster of AL glomeruli (Kelber et al. 2010). The absence of *S. basiconica*, together with the reduction of glomeruli in the T3 cluster, in honeybee drones suggests that ORNs from *S. basiconica* preferentially innervate glo- meruli in the T3 cluster and are associated with medial-tract PNs. To test this hypothesis, we investigated the axonal pro- jections of ORNs in the hair-like olfactory antennal sensilla of female worker bees, with a special focus on *S. basiconica* and, in particular, their glomerular innervation patterns and their association with PN output tracts. Furthermore, we retrogradely labeled the mALT in drones to analyze whether glomeruli associated with this tract are reduced.

Materials and methods

Animals

Honeybee workers and drones (Apis mellifera carnica) were collected from bee hives of the institutional bee station at the University of Würzburg. Workers were taken from the entrance of the hive and drones were caught directly in the hive. In both cases we did not control for age. The animals were cooled in a refrigerator (4 °C), fixed in custom made plastic holders and provided with sugar solution (40 %) ad libitum.

Staining of axonal projections

ORNs from hair-like sensilla on defined antennal segments were labeled by using a method previously described by Kelber et al. (2010). Cut glass microelectrodes were placed close to a defined segment of the antenna under visual control (280×) by using a photo-microscope (M 400, Wild, Heerbrugg, Germany) or an Olympus imaging system (200×-400×, upright microscope: BX51WI, filter set: U- MF2 excitation 395/440 FT 460 emission 540/50, objective: XLUMP, NA 0.95, light source: MT20, software: Cell R v2.5 [all Olympus Imaging Europa], camera: model 8484-03G [Hamamatsu Photonics]) and a micromanipulator (Junior Unit, Luigs & Neumann, Ratingen, Germany). This setup allowed the identification of individual sensilla (Fig. 1a, b). The electrode was mounted on a piezo element (Element, EPZ-Serie, Conrad Electronic, Hirschau, Germany) connected to a function generator (PM 5133, Fluke/Philips, Kassel, Germany). Vibration (2-13 kHz) of the piezo element and therefore also of the pipette was used to cut the hair-like sensilla and to expose the dendrites of the ORNs within sensilla of a defined antennal segment. Subsequently, a droplet of Biotin Dextran (Molecular Probes, D-7135, Leiden, Netherland) or Microruby (tetramethylrhodamine dextran with biotin, 3,000 MW, lysine-fixable, D-7162; Molecular Probes, Eugene, Ore., USA), 3-5 % in distilled water, was applied onto the remaining sensilla stumps to enable the dye to enter the ORN dendrites. This method allowed selective staining of hair-like sensilla (*S. trichoidea, S. basiconica*) and excluded the staining of *S. placodea*, as these sensilla are located beneath a plate-like structure of the antennal cuticle (Esslen and Kaissling 1976; Kelber et al. 2006). Animals were then kept in the dark for 24 h before the brains were dissected. For the staining of single sensilla, a microelectrode was placed close to one sensillum to cut only a single sensillum hair. Because of their small size, the cutting of individual basiconic sensilla was extremely difficult and the success rate for staining was

extremely low (only one staining after the approved cut of only one S. basiconicum). Therefore, in most cases, we moved the electrode, in particular in *S. basiconica*-rich regions close to the borders of antennal segments, to cut small groups of hair-like sensilla preferentially including *S. basiconica* (Fig. 1a, b). Larger numbers of *S. basiconica* could be found in ring-like arrangements in the distal region of the antennal segments 3-10, close to the transition to the next segment (Fig. 1; Esslen and Kaissling 1976; Nishino et al. 2009). These axonal projections in this staining technique were compared with the staining of ORN axons from *S. trichoidea* only. Larger groups of *S. trichoidea* in the middle of antennal segments that lacked any *S. basiconica* (Fig. 1) were cut with a sharp tungsten wire (diameter: 200 µm) attached to the piezo element. Microelectrodes used in all experiments (including mALT staining; see below) were pulled from thin-walled glass pipettes (1B100F-3, WPI, Sarasota, USA) with a DMZ-Universal Puller (Zeitz- Instruments, Martinsried, Germany).

Staining of medial tract projection neurons in drones

PNs of the mALT were retrogradely stained by using methods described in detail by Kirschner et al. (2006), Zube et al. (2008) and Rössler and Zube (2011). Head capsules were opened and glands and tracheae covering the brain were removed. The tissue between the vertical lobe of the MB and the AL was punctured with a fine glass electrode on the medial side, where mALT fibers run relatively close to the surface of the brain. A few crystals of either Microruby or Biotin Dextran were gently applied to the punctured tissue by means of a broken micropipette. Mass-staining of all AL output tracts was achieved by using a similar technique and application of dye crystals into the center of the AL. Mass- staining of AL glomeruli was performed by the cutting of the antennae and the application of a droplet of Microruby (about 3-5 % in distilled water) to the antennal nerve stump. In all cases, animals were kept for 4–6 h in the dark under moist conditions to allow the dye to be transported intracellularly.

Single PN staining

For single PN staining, the glial sheath was gently removed from the AL with fine forceps. PN cell bodies were approached with a patch-clamp pipette under visual control by using an upright microscope (BX51WI, Olympus Imaging Europa) and a micromanipulator (Junior Unit, Luigs & Neumann). We employed the intracellular [(K-gluconate (110 mM), HEPES (25 mM), KCl (10 mM), MgCl2 (5 mM), Mg-ATP (3 mM), Na-GTP (0.5 mM), EGTA (0.5

mM), pH 7.2, 284 mOsm)] and extracellular [(NaCl) (140 mM), KCl (5 mM), MgCl2 (1 mM), CaCl2 (2.5 mM), NaHCO3 (4 mM), NaH2PO4 (1.2 mM), HEPES (6 mM), glucose (14 mM), pH 7.4, 326 mOsm)] solutions of Palmeret al. (2013). For staining, 0.5-1 % Lucifer Yellow (L0259, Sigma-Aldrich Chemie, Steinheim, Germany) was added to the intracellular solution. Whole cell patch clamp recordings were established by using an Axon system (Axopatch 200B, Digidata 1440A, ClampEx, Molecular Devices, Oregon, USA) and the membrane voltage was kept at -60 mV.

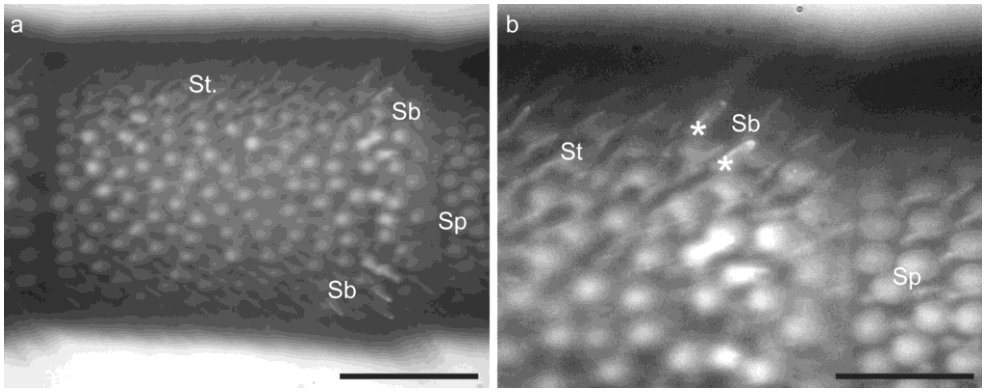

Fig. 1 Light microscopic images of *Sensilla basiconica* (*Sb*), *Sensilla placodea* (*Sp*) and *Sensilla trichoidea* (*St*., *St*) on a honeybee worker antenna. **a** Overview of the ninth segment. *Bar* 100 µm. **b** Detailed view of the *S. basiconica*-rich region on the ninth segment (*white asterisks* bases of two identifiable *S. basiconica*). *Bar* 25 µm.

Neuranatomical analyses

Brains were placed in fixative solution (4 % formaldehyde) overnight, following the staining procedure and then rinsed five times for 10 min in PBS (phosphate-buffered saline, pH 7.2). Biotin-Dextran-injected brains were stained with Alexa- 488-conjugated Streptavidin (S-11226, Molecular Probes, Eugene, Ore., USA) in PBS with 0.2% Triton X (1:125) for 48 h. Subsequently, brains were again rinsed five times for 10 min in PBS. Microruby- and Biotin-Dextran-labeled brains were dehydrated in an ascending ethanol series (50, 70, 90, 95, 2× 100 %, each 10 min) and cleared and mounted in methyl salicylate (M2047, Sigma-Aldrich Chemie) for confocal microscopy. Afterwards, brains were scanned with a con- focal laser-scanning microscope (Leica TCS SP2; Leica Microsystems, Wetzlar, Germany). Images were processed with AMIRA 3.1.1 and 5.4 software (Mercury Computer Systems, Berlin, Germany) and AL glomeruli in one prepara- tion were reconstructed by using the AMIRA wrapping tool. Image stacks were further processed with ImageJ 1.46j (Wayne Rasband, National Institutes of Health, Befesta, Md., USA). To count the glomeruli in all other

successful mALT stainings (that were not three-dimensionally recon- structed in detail), we marked glomeruli in image stacks by using the segmentation editor implemented in ImageJ. Contrast and brightness were adjusted with GIMP 2.8.2 (GNU Image Manipulation Program, http://www.gimp.org) and images in figures were arranged with CorelDrawX6 (Corel, Ottawa, ON, Canada).

Identification of glomeruli

After the successful staining of axonal projections, AL reconstructions in workers were mapped onto a template AL by using the VOI (volume of interest) method described in Kelber et al. (2006). The antennal nerve, the T1 tract and a specific glomerulus (A17; after Galizia et al. 1999) were used as landmarks. Additionally, one AL reconstruction of a mass- staining of ORN axons of the whole antennal nerve was mapped onto the same template AL. This reconstruction allowed the identification of the AL input tracts in the template AL. With the identified glomeruli and the input tracts in the template AL, the matching of sensilla-stained ALs allowed the assignment of axonal projections of ORNs to a specific input tract and to particular glomeruli.

Statistics

Relative innervation frequencies of the input clusters (T1-T4) were analyzed with a Friedman analysis of variance (ANOVA) and a post-hoc Wilcoxon rank sum test with Bonferroni correction for multiple comparisons. The distribution of ORN axons in the various glomerular clusters originating from the staining of *S. basiconica*-rich regions was compared with a hypothetical distribution in the glomerular input clusters based on the natural distribution by using Fisher's exact test. All statistic tests were performed with R 2.10.1 (R Foundation for Statistical Computing, Vienna, Austria

Results

ORN axon projections from many *S. trichoidea* and *S. basiconica* are broadly distributed into AL glomeruli

In the honeybee, ORN axons from *S. placodea* are broadly distributed across glomeruli of the AL and do not preferentially terminate in a specific sensory input cluster (Kelber et al. 2006). To determine whether this also held true for hair-like sensilla, we started with unselective mass-stainings of hair- like sensilla (*S. trichoidea* and *S. basiconica*) on a proximal (4th) and a distal (9th) segment of the same antenna by using two fluoresecent tracers. With this mass-staining method, no specific tract preferences of axons from ORNs housed in hair- like sensilla was found. However, the trajectories of axonal projections revealed a conspicuous axon-sorting-zone-like region at the AL entrance in which axons from the two stained axon bundles in the antennal nerve intermingled (Fig. 2a). Similarly, at the end of the antennal sensory input tracts, ORN axons showed a typical crossing pattern before they diverged to form terminal arborizations in specific subcompartments of individual glomeruli (Fig. 2a).

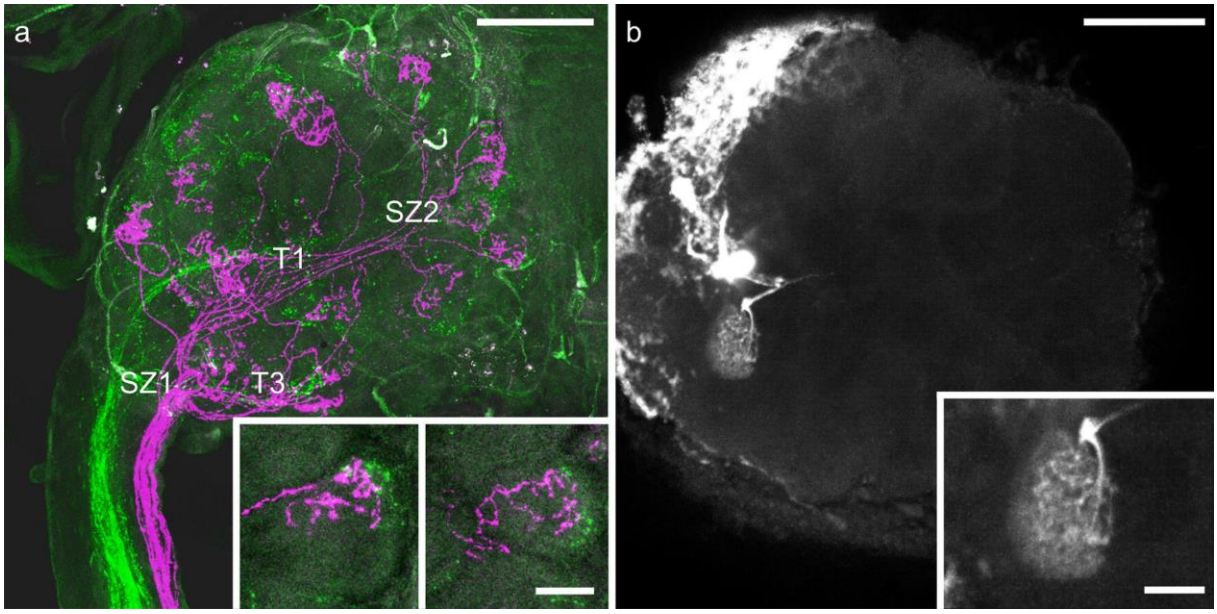

Fig. 2 a Z-projection of a double-mass-staining of hair-like sensilla on segment 9 (*magenta*) and segment 4 (*green*) of honey bee antenna. The input tracts *T1* and *T3* are indicated. Note the two sorting zones (*SZ1*, *SZ2*). *Bar* 100 µm. *Insets* Detailed views of two glomeruli that are innervated by axons from olfactory receptor neurons from both the distal and the proximal parts of segment 9 in a layered fashion. *Bar* 25 µm. **b** Z- projection of an antennal lobe with an intracellularly stained projection neuron innervating a single glomerulus. *Bar* 100 µm. *Inset* Stained glomerulus in more detail; the dendritic arborizations of a projection neuron ramify throughout the entire glomerulus. *Bar* 25 µm

Several glomeruli were innervated by ORN axons from the distal and the proximal segments. Interestingly, ORN axons from different antennal segments arborized in different layers within the same glomerulus (Fig. 2a, b). The dendritic arborizations of a single PN, in contrast to ORN axons, ramified across the entire volume of a glomerulus (Fig. 2b).

Axons from ORNs in *S. trichoidea* of a single antennal segment arborize in the T1, T2 and T3 cluster of glomeruli

As we found no specific preference of ORN projections for a certain glomerular cluster with unselective mass-staining of hair-like sensilla on different antennal segments, we set out to focus on the staining of ORNs from *S. trichoidea* only. Selective mass-labeling of axons from ORNs in *S. trichoidea* in honeybee workers was performed by cutting sensilla only at the middle region of the fifth antennal segment (Fig. 1). This mass-labeling technique excludes S. basiconia, which are located at the segment borders only but might well contain some mechanosensitive *S. trichoidea* (Lacher 1964) in addition to the olfactory sensilla. This staining (n=13) revealed bundles of ORN axons terminating in the AL; a typical example is shown in Fig. 3. The trajectories of labeled ORN axons clearly changed from a more or less parallel organization into sorting-zone-like crossing patterns close to the entrance to the AL. From there, axonal projections proceeded into three tracts (T1, T2, T3) leading to the associated glomerular clusters of the AL. The T4 input tract and the associated glomerular cluster were not stained in any of the 13 preparations (Fig. 3d). A few axons proceeded into the dorsal lobe indicating that some of the stained sensilla stained were mechanosensory in nature (data not shown).

Axons from ORNs in *S. basiconica* preferentially innervate the T3 cluster of glomeruli

As *S. basiconica* are far less numerous compared with *S. trichoidea*, a preference of axons from ORNs housed in *S. basiconica* for a certain input cluster might be masked in the mass-staining of hair-like sensilla. We therefore selectively stained sensilla in *S. basiconica*-rich regions; this was successful in 15 worker bees. In all cases, axonal branches of stained ORN axons were mainly restricted to the outer regions of individual glomeruli (Fig. 4). Glomerular borders were visualized by autofluorescence. Between 3 and 29 glomeruli per bee were stained in the different preparations. All stained glomeruli were mapped into the template AL and

assigned to their input-tract glomerular clusters. In 13 out of 15 bees, T3-associated glomeruli were the most frequently stained glomeruli. In total, 180 ORN axons were stained in 15 bees; 57 projected to T1, four to T2, 111 to T3 and eight to T4 (Fig. 5; exact numbers of stained glomeruli can be found in supplementary Table 1). In one case, we were able to determine, by visual inspection, that the staining was from only a single S. basiconicum that had been cut (Fig. 4g-i).

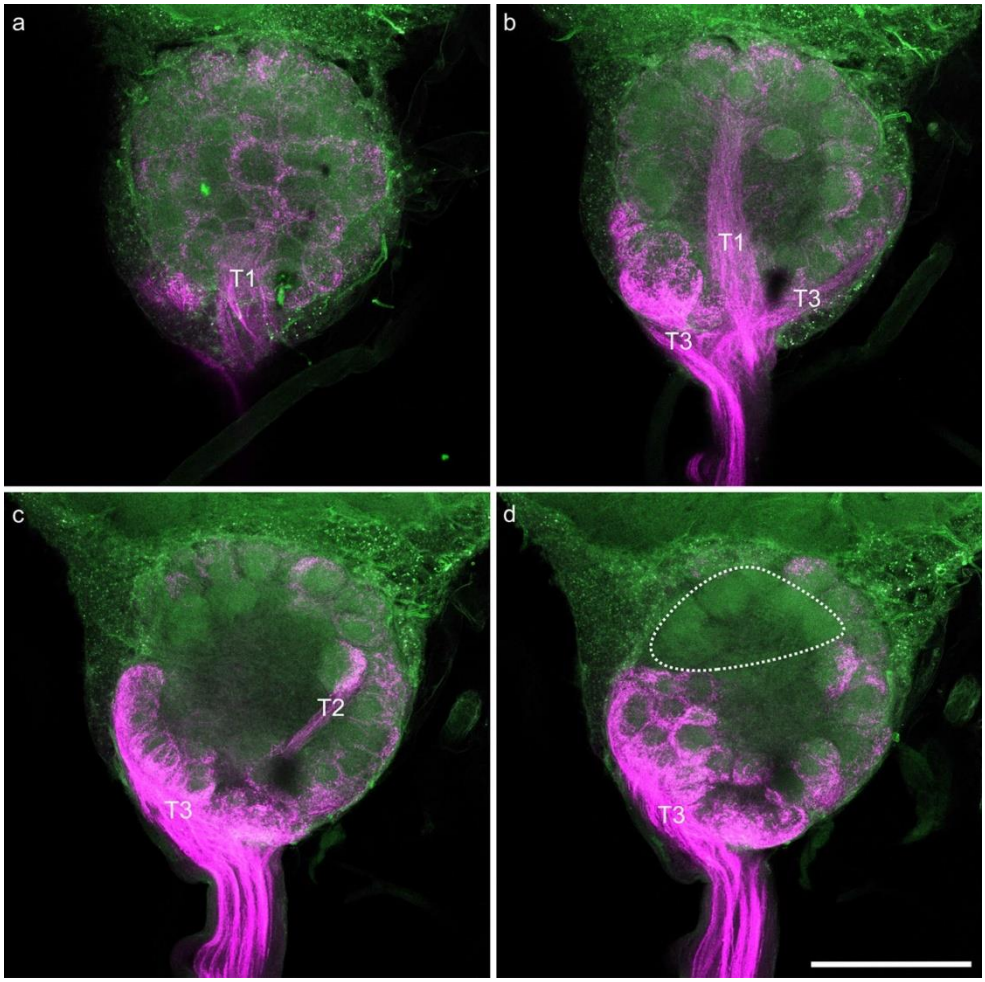

Fig. 3 Images of a representative mass-staining of the axons of olfactory receptor neurons in *Sensilla trichoidea* of segment 5 of the honeybee worker antenna. Axons of olfactory receptor neurons are shown in *magenta*; the background was visualized via autofluorescence of the tissue and is shown in *green*. **a** Z- projection of 20 µm of the dorsal part of the stained antennal lobe; the glomeruli innervated from T1 input tract (*T1*) are clearly visible. **b** Z-projection of 20 µm of the dorsal middle part of the stained antennal lobe. Glomeruli innervated from the T3 input tract (*T3*) and the T1 input tract (*T1*) are clearly visible. **c** Z-projection of 20 µm of the ventral middle part of the stained antennal lobe. Glomeruli innervated from the T3 input tract (*T3)* and the T2 input tract (*T2*) are clearly visible. **d** Z- projection of 20 µm of the ventral part of the stained antennal lobe. Glomeruli innervated from the T3 input tract (*T3*) are clearly visible; the only non-innervated glomeruli (probably associated with T4 input tract) are indicated by the *dashed circle*. *Bar* 200 µm

In this case, a single glomerulus was labeled in the T1 cluster and nine glomeruli were innervated in the T3 cluster. As *S. trichoidea* were also present in the segmental border regions of the antennae enriched with *S. basiconica*, we could not completely exclude that some *S. trichoidea* were also stained in most of the other group stainings of sensilla in the *S. basiconica*-enriched regions. To test this statistically, we calculated the relative innervation frequencies for each specimen. We compared these frequencies with a Friedman ANOVA (P=5.28*10-8, chi2 =36.72, n=15) and observed differences between at least two groups within the data.

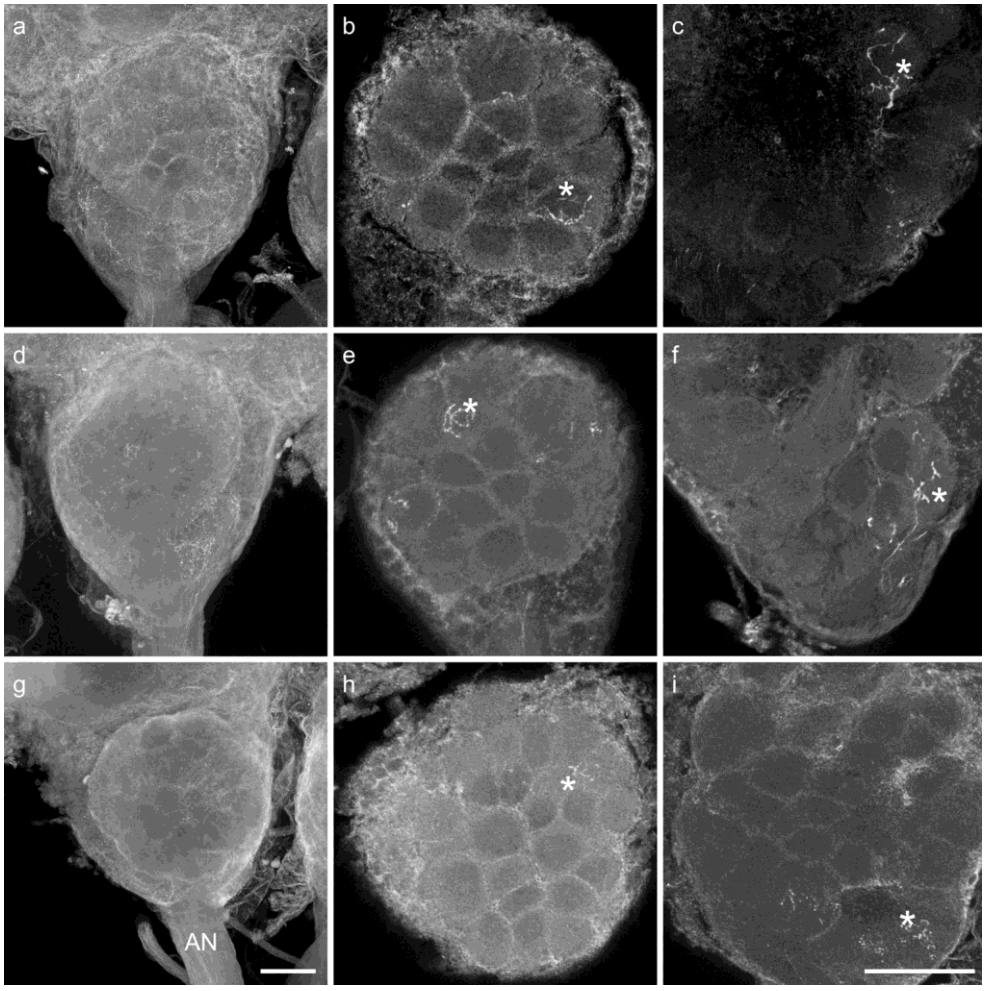

Fig. 4 Confocal image stacks from two antennal lobes after staining of *Sensilla basiconica*-rich regions of the antenna (**a**–**f**) and image stacks of a single-sensillum staining of a *S. basiconicum* (**g**–**i**). Stained glomeruli (*asterisks*). **a**, **d**, **g** Complete stacks of antennal lobes with the antennal nerves (*AN*) and olfactory receptor neuron (OR*N*) arborizations in single glomeruli can hardly be identified in the complete image stacks. *Bar* 100 μm. **b**, **e**, **h** Substacks of the antennal lobes with identifiable ORN innervation in individual glomeruli in the T1 glomerular cluster. **c**, **f**, **i** Substacks of the antennal lobe with identifiable ORN innervation in individual glomeruli in the T3 glomerular cluster region. *Bar* 100 μm

A post-hoc Wilcoxon rank sum test with Bonferroni correction for multiple comparisons revealed T3 as the most frequently stained cluster of glomeruli. Significant differences were found between all clusters, except between T2 and T4 (Fig. 5, exact P-values: T1:T2 4.9 × 10-4 T1:T3 6.3 × 10-4 T1:T4 2.3 × 10-3 T2:T3 9.5 × 10-6 T2:T4 1.0 T3:T4 1.5 × 10-5). As the distribution of glomeruli among the input clusters is not homogenous (Flanagan and Mercer 1989; Galizia et al. 1999), we calculated a hypothetical distribution of glomeruli (T1: 79, T2: 8, T3: 85, T4: 8) by using the total number of glomeruli (180) stained in our experiments. Use of Fisher's exact test between the hypothetical distribution of glomeruli and the observed distribution revealed a significant difference between the two distributions (P=0.032). When we tested only the two major glomerular clusters (T1 and T3), the difference between the expected and the observed distribution had an even higher significance level (P = 0.0076). The projection patterns of sensilla in *S. basiconica*-enriched zones of the antenna, therefore, further indicate that axons of ORNs housed in *S. basiconica* preferentially, although not exclusively, project to the T3 cluster of olfactory glomeruli in the AL of worker bees.

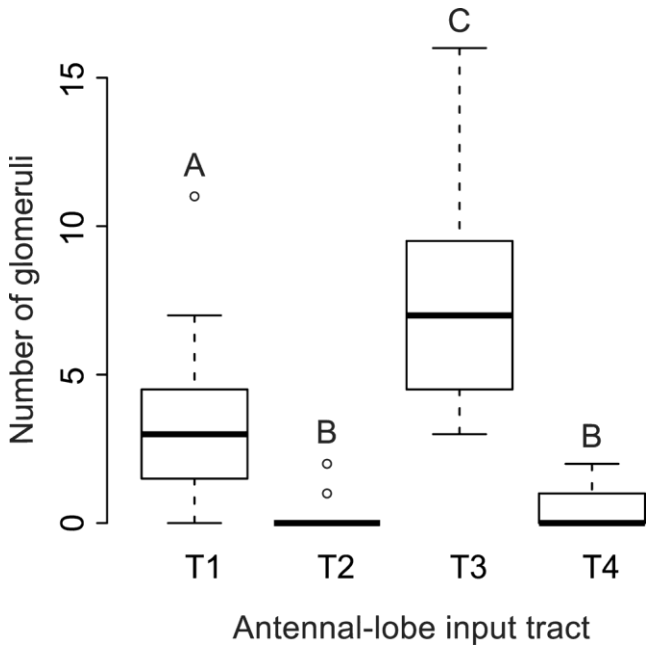

Fig. 5 Numbers of glomeruli containing axonal projections from selective staining of ORNs in multiple *Sensilla basiconica*. Antennal lobe input tract T3 glomeruli were stained significantly more often compared with T1 glomeruli and T1 glomeruli were stained more often than T2 and T4 glomeruli (Friedman ANOVA, post-hoc Wilcoxon rank sum test with Bonferroni correction for multiple comparisons, *n*=15, *A–C* significant differences between clusters)

Number of glomeruli innervated by mALT projection neurons is reduced in honeybee drones

We have shown that ORNs from *S. basiconica* preferentially project to the T3 glomerular cluster in honeybee workers. This glomerular cluster is however reduced in honeybee drones (Nishino et al. 2009) and is associated with the mALT in honeybee workers (Kirschner et al. 2006). Thus, we assumed that the mALT should also be reduced in drones. Anterograde fluorescent staining of the output tracts of the AL did not reveal any obvious differences in tract diameters between the mALT and lALT in confocal images (Fig. 6a). In drones, as in workers, mALT PNs project via the MBs to the LH, whereas lALT PNs project first to the LH and then to the MBs (Fig. 6a). One preparation with a mass-staining of ORN axons in drones was used to reconstruct all glomeruli of the AL (Fig. 6c). This revealed a total of 109 glomeruli (107 glomeruli were counted in a second mass-staining). Specific staining of the mALT was used to determine the number of mALT glomeruli. One backfill of the mALT PNs (Fig. 6b) was reconstructed (Fig. 6d) and revealed a total of 45 glomeruli innervated by mALT PNs. In the remaining successful mALT labelings, a similar or even smaller number of glomeruli was counted (numbers from all successful mALT stainings: specimen 1: 39, specimen 2: 45, specimen 3: 45, specimen 4: 39, specimen 5: 43, n=5). For further calculations, we used the highest number of labeled glomeruli, as some glomeruli might not have been stained by retrogradely labeling the PN arborizations in the AL. In honeybee workers, ~920 PNs innervate ~161 glomeruli (Rybak 2012), resulting in a hypothetical ratio of 5-6 PNs per glomerulus.

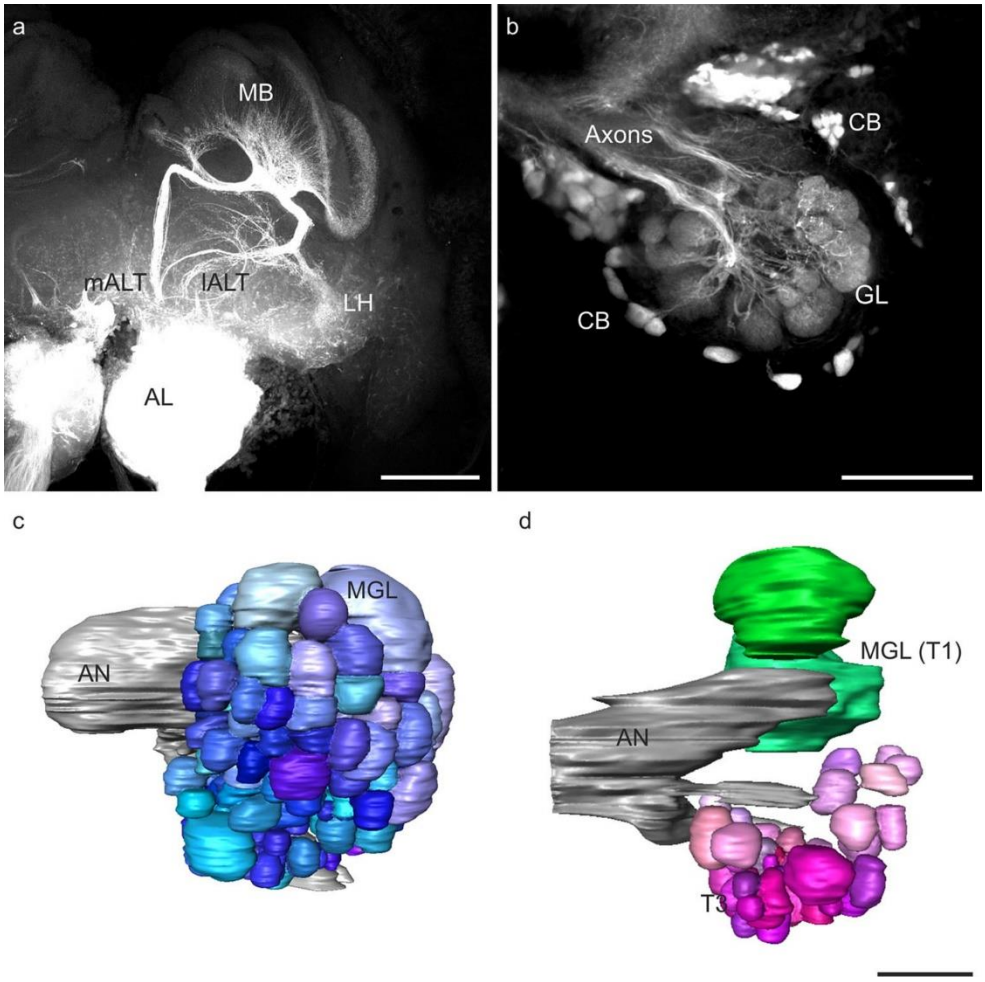

Fig. 6 a Z-projection of a mass-staining of antennal lobe (*AL*) projection neurons in the honeybee drone; the AL, the medial and the lateral AL tract (*mALT*, *lALT*) and arborizations in the mushroom bodies (*MB*) and the lateral horn (*LH*) are visible. *Bar* 200 µm. **b** Z-projection of mALT staining in a honeybee drone. The axons, cell bodies (*CB*) and dendritic glomerular (*GL*) innervation are visible. *Bar* 100 µm. **c** Three-dimensional reconstruction of a drone AL with the antennal nerve (*AN*) after staining of all olfactory receptor neuron axons. Two macroglomeruli (*MGL*) are indicated. **d** Reconstruction of the mALT proportion of glomeruli and two macroglomeruli (*MGL*) within the T1 glomerular cluster (*T1*) as landmarks in a drone AL. The two lALT-associated MGL are shown in *green*, whereas mALT glomeruli in the T3 glomerular cluster (*T3*) are shown in shades of *magenta*. *Bar* 100 µm

No data on the number of PNs in drones are available but by assuming multiple PNs per glomerulus and by considering the fact that only one PN needs to be stained to identify a glomerulus, we assumed that the highest numbers of glomeruli counted in our results were representative of the total number of mALT innervated glomeruli. Subtraction of the average number of maximally counted mALT-associated glomeruli (45) from the total number of 109 glomeruli revealed an estimated number of 64 lALT-associated glomeruli (numbers in Fig. 7). Compared with the situation in females (~161 glomeruli in total; Kirschner et al. 2006), this indicates that most of the glomeruli missing in drones can be assigned to the mALT hemilobe

of the AL. In total, 24 % of the lALT glomeruli and 42 % of the mALT glomeruli were absent in drones compared with workers. Whereas the mALT to lALT ratio of the AL in females is roughly 1:1, only ~39 % of all AL glomeruli in drones were associated with the mALT compared with ~61 % glomeruli associated with the lALT. The combination of our present results with the data from Kirschner et al. (2006) indicates that ORNs from *S. basiconica* in female worker bees preferentially innervate the T3 cluster of glomeruli and that this mALT-innervated cluster of glomeruli is reduced in drones (Fig. 7).

Discussion

This study shows that axons of ORNs from *S. basiconica*, which are absent on drone antennae, mainly project into the T3 cluster of glomeruli in the AL of worker bees (Fig. 7). The T3 cluster of glomeruli has been demonstrated to be reduced in drones (Nishino et al. 2009) and our results reveal that mALT PNs (which, in the female AL, receive input from the T3 cluster) innervate fewer glomeruli in drones compared with workers. This indicates that information from the *S. basiconica* is associated with the mALT pathway in females and further suggests that this part of the mALT pathway is reduced in drones compared with workers. A similar reduction of the mALT- associated portion of AL glomeruli has been shown in males of the ant *Camponotus floridanus* (Zube and Rössler 2008).

General features and sorting of axonal projections of ORNs

The trajectories of individual axons in the mass-stainings indicate that ORN axons are guided to their glomerular targets via a two-step sorting process, one at the segregation into T1- T4 at the entrance of the antennal nerve and a second one at the end of the tracts, just before the axons diverge to their glomerular targets. We show that ORN axons from the various antennal segments run in parallel along the antennal nerve until they reach the AL entrance. This is analogous to the ORN axon-sorting zone in the moth Manduca sexta (Rössler et al. 1999). After the initial rearrangements at the AL entrance, however, axonal projections in the honeybee proceed again in parallel along the tracts (T1-T4) until they reach the glomerular clusters. At these glomerular clusters, ORN axons appear to be rearranged in another crossing pattern until they terminate in distinct layers within individual glomeruli.

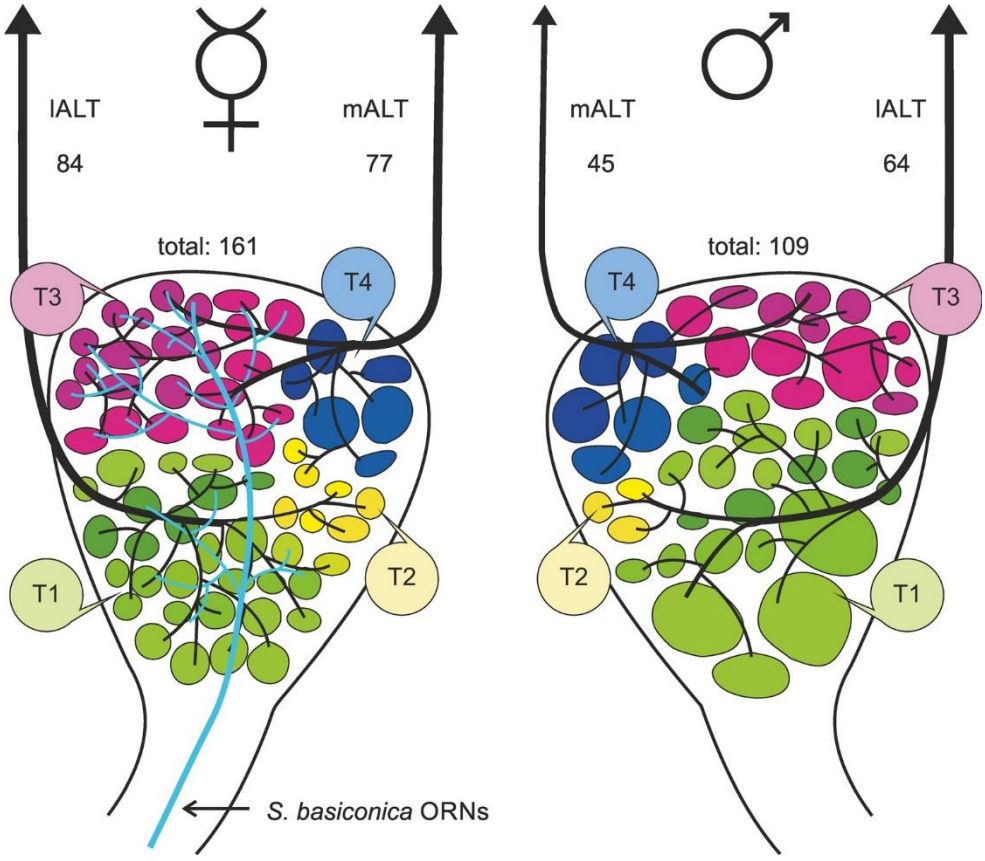

Fig. 7 Representations of a honeybee worker (*left*) and drone (*right*) antennal lobe (AL). Olfactory receptor neuron axons housed in *S. basiconica* are only present in workers and project via the antennal nerve mainly to the T3 glomerular cluster (*T3*) in the AL (*light blue projections*). The T1 glomerular cluster (*T1*) is drawn in *shades of green*, the T2 in *shades of yellow* (*T2*) and the T4 cluster in *shades of blue* (*T4*). The medial AL tract (*mALT*) innervates mainly T3 glomeruli and the lateral AL tract (*lALT*) mainly T1 glomeruli. The T3 glomerular cluster and the mALT output tract are reduced in drones. The estimated numbers of glomeruli innervated by mALT and lALT projection neurons and the total numbers of glomeruli in the female (from Kirschner et al. 2006) and male AL are indicated (ORNs olfactory receptor neurons)

This indicates that the organization in the four olfactory sensory tracts in the honeybee involves a more complex sorting process compared with the single sorting zone at the AL entrance shown in moths (Rössler et al. 1999). This process requires further clarification in future developmental studies. Within individual glomeruli, ORN axons of sensilla from the distal and proximal segments of the antenna terminate in different layers (Fig. 2). These projection patterns indicate a change from the topographic position of sensilla on the antenna to the spatial organization of ORN target fields within single AL glomeruli. In contrast to the ORN projections, PN dendrites might arborize throughout the entire glomerulus (Fig. 2c, d;

see also Müller et al. 2002; Krofczik et al. 2008) indicating that individual PNs receive convergent input from ORNs from widely separated topographical locations that innervate the same glomerulus.

Glomerular targets of ORN axons from *S. trichoidea*

Selective mass-staining of *S. trichoidea* labels bundles of ORN axons projecting to the AL (Fig. 3). The trajectories of ORN axons can be followed along three tracts (T1, T2, T3; Fig. 3). In none of the 13 preparations have we found staining of T4 glomeruli (Fig. 3d). Interestingly, despite a wide distribution of axons in almost all glomeruli of the AL, slightly brighter staining has been detected in T3 glomeruli compared with T1 glomeruli. Whether this is attributable to a higher density and/or brighter labeling of individual axons cannot be resolved with our method. ORN axons from *S. placodea* have also been shown to project into all four glomerular clusters in the honeybee (Kelber et al. 2006). For a more detailed analysis, single fills of *S. trichoidea* ORNs would be necessary. Our staining demonstrates that ORN projections from *S. trichoidea* from only one antennal segment are widely distributed across three glomerular clusters (T1-T3) that contain >95 % of all AL glomeruli in the honeybee (Kirschner et al. 2006). Assuming that this is true for all antennal segments (we found similar results for segments 3, 5, 6, 7 and 8), this implies a high redundancy of the antennal segments within individual glomeruli. This ensures that the antenna efficiently captures sufficient odor molecules for odor identification but rather excludes a topographical resolution of odor reception (e.g., ORNs at the proximal or distal part of the antenna). In contrast to ORNs, PNs have dendritic arborizations across entire glomeruli (Fig. 2c, d). Whether the position of ORN projections in a distinct layer of the glomerulus (and its position on the antenna) in the honeybee has any physiological impact on PN responses, however, needs to be investigated in physiological recordings.

Projection patterns of ORN axons from *S. basiconica*

Mass-staining techniques of hair-like sensilla on entire antennal segments have not allowed us to resolve glomerular cluster preferences of *S. basiconica*-associated ORN axons, as even the *S. basiconica*-rich segment 9 contains over 10× more *S. trichoidea* than *S. basiconica* (Esslen and Kaissling 1976). To increase the proportion of *S. basiconica*-associated ORNs, we selectively stained hair-like sensilla in the distal regions of individual antennal segments

that show a ring-like arrangement of *S. basiconica* (Fig. 1). These experiments revealed that ORN axons from these sensilla terminate to a significantly higher proportion in glomeruli of the T3 cluster of AL glomeruli (Figs. 5, 7). In these staining experiments, we have preferentially aimed to cut *S. basiconica* but because of the small size of these sensilla in the honeybee, staining of *S. trichoidea*, in most cases, cannot be completely excluded. Therefore, we used a statistical method to analyze cluster preference in these selective stainings. Furthermore, the approved staining (by visual inspection) of a single S. basiconicum has shown that nine of the T3 glomeruli and only one T1 glomerulus are innervated thereby supporting the multiple sensilla staining results. The single S. basiconicum stained in our experiments comprised 10 ORNs. This is in agreement with results from histological investigations showing that *S. basiconica* in the honeybee contain 8-12 ORN dendrites (Nishino et al. 2009). In other Hymenoptera, ORN numbers in *S. basiconica* have been demonstrated to range between 30-40 ORNs in wasps (Lacher 1964) and 3-53 ORNs in ants (Kelber et al. 2010). Until now, the notion that *S. basiconica* are indeed olfactory sensilla is mainly based on morphological criteria. Whereas the morphological evidence is strong, however, clear physiological evidence is still lacking. Recordings from *S. basiconica* have only been mentioned as unpublished results in Akers and Getz (1993). Our anterograde staining of the axonal projections of ORNs housed in *S. basiconica* has revealed innervations of relatively high numbers of preferentially T3 glomeruli in the AL. This adds further evidence to the assertion that *S. basiconica* are olfactory sensilla (Slifer and Sekhon 1961; Lacher 1964). Our results suggest that axons of *S. basiconica*-associated ORNs preferentially project to glomeruli of the T3 cluster and only partially to glomeruli of the T1 cluster.

Differences between honeybee drones and workers and potential functional consequences

Interestingly, *S. basiconica* are present in honeybee workers and queens but not in drones (Esslen and Kaissling 1976). The absence of *S. basiconica* in males seems to be a typical feature in Hymenoptera including the honeybee, bumblebees, solitary bees and ants (Ågren 1977; 1978; Wcislo 1995; Ågren and Hallberg 1996; Nakanishi et al. 2009, 2010; Mysore et al. 2010; Nishikawa et al. 2012; Streinzer et al. 2013). Wcislo (1995) argued that drones have reduced the number of a certain type of olfactory sensilla to increase their capabilities for pheromone detection and thereby to increase their probability for encountering a queen faster than other drones. The finding that drones have extremely high numbers of pore plates (*S.*

placodea), which also house the pheromone- specific sensilla (Kaissling and Renner 1968), supports this view. Three of the enlarged glomeruli (macroglomeruli) are located in the T1 cluster of glomeruli (Nishino et al. 2009) and calcium-imaging studies have shown that components of the queen mandibular pheromone are processed in one of these enlarged glomeruli (Sandoz 2006). The processing of pheromone information in macroglomeruli is well known from sex pheromone communication in various species of moths (e.g., Christensen and Hildebrand 1987; Anton and Hansson 1994; Greiner et al. 2004) and has also been shown for an enlarged glomerulus which processes components of the trail pheromone in large leaf-cutting ant workers (Kleineidam et al. 2005; Kelber et al 2009; Kuebler et al 2010). The reduced number of *S. trichoidea* and the complete absence of *S. basiconica* and the associated neuronal pathway in the AL of drones might allow higher capacities for queen-pheromone-specific sensilla and a larger sex-pheromone-processing neuronal circuitry in the AL (Fig. 7).

Female-specific olfactory subsystems and their possible function

We have been able to demonstrate that the reduction of glomeruli in the AL of honeybee drones is higher in the mALT- compared to the lALT-innervated hemilobe of the AL. ORN axons in the glomeruli of the T3 cluster are innervated by mALT PNs in females (Kirschner et al. 2006). This cluster is reduced in drones, whereas the T1 cluster is less reduced compared with that in the female AL. As drones lack *S. basiconica*, the reduction of the mALT-associated parts of the T3 glomeruli is likely to be related to the absence of ORNs from the *S. basiconica*. As three enlarged glomeruli (macroglomeruli, as indicated in Fig. 7) are present in the T1 cluster in drones (Sandoz 2006; Nishino et al. 2009), the slight reduction in the number of T1 glomeruli in drones might favor the macroglomeruli. Several physiological studies, so far, have shown that no part of the honeybee AL and therefore neither the mALT or the lALT, is selectively specialized for either only social or floral odorants (Abel et al. 2001; Brill et al. 2013; Carcaud et al. 2012; Galizia et al. 2012; Krofczik et al. 2008; Müller et al. 2002; Rössler and Brill 2013; Yamagata et al. 2009). However, as honeybees are exposed to an enormous odor space in their natural environments, more odorants, in particular social (colony) cues and pheromones, remain to be tested in more detail and might give further indications concerning selective physiological properties and the molecular receptive range of *S. basiconica* ORNs. The ants *Camponotus floridanus* (Zube and Rössler 2008), *Camponotus japonicus* (Nishikawa et al. 2012) and *A. vollenweideri* (Kelber et al. 2010) have similarly been demonstrated to have a reduced number of glomeruli in males compared with females.

Kelber et al. (2010) investigated projection patterns of *S. trichoidea* and *S. basiconica* ORNs in A. vollenweideri. Here, the ants possess six AL glomerular clusters (T1-T6) and *S. trichoidea* ORNs have been shown to project to all of them. Up to five different glomerular clusters have been found to be innervated by ORNs from a single S. trichoideum. In contrast, *S. basiconica* ORNs only projected to the T6 cluster (Kelber et al. 2010). In honeybee workers, we were able to reveal that *S. basiconica* preferentially project into the T3 cluster. *C. japonicus* ALs comprise seven glomerular clusters (T1-T7) and the glomerular cluster T6 is also worker-specific, similar to the T6 cluster in *A. vollenweideri* (Kelber et al. 2010; Nishikawa et al. 2012). Furthermore, here the T6 output neurons were demonstrated to project to specific subregions within the MBs and the LH and the authors speculate that the input to these glomeruli origins from *S. basiconica*-associated ORNs (Nishikawa et al. 2012). Nishikawa et al. (2012) argued that these brain regions are likely to be involved in social tasks in C. japonicus, as drones do not need to fulfil extensive social duties within the colony. Another important aspect is that in several solitary bee species, the males also lack *S. basiconica* (Ågren 1977, 1978; Ågren and Hallberg 1996; Galvani 2012; Streinzer et al. 2013). In parasitoid wasps, cuticular hydrocarbon pro- files have been shown to vary between closely related species, between sexes and according to the developmental environment (Khidr et al. 2013). Better detection abilities for cuticular hydrocarbons could serve females in kin detection and thus help them to avoid insemination by related males or even by males from other species. Another major distinction between drones and workers in both ants and social bees is that drones do not forage. This implies the involvement of *S. basiconica* in the detection of floral odorants. These studies show that various hymenopteran species possess female-specific olfactory subsystems consisting in specific sensilla, their respective ORNs and downstream odor-processing brain structures. The separation of these subsystems from the sexual isomorphic structures can be more (*A. vollenweideri*, *C. japonicus*) or less (*A. mellifera*) pronounced. Thus, variations in olfactory tasks and structures between males and females might differ across species. Based on these differences described so far with regard to behaviors between male and female honeybees, we conclude that the *S. basiconica* might equally well be specialized for flower odorant detection or the detection of social olfactory cues or might even be generalistic.

Concluding remarks

Honeybee workers possess a specific olfactory subsystem comprising *S. basiconica*, parts of the T3 cluster of glomeruli and a significant proportion of mALT PNs. Drones completely lack this olfactory subsystem (Fig. 7) and, additionally, have far fewer *S. trichoidea*, all features that might favor a more elaborated queen-pheromone-processing system and the associated higher numbers of *S. placodea* present in drones (Brockmann et al. 2006; Kaissling and Renner 1968; Sandoz 2006). At the behavioral level, drones, therefore, are likely to have more limited odor discrimination and recognition abilities compared with females. This limitation is likely to be associated with social (colony) odors and/or floral odors. The adaptation in drones for improved queen-pheromone detection including high numbers of *S. placodea* and pheromone-processing macroglomeruli is likely to increase mating probabilities. Honeybee workers, in contrast, are ex- posed to high selective pressure to identify and locate correct- ly a wide variety of odorants, including floral odorant mixtures, a large variety of pheromones and colony (social) cues. The different types of sensilla and the associated olfactory subsystems of glomeruli and output tracts in the AL appear to be well adapted for these tasks.

Acknowledgments We thank Cornelia Grübel for expert help with tract staining and confocal microscopy, Dirk Ahrens for beekeeping and Johannes Spaethe for fruitful discussions and help with statistics.

References

Abel R, Rybak J, Menzel R (2001) Structure and response patterns of olfactory interneurons in the honeybee, *Apis mellifera*. J Comp Neurol 437:363–383

Ache BW, Young JM (2005) Olfaction: diverse species, conserved principles. Neuron 48:417–430

Ågren L (1977) Flagellar sensilla of some colletidae (Hymenoptera: Apoidea). Int J Insect Morphol Embryol 6:137–146

Ågren L (1978) Flagellar sensilla of two species of *Andrena* (Hymenoptera: Andrenidae). Int J Insect Morphol Embryol 7:73–79 Ågren L, Hallberg E (1996) Flagellar sensilla of bumble bee males (Hymenopera, Apidae, *Bombus*). Apidologie 27:433–444

Ai H, Nishino H, Itoh T (2007) Topographic organization of sensory afferents of Johnston's organ in the honeybee brain. J Comp Neurol 502:1030–1046

Akers RP, Getz WM (1993) Response of olfactory receptor neurons in honeybees to odorants and their binary mixtures. J Comp Physiol A 173:169–185

Anton S, Hansson BS (1994) Central processing of sex pheromone, host odour, and oviposition deterrent information by interneurons in the antennal lobe of female *Spodoptera littoralis* (Lepidoptera: Noctuidae). J Comp Neurol 350:199–214

Anton S, Homberg U (1999) Antennal lobe structure. In: Hansson B (ed) Insect olfaction. Springer, Berlin, pp 97–124

Arnold G, Masson C, Budharugsa S (1985) Comparative study of the antennal lobes and their afferent pathway in the worker bee and the drone (*Apis mellifera*). Cell Tissue Res 242:2379–2383

Brill MF, Rosenbaum T, Reus I, Kleineidam CJ, Nawrot MP, Rossler W (2013) Parallel processing via a dual olfactory pathway in the honeybee. J Neurosci 33:2443–2456

Brockmann A, Brückner D (1995) Projection pattern of poreplate sensory neurones in honey bee worker, *Apis mellifera* L. (Hymenoptera: Apidae). Int J Insect Morphol Embryol 24:405–411

Brockmann A, Dietz D, Spaethe J, Tautz J (2006) Beyond 9-ODA: sex pheromone communication in the European honey bee *Apis mellifera* L. J Chem Ecol 32:657–667

Carcaud J, Hill T, Giurfa M, Sandoz J-C (2012) Differential coding by two olfactory subsystems in the honeybee brain. J Neurophysiol 108:1106–1121

Cervantes-Sandoval I, Martin-Peña A, Berry JA, Davis RL (2013) System-like consolidation of olfactory memories in *Drosophila*. J Neurosci 33:9846–9854

Christensen TA, Hildebrand JG (1987) Male-specific, sex pheromone- selective projection neurons in the antennal lobes of the moth, *Manduca sexta*. J Comp Physiol A 160:553–569

Dacks AM, Nighorn AJ (2011) The organization of the antennal lobe correlates not only with phylogenetic relationship, but also life history: a basal hymenopteran as exemplar. Chem Senses 36:209–220

Davis RL (2005) Olfactory memory formation in *Drosophila*: from molecular to systems neuroscience. Annu Rev Neurosci 28:275–302

Esslen J, Kaissling K (1976) Zahl und Verteilung antennaler Sensillen bei der Honigbiene *Apis mellifera* L. Zoomorphology 83:227–251

Flanagan D, Mercer A (1989) An atlas and 3-D reconstruction of the antennal lobes in the worker honey bee, *Apis mellifera* L. (Hymenoptera: Apidae). Int J Insect Morphol Embryol 18:145–159

Galizia CG, Franke T, Menzel R, Sandoz J-C (2012) Optical imaging of concealed brain activity using a gold mirror in honeybees. J Insect Physiol 58:743–749

Galizia CG, McIlwrath SL, Menzel R (1999) A digital three-dimensional atlas of the honeybee antennal lobe based on optical sections acquired by confocal microscopy. Cell Tissue Res 295:383–394

Galizia CG, Rössler W (2010) Parallel olfactory systems in insects: anatomy and function. Annu Rev Entomol 55:399–420

Galvani G (2012) Distribution and morphometric studies of flagellar sensilla in Emphorini bees (Hymenoptera, Apoidea). Micron 43: 673–687

Gary NE (1962) Chemical mating attractants in the queen honey bee. Science 136:773–774

Gerber B, Tanimoto H, Heisenberg M (2004) An engram found? Evaluating the evidence from fruit flies. Curr Opin Neurobiol 14: 737–744

Getz WM, Akers RP (1993) Olfactory response characteristics and tuning structure of placodes in the honey bee *Apis mellifera* L. Apidologie 24:195–217

Giurfa M (2007) Behavioral and neural analysis of associative learning in the honeybee: a taste from the magic well. J Comp Physiol A 193: 801–824

Greiner B, Gadenne C, Anton S (2004) Three-dimensional antennal lobe atlas of the male moth, *Agrotis ipsilon*: a tool to study structure- function correlation. J Comp Neurol 475:202–210

Groh C, Rössler W (2008) Caste-specific postembryonic development of primary and secondary olfactory centers in the female honeybee brain. Arthropod Struct Dev 37:459–468

Hildebrand JG, Shepherd GM (1997) Mechanisms of olfactory discrim- ination: converging evidence for common principles across phyla. Annu Rev Neurosci 20:595–631

Hourcade B, Muenz TS, Sandoz J-C, Rössler W, Devaud J-M (2010) Long-term memory leads to synaptic reorganization in the mushroom bodies: a memory trace in the insect brain? J Neurosci 30:6461–6465

Ito K, Shinomiya K, Ito M, Armstrong JD, Boyan G, Hartenstein V, Harzsch S, Heisenberg M, Homberg U, Jenett A, Keshishian H, Restifo LL, Rössler W, Simpson JH, Strausfeld NJ,

Strauss R, Vosshall LB, Insect Brain Name Working Group (2014) A systematic nomenclature for the insect brain. Neuron 81:755–765

Kaissling KE, Renner M (1968) Antennal receptors for queen substance and scent gland odour in honeybees. Z Vergl Physiol 59:357–361

Kelber C, Rössler W, Kleineidam CJ (2006) Multiple olfactory receptor neurons and their axonal projections in the antennal lobe of the honeybee *Apis mellifera*. J Comp Neurol 496:395–405

Kelber C, Rössler W, Roces F, Kleineidam CJ (2009) The antennal lobes of fungus-growing ants (Attini): neuroanatomical traits and evolutionary trends. Brain Behav Evol 73:273–284

Kelber C, Rössler W, Kleineidam CJ (2010) Phenotypic plasticity in number of glomeruli and sensory innervation of the antennal lobe in leaf- cutting ant workers (*A. vollenweideri*). Dev Neurobiol 70:222–234

Khidr SK, Linforth RST, Hardy ICW (2013) Genetic and environmental influences on the cuticular hydrocarbon profiles of *Goniozus* wasps. Entomol Exp Appl 147:175–185

Kirschner S, Kleineidam CJ, Zube C, Rybak J, Grünewald B, Rössler W (2006) Dual olfactory pathway in the honeybee, *Apis mellifera*. J Comp Neurol 499:933–952

Kleineidam CJ, Obermayer M, Halbich W, Rössler W (2005) A macroglomerulus in the antennal lobe of leaf-cutting ant workers and its possible functional significance. Chem Senses 30:383–392

Krofczik S, Menzel R, Nawrot MP (2008) Rapid odor processing in the honeybee antennal lobe network. Front Comput Neurosci 2:9

Kuebler LS, Kelber C, Kleineidam CJ (2010) Distinct antennal lobe phenotypes in the leaf-cutting ant (*Atta vollenweideri*). J Comp Neurol 518:352–365

Lacher V (1964) Elektrophysiologische Untersuchungen an einzelnen Rezeptoren für Geruch, Kohlendioxyd, Luftfeuchtigkeit und Tempratur auf den Antennen der Arbeitsbiene und der Drohne (*Apis mellifica* L.). Z Vergl Physiol 48:587–623

Le Conte Y, Hefetz A (2008) Primer pheromones in social Hymenoptera. Annu Rev Entomol 53:523–542

Maronde U (1991) Common projection areas of antennal and visual pathways in the honeybee brain, *Apis mellifera*. J Comp Neurol 309:328–340

Martin JP, Beyerlein A, Dacks AM, Reisenman CE, Riffell JA, Lei H, Hildebrand JG (2011) The neurobiology of insect olfaction: sensory processing in a comparative context. Prog Neurobiol 95:1–21

Mobbs PG (1982) The brain of the honeybee *Apis mellifera*. I. The connections and spatial organization of the mushroom bodies. Proc R Soc Lond [Biol] 298:309–354

Müller D, Abel R, Brandt R, Zöckler M, Menzel R (2002) Differential parallel processing of olfactory information in the honeybee, *Apis mellifera* L. J Comp Physiol A 188:359–370

Mysore K, Shyamala BV, Rodrigues V (2010) Morphological and devel- opmental analysis of peripheral antennal chemosensory sen- silla and central olfactory glomeruli in worker castes of *Camponotus compressus* (Fabricius, 1787). Arthropod Struct Dev 39:310–321

Nakanishi A, Nishino H, Watanabe H, Yokohari F, Nishikawa M (2009) Sex-specific antennal sensory system in the ant *Camponotus japonicus*: structure and distribution of sensilla on the flagellum. Cell Tissue Res 338:79–97

Nakanishi A, Nishino H, Watanabe H, Yokohari F, Nishikawa M (2010) Sex-specific antennal sensory system in the ant *Camponotus japonicus*: glomerular organizations of antennal lobes. J Comp Neurol 518:2186–2201

Nishikawa M, Watanabe H, Yokohari F (2012) Higher brain centers for social tasks in worker ants, *Camponotus japonicus*. J Comp Neurol 520:1584–1598

Nishino H, Nishikawa M, Mizunami M, Yokohari F (2009) Functional and topographic segregation of glomeruli revealed by local staining of antennal sensory neurons in the honeybee *Apis mellifera*. J Comp Neurol 515:161–180

Palmer MJ, Moffat C, Saranzewa N, Harvey J, Wright GA, Connolly CN (2013) Cholinergic pesticides cause mushroom body neuronal inactivation in honeybees. Nat Commun 4:1634

Rössler W, Brill MF (2013) Parallel processing in the honeybee olfactory pathway: structure, function, and evolution. J Comp Physiol A 199: 981–996

Rössler W, Zube C (2011) Dual olfactory pathway in Hymenoptera: evolutionary insights from comparative studies. Arthropod Struct Dev 40:349–357

Rössler W, Oland LA, Higgins MR, Hildebrand JG, Tolbert LP (1999) Development of a glia-rich axon-sorting zone in the olfactory path- way of the moth *Manduca sexta*. J Neurosci 19:9865–9877

Rybak J (2012) The digital honey bee brain atlas. In: Eisenhardt D, Giurfa M, Galizia CG (eds) Honeybee neurobiology and behavior— a tribute to Randolf Menzel. Springer, The Netherlands, pp 125–140

Sandoz J-C (2006) Odour-evoked responses to queen pheromone com- ponents and to plant odours using optical imaging in the antennal lobe of the honey bee drone *Apis mellifera* L. J Exp Biol 209:3587– 3598

Slessor KN, Winston ML, Le Conte Y (2005) Pheromone communication in the honeybee (Apis mellifera L.). J Chem Ecol 31:2731–2745 Slifer EH, Sekhon SS (1961) Fine structure of the sense organs on the antennal flagellum of the honey bee, *Apis mellifera* Linnaeus. J Morphol 109:351–381

Streinzer M, Kelber C, Pfabigan S, Kleineidam CJ, Spaethe J (2013) Sexual dimorphism in the olfactory system of a solitary and a eusocial bee species. J Comp Neurol 521:2742–2755

Touhara K, Vosshall LB (2009) Sensing odorants and pheromones with chemosensory receptors. Annu Rev Physiol 71:307–332

Wanner KW, Nichols AS, Walden KKO, Brockmann A, Luetje CW, Robertson HM (2007) A honey bee odorant receptor for the queen substance 9-oxo-2-decenoic acid. Proc Natl Acad Sci U S A 104: 14383–14388

Wcislo WT (1995) Sensilla numbers and antennal morphology of parasitic and non-parasitic bees (Hymenoptera: Apoidea). Int J Insect Morphol Embryol 24:63–81

Yamagata N, Schmuker M, Szyszka P, Mizunami M, Menzel R (2009) Differential odor processing in two olfactory pathways in the honeybee. Front Syst Neurosci 3:16

Zube C, Rössler W (2008) Caste- and sex-specific adaptations within the olfactory pathway in the brain of the ant Camponotus floridanus. Arthropod Struct Dev 37:469–479

Zube C, Kleineidam CJ, Kirschner S, Neef J, Rössler W (2008) Organization of the olfactory pathway and odor processing in the antennal lobe of the ant *Camponotus floridanus*. J Comp Neurol 506:425–441

Manuscript II: Complex and sparse coding along the honeybee's olfactory pathway: potential contribution of ionic currents of medial and lateral projection neurons and Kenyon cells

Jan Kropf, Wolfgang Rössler

Abstract

In the olfactory system of the honeybee an intriguing pattern of convergence and divergence between the individual neuronal types within the olfactory pathway exists: approximately 60.000 olfactory sensory neurons (OSN) convey olfactory information on 900 projection neurons (PN) in the antennal lobe. In order to transmit all information from the OSNs reliably, PNs need to employ relatively high spiking frequencies. PNs then project via a dual olfactory pathway to the mushroom bodies (MB) .This pathway comprises two tracts, the medial (mALT) and the lateral antennal lobe tract (lALT). Although both tracts receive input from different OSNs, they were shown to transmit information from a similar set of odors, yet with slight differences. LALT PNs respond faster but mALT PNs are more odor specific (Brill et al. 2013). In the MBs, PNs form synaptic complexes with ~184.000 Kenyon cells (KC), the MB intrinsic neurons. Generally, insect MBs are regarded as the centers for sensory integration and learning and memory. As KCs drastically outnumber PNs, they are likely to employ much lower spiking frequencies than PNs. Indeed, they were shown to respond in a very phasic and sparse fashion to odor stimulation using Ca^{2+}-imaging (Szyszka et al. 2005). In the present study, we aim to identify the neuronal properties leading to the differences between m- and lALT PNs and KCs. In PNs, we could identify a set of Na^+ currents and diverse K^+ currents depending on voltage and Na^+ or Ca^{2+}relatively similar to currents observed in locust DUM (dorsal unpaired median) neurons that support spiking activity (Wicher et al. 2006). Conversely in KCs, we found very prominent K^+ currents, which are likely to contribute to the sparse response fashion observed in KCs.

Introduction

Olfaction is a crucial sense for honeybees needed for the location and evaluation of food sources, for communication with other colony members, for the identification of nestmates and non-nestmates, and for finding mating partners (reviewed for example by Slessor et al. 2005). The olfactory system in honeybees has been under investigation for at least 50 years, and many details of its anatomy and physiology have been worked out (reviewed for example by Galizia and Rössler 2010 and Sandoz 2011).

Odorants are received by olfactory receptors, which are located in olfactory sensory neurons (OSNs) of different types of sensilla on the antennae. Approximately 60.000 OSNs project their axons to the antennal lobe (AL) (Esslen and Kaissling 1976). In the AL, they form synapses with projection neurons (PNs) and local interneurons (LNs). The OSN axons form two bundles running along the antenna to the AL entrance. Here, they diverge into four distinct tracts (T1-T4) that proceed further into the AL (Kirschner et al. 2006). In the AL, OSN axons synapsing on PNs and LNs form spheroidal structures commonly termed glomeruli (Hildebrand and Shepherd 1997). Each glomerulus was shown to receive information from OSNs expressing the same odorant receptor gene (Gao et al. 2000; Vosshall et al. 2000). This principle is broadly accepted for vertebrates and invertebrates (reviewed by Ache and Young 2005) and receives support from studies which analyzed the number of olfactory receptor genes (OR) and of olfactory glomeruli (honeybee: 163 ORs Robertson and Wanner 2006; 163 glomeruli Kirschner et al. 2006). Accordingly, the glomeruli represent functional units of the AL and encode odor information in a combinatorial fashion, which, theoretically, allows for coding almost infinite numbers and combinations of odors (for example Galizia et al. 1999; Sachse et al. 1999). Numerous synaptic interactions across glomeruli can then influence the separation of odors by the array of glomeruli (Deisig et al. 2010). This interaction is likely mediated by LNs (~3.000-4.000 around the honeybee AL; reviewed by Galizia and Rössler 2010; Galizia and Kreissl 2012), which were shown to have a variety of anatomical features and response properties (Galizia and Kimmerle 2004; Meyer et al. 2013). The exact synaptic connectivity in the honeybee AL between OSNs, LNs and PNs is not known. There are three tracts of PNs, which convey the information to the mushroom bodies (MBs) and the lateral horn (LH) in the honeybee: the medial antennal lobe tract (mALT), the lateral antennal lobe tract (lALT), and the medio-lateral antennal lobe tract (mlALT) (after the unified nomenclature of Ito et al. 2014, the ALTs were formerly termed antenno-cerebral tract ACT; e.g. Kirschner et al. 2006 and antenno-protocerebral tract APT; e.g. Galizia and Rössler 2010). The mALT exits the AL

medially and proceeds medially from the vertical lobe to the MBs and finally reaches the LH, whereas the lALT runs in the opposite direction and reaches the LH before the MBs. Both m- and lALT PNs have axonal arborizations in the LH and the MBs, where they form distinct synaptic complexes, so called microglomeruli, with the MB intrinsic neurons, the Kenyon cells (KC) (Homberg et al. 1989; Groh et al. 2004). PNs belonging to the mlALT do not innervate the MBs and project directly to the LH. MlALT PNs and lALT PNs can be found in various insects including *Drosophila melanogaster* (Tanaka et al. 2012) and *Manduca sexta* (Homberg et al. 1988). The two parallel tracts of PNs projecting in opposing directions to the MBs and LH form a dual olfactory pathway, which represents a typical feature in Hymenoptera (Rössler and Zube 2011). The detailed function of the dual olfactory pathway still remains uncertain. However, the baseline is that both tracts seem to convey information about largely similar odors (Müller et al. 2002; Krofczik et al. 2008; Carcaud et al. 2012; Galizia et al. 2012; Brill et al. 2013). Individual mALT PNs were shown to be more narrowly tuned than lALT PNs with a broad response spectrum. Furthermore, the mean spontaneous as well as the response action potential (AP) frequencies are higher in lALT than in mALT PNs, and lALT PNs, on average, have shorter response latencies (Brill et al. 2013). Differences in odor response complexity between both tracts are not completely consistent, as both tracts exhibit tonic response patterns, phasic-tonic response patterns, burst with a post burst hyperpolarization phase response patterns and even inhibitory responses (Abel et al. 2001; Müller et al. 2002). The reason for this complexity of response patterns may be that a relatively small number of PNs needs to convey a lot of information (bottleneck). Approximately 60.000 OSNs (Esslen and Kaissling 1976) synapse on only ~900 PNs (Rybak 2012), which have to transmit the odor information reliably to the KCs. In contrast to PNs, KCs are far more numerous (~184.000, after Witthoeft 1967 combined with Strausfeld 2002). Thus KCs should not employ such complex response dynamics and, indeed, KCs in honeybees were shown to exhibit temporal as well as spatial sparse coding of information (Szyzska et al. 2005). Locust KCs also employ strict temporal sparse coding, *Drosophila* KCs have a slightly less pronounced sparse code, but are also silent until stimulation (Turner et al. 2008; Murthy and Turner 2013). From the calyces of the MBs, KC axons project further via the peduncle to the vertical lobe, where they form synapses with the extrinsic mushroom body neurons (EN) (Rybak and Menzel 1993). Again, KCs are far more numerous than ENs (~400 after Rybak and Menzel 1993). In the same line, ENs have spontaneous and odor response spiking frequencies, which are even slightly higher than PN response frequencies (Strube-Bloss et al. 2011; 2012; Brill et al. 2013). In summary, the number of neurons per population and the connectivity between OSNs, PNs, KCs and ENs demands

that PNs and ENs have relatively high spiking frequencies with complex odor coding properties, whereas KCs have to employ a sparse information code. The differences in information coding between these neuronal populations may be caused by the sensory input, the synaptic connections between them, by intrinsic properties of these neurons, or by a combination of these parameters.

Intrinsic properties of PNs and KCs have been mostly studied in primary cell cultures of honeybee neurons. PNs were shown to possess Na^+, K^+ and Ca^{2+} currents, which are commonly known to be involved in AP generation and to contain Ca^{2+} dependent K^+ channels providing an intrinsic self-inhibitory mechanism (Grünewald 2003; Perk and Mercer 2005). The whole cell currents of KCs in primary cultures differ drastically from the ones found in PNs: KCs have very prominent A-type K^+ channels, which are likely to be involved in sparse coding (Schäfer et al. 1994; Pelz et al. 1999; Grünewald 2003; Wüstenberg et al. 2004). However, the studies on KCs are not completely consistent. In some studies Ca^{2+} dependent K^+ currents, which cause an N-shape in the current voltage (IV) plot, were observed (*in vitro*: Schäfer et al. 1994; *in situ* in isolated brain preparations: Palmer et al. 2013). In contrast, Grünewald (2003) did not find an N-shaped I-V plot in pupal honeybee KCs maintained in primary cultures. Due to these differences found between different cell-cultured KCs together with the fact that m- and lALT PNs could not be distinguished in primary cultures, we set out to perform *in situ* whole cell recordings from honeybee mALT PNs, lALT PNs and KCs using a novel head preparation and combined staining and recording techniques.

In the present study, we aim to identify neuronal properties supporting the complex odor response patterns of PNs and the sparse coding properties of KCs. Additionally we set out to investigate whether the differences in AP frequencies and latencies between m- and lALT (Brill et al. 2013) are caused by differences in intrinsic properties or different synaptic interactions of the two populations of PNs.

Material and methods

Animals

All honeybees (*Apis mellifera carnica*) were taken from colonies of our departmental bee station at the University of Würzburg. Only adult bees were used, but we did not control for the exact age of the bees. The bees were cooled in a refrigerator (4°C) and harnessed in custom-built plastic holders. Immediately after the bees had recovered from cooling, they were fed with a ~50% sucrose solution in aqua dest.

Pre-experimental PN staining

To distinguish PN cell bodies from LN cell bodies in the AL, we stained PNs 10 to 20 hours before recording. A small window above the MB calyces was cut into the cuticle, and glands and trachea covering the calyces were removed manually using fine forceps. Thin-walled glass micropipettes (1B100F-3, WPI, Sarasota, USA) were pulled with a Zeitz Puller (Zeitz-Instruments, Martinsried, Germany) and coated with Microruby™ (tetramethylrhodamine dextran with biotin, 3.000 MW, lysine-fixable, D-7162; Molecular Probes, Eugene, Oregon, USA) dissolved (3-5%) in aqua dest. The dye loaded micropipettes were used to punctuate both calyces of both MBs, to have the dye subsequently taken up by the neurons. After the staining procedure, a two component tissue glue (Kwik-Sil™ World Precision Instruments, Sarasota, USA) was used to seal the window and to prevent dessication of the brain.

Preparation for lALT PN and KC recordings

The mandibles were put into gently heated dental wax (Flexaponal white, Dentaurum, Ispringen, Germany) in an upright fashion to avoid movements. We used a soldering iron with a fine soldering head controlled with an adjustable power source (ouput: ~3.2V, 1.5A, Voltcraft PS-1152A, Conrad Electronics, Hirschau, Germany) to melt the dental wax. Once the mandibles were covered with wax, the preparation was put in a refrigerator for approximately 10 seconds to harden the dental wax. All cuticle covering the ALs and the MBs as well as the Kwik-Sil™ was removed. The cuticle below the brain as well as the eyes were left intact to stabilize the brain. All glands and trachea covering the brain were manually removed using fine forceps. Then, the heads were severed from the thorax. The brain was fixed in the recording chamber (RC-22C, Warner Instruments, LLC, Hamden, Connecticut, USA) by pressing the

hardened dental wax surrounding the mandibles into slightly softer peripheral wax (Surgident, Heraeus Kulzer GmbH, Hanau, Germany) in the recording chamber. As the head was orientated in an upright fashion, this preparation allowed access to mALT and KC cell bodies. An Olympus imaging system (200×-400×, upright microscope: BX51WI, filter set: excitation 560/40 DCTX 590 emission 610 LP, objective: XLUMP, NA 0.95, light source: MT20, software: Cell R v2.5, all Olympus Imaging Europa, camera: model 8484-03G Hamamatsu Photonics) was used to identify stained neuronal cell bodies. The only neurons connecting the MBs with the AL are PNs, therefore stained cell bodies in the AL could be clearly identified as PNs. KC cell bodies are numerous and can be easily identified. Differentiation between clawed and spiny KCs is possible according to their anatomical location. Only type II (clawed) KCs with cell bodies outside the calyx cup (Strausfeld 2002) were recorded in our experiments.

Preparation for mALT PN recordings

The cell bodies of mALT PNs are located on the dorsal site of the AL, therefore slight adjustments of the preparation were necessary. The complete preparation was turned upside down, and the mandibles were fixed with dental wax in an approximate angle of 45°. The proboscis and the cuticle beneath the brain were removed using microscissors. Glands, muscles and tracheae covering the brain were gently removed. Additionally, the subesophageal ganglion (SEG) was removed by pushing it in the direction of the MBs. Afterwards, the brain was mounted in the recording chamber as described above. Two large mALT PN cell body clusters were visible and accessible after this procedure.

Patch Clamp recordings

Patch clamp electrodes were pulled from thick-walled borosilicate glass with filament (GB150F-8P, Science Products, Hofheim, Germany) with a Zeitz Puller. Electrodes had tip resistances of 4-6 MOhm (PN-recording) and 6-8 MOhm (KC-recording) measured in the extracellular solution. The patch clamp electrodes were moved to the cell bodies by using an electrical micormanipulator (Junior Unit, Luigs & Neumann, Ratingen, Germany). We used an Axopatch 200b amplifier, a Digidata 1440A acquisition board and the ClampEx software (all Molecular devices, Sunnyvale, California, USA). The extracellular solution comprised in mmol: NaCl (140), KCl (5), $MgCl_2$ (1), $CaCl_2$ (2.5), $NaHCO_3$ (4), NaH_2PO_4 (1.2), HEPES (6) and glucose (14), adjusted to pH 7.4 with NaOH. The intracellular solution contained in mmol:

K- gluconate (110), HEPES (25), KCl (10), $MgCl_2$ (5), Mg-ATP (3), Na-GTP (0.5) and EGTA (0.5), pH 7.2. Currents were isolated by blocking Na^+ currents and Na^+ dependent currents with Tetrodotoxin (TTX, 10^{-7} mmol) and by blocking Ca^{2+} currents and Ca^{2+} dependent currents with $CdCl_2$ ($5x10^{-5}$ mmol) in the extracellular solution. For staining of neurons via the patch-clamp electrode, 0.5-1 % Lucifer Yellow (L0259, Sigma-Aldrich Chemie, Steinheim, Germany) was added to the intracellular solution. All chemicals were purchased at Sigma-Aldrich Chemie Gmbh (Munich, Germany) or at Carl Roth GmbH + Co. KG (Karlsruhe, Germany).

Data analysis and statistics

All patch clamp raw data traces were analyzed with the "statistics" function implemented in pClamp (Molecular devices, Sunnyvale, California, USA). The positive and negative maximal values at the transient peak and during the persistent phase were determined. Membrane voltages were directly measured with the digital meter on the amplifier and corrected by subtracting the liquid junction potential of our solutions (-13mV). Cell capacitances were obtained with the electrode test function implemented in ClampEx. The obtained data sets were further processed with Excel (Microsoft Corporation Redmond, Washington, USA), I-V plots were also generated with Excel. All statistics as well as box plots were made with R (R Foundation for Statistical Computing, Vienna, Austria). Conductance values for a specific ion were calculated by using the equilibrium potentials of Na^+ (143.26 mV), Ca^{2+} (23.15mV) and K^+ (-78.1mV) ions for our given intra-and extracellular solutions. The conductance/maximal conductance values (G/Gmax) were plotted as a function of the increasing voltage and were fitted with a first-order Boltzmann fit. G/Gmax plots, fitting of G/Gmax plots with first-order Boltzman equations and the determination of half maximal activation voltages was done with OriginLab (OriginLab Corporation, Northampton, Massachusetts, USA).

Neuranatomical analyses and image composition

Both, brains stained with MicrorubyTM and brains with single cell staining with lucifer yellow (L0259, Sigma-Aldrich Chemie Gmbh, Munich, Germany) were put into fixative solution (4 % formaldehyde) overnight and rinsed five times for 10 min in PBS (phosphate-buffered saline, pH 7.2) the next day. Afterwards, the brains were dehydrated in an ascending ethanol series (50, 70, 90, 95, 2× 100 %, each 10 min) and cleared in methyl salicylate (M2047, Sigma-Aldrich

Chemie Gmbh, Munich, Germany). The brains were then mounted in methyl salicyate in custom made microscopy slides and scanned with a confocal laser-scanning microscope (Leica TCS SP2; Leica Microsystems, Wetzlar, Germany). Further on, the image stacks were processed with ImageJ 1.46j (Wayne Rasband, National Institutes of Health, Befesta, Md., USA) to using the Z-project function. All images were finally arranged with CorelDrawX6 (Corel, Ottawa, ON, Canada).

Results

Pre-experimental identification of neurons

One important prerequisite for selectively recording from l- or mALT PNs was the identification of the neuronal cell bodies in the AL tissue, as they are embedded in many cell bodies of AL local interneurons. The injection of dextran coupled dyes into the brain leads to the uptake of the dye in neurons with either pre- or post-synaptic profiles in the area where the dye was injected. The dye then is transported retrogradely as well as anterogradely along the respective neurites.

Confocal light microscopic analyses after the injection of Microruby^{TM} into the MBs, revealed that the dye was taken up by KCs, visual, gustatory and olfactory PNs. In a broad overview, KCs proceeding from the MBs to the vertical lobe, visual commisures connecting the optic lobes, gustatory PNs ascending from the SEG to the MBs and olfactory PNs ascending from the AL to the MBs can be distinguished (Fig. 1a).

However, the only cells with axonal arborizations in the MBs and cell bodies in the AL are olfactory PNs. Therefore, cell bodies in the AL stained after dye injection into the MBs could be identified as PNs. By focusing on the AL, the two tracts leaving the AL could be easily identified (Fig. 1c). PN ramifications in the glomeruli as well as stained cell bodies clustered around the AL are visible (Fig. 1b, c). AL reconstructions from Kirschner et al. (2006) show the location of the PN cell-body clusters color coded in red and green for the m- and the lALT (Fig. 1d). By comparing these with the Microruby^{TM} stainings of both tracts, it was possible to identify the individual soma clusters (Fig. 1b, c, d). These cell bodies can also be identified *in situ* using a fluorescence light microscope (Fig. 2a, b). By comparing the location of the cell bodies with the reconstructions from Kirschner et al. (2006), it was possible to distinguish between m- and lALT cell bodies *in situ*. To avoid false identification of a cell body, mALT PNs were only recorded when the whole brain was turned upside down and the SEG was cut away. The only region where mALT cell bodies can be approached with a patch pipette in an upright preparation is lateral to the region where the antennal nerve enters the AL (Fig. 1d). This part of the AL was excluded from recording to avoid the wrong tract association of a cell body. In contrast, KCs are far more numerous than PNs, and their cell bodies can be found all over the MBs. We recorded exclusively from Class II KCs, also termed clawed KCs, which are located around the outer border of the MB calyx, outside the calyx cups (Strausfeld 2002).

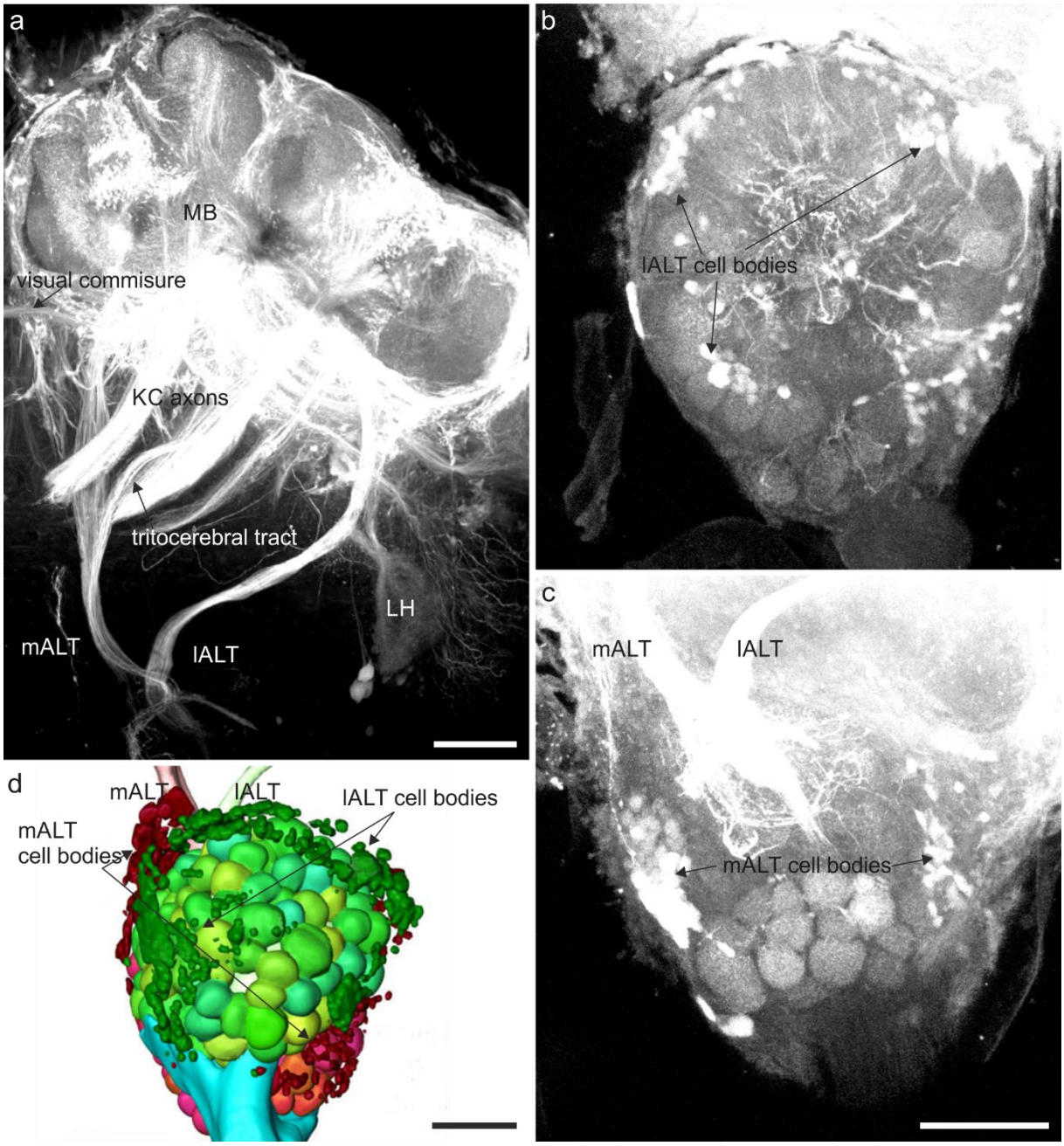

Fig. 1 Pre-experimental identification of projection neurons. **a** Confocal microscopy stack showing the neurons stained in the mushroom body (*MB*) with Microruby^{TM} prior to patch clamp recordings. The medial and the lateral antennal-lobe tract (*mALT*/*lALT*) as well as their arborizations in the lateral horn (*LH*) are clearly visible. Furthermore, the tritocerebral tract, the visual commisure and KC axons were stained. *Bar* 100 µm. **b** Substack of the ventral part of the antennal lobe (AL), *lALT* cell bodies and glomerular branching are clearly visible. **c** Substack of the dorsal part of the AL, *mALT* cell bodies, *mALT* and *lALT* axons are clearly visible. *Bar* 100 µm. **d** Reconstruction of the honeybee AL, the *lALT* cell bodies (*green*) and *mALT* cell bodies (*magenta*) can be matched to the cell bodies visible in **b** and **c**. The PN axons of *mALT* and *lALT* are indicated. *Bar* 100 µm. Adapted from Kirschner et al. 2006.

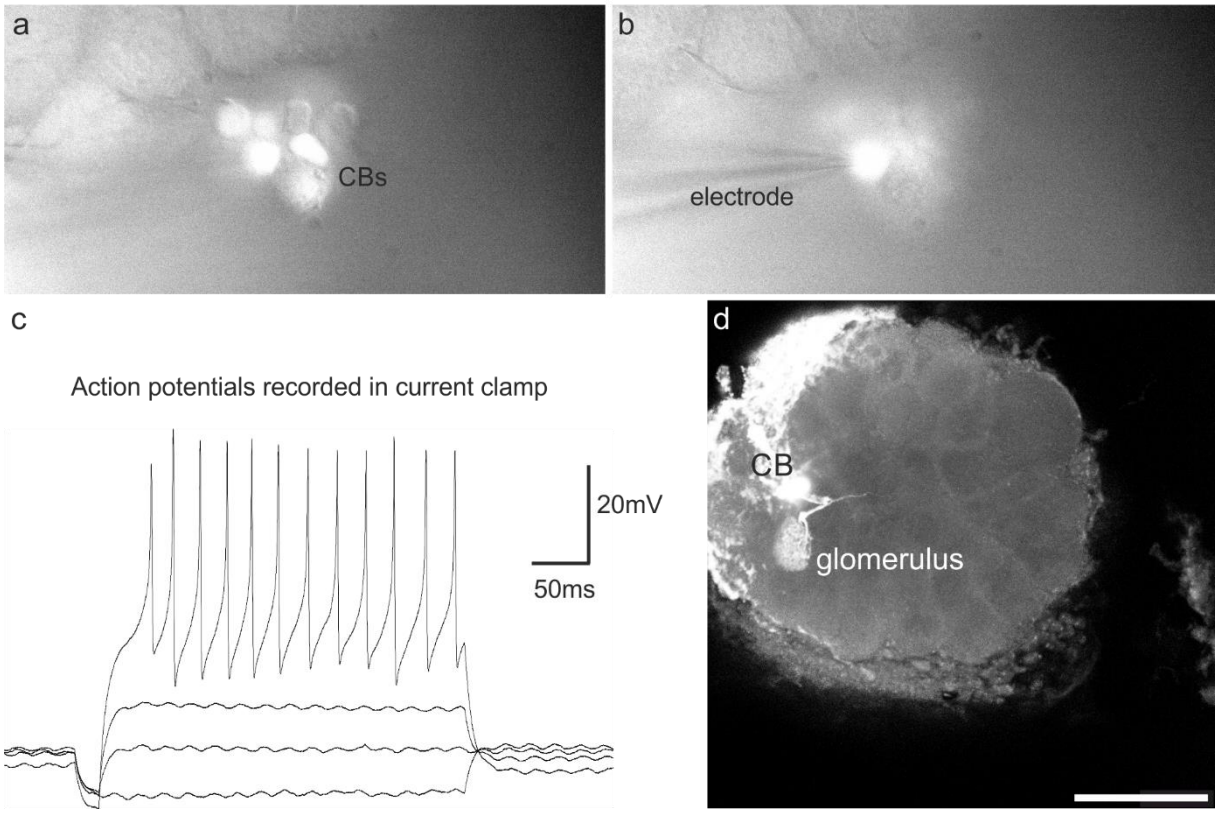

Fig. 2 Patch-clamp recording of visually identified dye-labeled projection neurons (PN). **a** A cluster of stained and not stained cell bodies (*CBs*) viewed with a fluorescence microscope. Only stained cell bodies were used for PN recordings. **b** Patch-clamp electrode attached to a stained PN cell body. **c** Action potentials (AP) of a honeybee PN elicited in current-clamp mode - the PN started to generate APs at ~ -40mV. **d** PN stained with Lucifer Yellow via the patch-clamp electrode. The *CB* and the dendritic arborizations in the glomerulus are clearly visible. *Bar* 100 µm

Recording under standard conditions

As this represents the first study, which investigates the ion channel composition of honeybee PNs and KCs *in situ*, we started by analyzing and comparing basic neuronal properties of the three neuronal classes under standard conditions. The membrane voltages of lALT PNs in our recordings ranged from -30 to -50mV, the mean membrane voltage of all cells was -41.5mV (N=9). Similarly, membrane voltages of mALT PNs ranged from -33 to -45mV with a mean of -39.4mV (N=4). In contrast, KC membrane voltages were slightly more negative and ranged from -42 to- 58mV (mean= -50.5mV, N=6). As the whole cell patch clamp technique can induce slight leakage currents, which potentially depolarize the cells, we assume even lower membrane voltages in intact cells. Therefore, during current clamp recordings, a minimal negative current was injected to achieve resting potentials of around -60mV. PNs recorded in current clamp

started to fire action potentials at membrane voltages from -50 to -40mV (Fig. 2 c). Staining of whole cells with a neuronal tracer via the patch pipette proved to be extremely difficult and is shown for a single case in Fig. 2d. The cell body of a lALT PN is visible, as well as dense dendritic branches within the gomerulus and the first part of the axon. Additionally, two varicosities of the neuron are visible, one at the branching point of the axon, the primary neurite and dendritic neurite and the other at the branching point of the dendritic ramifications within the glomerulus (Fig. 2d).

I-V plots obtained under standard conditions

As introduction of an olfactory stimulation devise would have complicated the experimental setup drastically, we decided to perform *in situ* voltage clamp recordings with pharmacological isolation of currents to identify basic electrical properties of the three neuronal classes. In voltage-clamp recordings under standard conditions, all three types of recorded neurons (lALT PNs, mALT PNs and KCs) showed transient inward, transient outward and persistent outward currents (Fig. 3a). Based on the ion concentrations used for recording under standard conditions, we conclude that the inward currents were mainly Na^+ currents and only partly Ca^{2+} currents, whereas all outward currents were likely K^+ currents. The currents which were activated first during the voltage step protocol (-70 to 70mV in PNs, -90 to 70mV in KCs) were inward currents. The inward currents of m- and lALT PNs were activated at approximately -50mV, the inward currents of KCs at -30mV (Fig. 3b). The transient K^+ currents were activated right after the inwards currents at -40mV in PNs and KCs (Fig. 3b). These currents deactivated very fast in PNs and were only slightly higher than the persistent K^+ currents. In contrast, KCs exhibited a very prominent transient outward current with about twice the amplitude of the persistent KC current. This current activated and deactivated significantly slower than the transient current in PNs (Fig. 3a). Persistent currents activated at -30mV in all three neuron types, yet they showed different IV relations in PNs and KCs. PN persistent currents increased with increasing membrane voltages in a linear IV relationship (Fig. 3b). Conversely, the persistent K^+ current of KCs shows a nonlinear, distinct N-form in the I-V plot which increases until 30mV, decreases slightly until 50mV and increases again at higher membrane voltages (Fig. 3b). This N-form hints at the presence of purely Ca^{2+}-dependent K^+ currents, which deactivate once the Ca^{2+} reversal potential is reached (see for example: Demmer and Kloppenburg 2009).

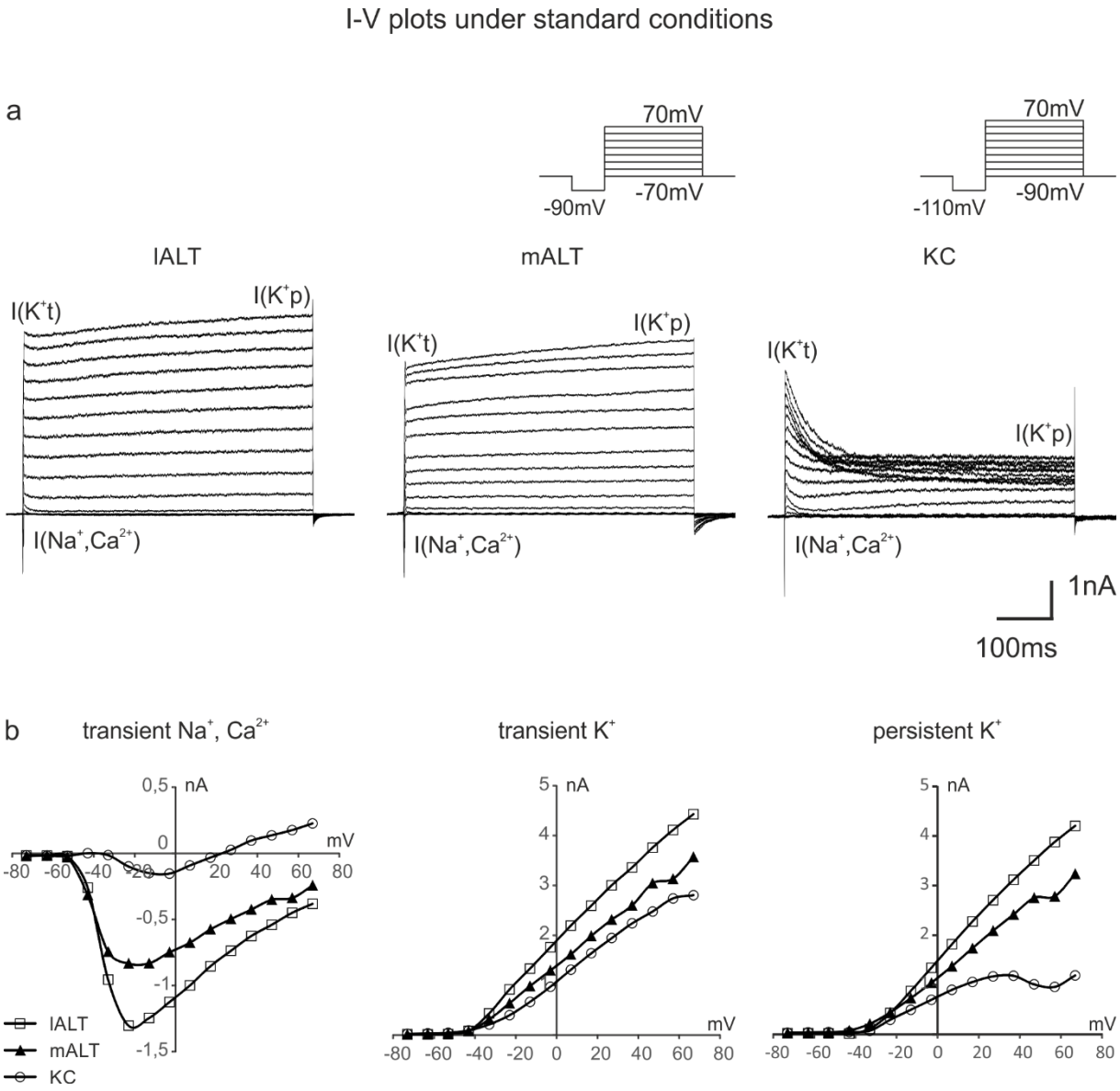

Fig. 3 Current-voltage (*I-V*) plots showing relations in lateral and medial antennal-lobe tract (lALT/mALT) projection neurons (PN) and Kenyon cells (KC). **a** Representative voltage clamp recordings of *lALT* and *mALT* PNs and *KCs*. The time points at which the transient Na^+ and Ca^{2+} currents (*I(Na*$^+$*,Ca*$^{2+}$*)*), the transient K^+ (*I(K*$^+$*t)*) and the persistent K^+ currents (*I(K*$^+$*p)*) were measured are indicated. *lALT* and *mALT* PNs have similar currents, *KCs* differ drastically as they have only small *I(Na*$^+$*,Ca*$^{2+}$*)* and a prominent *I(K*$^+$*t)* with about twice the size as the *I(K*$^+$*p)*. PNs were kept at -70mV, KCs at -90mV. In both PNs and KCs, a quick hyperpolarizing step of -20mV was used, then the membrane voltage was increased in 10mV increments. **b** I-V plots of the three neuronal types (lALT: N=9, mALT: N=4, KC: N=6). Note the N-form hinting Ca^{2+} dependent K^+ currents in the *I(K*$^+$*p)* in KCs.

Capacitance and current densities

Generally, PNs exhibited significantly larger currents than KCs (Fig 3a, b). As, theoretically, the current flow over all ion channels in the neuron's membrane is measured in whole-cell voltage-clamp experiments, the number and conductance of ion channels directly influences the amplitude of the measured current. The number of ion channels itself depends on the ion channel density and the size of the surface of the neuron. Therefore, larger neurons with an increased surface will have larger currents. One measure of the size of a cell is its capacitance. KCs (mean: 6.51pF) had significantly lower capacitances than lALT PNs (mean: 14.25pF) and showed a trend to have lower capacitances than mALT PNs (mean: 17.27pF). L- and mALT PNs did not differ from each other regarding these properties (Kruskal Wallis test: p=0.00611, post hoc Wilcoxon tests with bonferroni correction: lALT vs mALT: p=0.780300, lALT vs KC: p=0.008391, mALT vs KC: p=0.057150, Fig. 4a). To compensate for the size of the cell, we calculated the current density by dividing the mean maximal currents by the capacitance of the cell. Both l- and mALT PNs showed similar current densities, whereas in KCs the Na^+ current density is especially low and the transient K^+ current density relatively high (Fig. 4b).

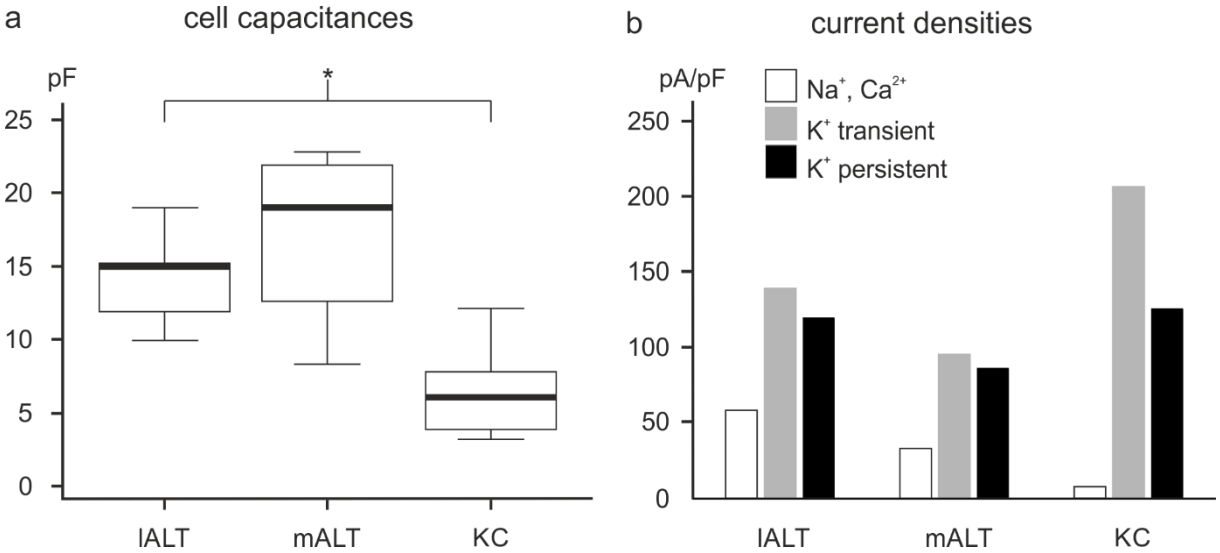

Fig. 4 a Mean cell capacitances of lateral and medial antennal-lobe tract (*lALT*/*mALT*) projection neurons (PN) and Kenyon cells (*KC*). The mean capacitance of the *lALT* neurons is significantly larger than the mean *KC* capacitance (Kruskal Wallis test: p=0.00611, post hoc Wilcoxon tests with bonferroni correction: lALT vs mALT: p=0.780300, lALT vs KC: p=0.008391, mALT vs KC: p=0.057150, lALT: N=9, mALT: N=4, KC: N=6). **b** Mean current densities of *lALT* and *mALT* PNs and *KCs*. Note the high current density of the transient K^+ current and the low current densities of the Na^+, Ca^{2+} currents (lALT: N=9, mALT: N=4, KC: N=6).

Mean maximal currents and their relation

In the current density measurements, PNs had a higher ratio of Na^+ to K^+ currents than KCs, and KCs had an especially high transient K^+ to persistent K^+ current ratio. To calculate the exact ratios, we determined the mean maximal currents of all cells (fig. 5a). Na^+ and Ca^{2+} mean maximal currents were determined at membrane voltages ranging from -50 to 40 mV, K^+ mean maximal currents were determined from -40 to 50 mV. The mean maximal Na^+ and Ca^{2+} currents in PNs are much larger than in KCs, and the ratio of the transient Na^+ and Ca^{2+} current to the transient K^+ current was significantly larger in m- and lALT PNs than in KCs (Kruskal Wallis test: p=0.002526, post hoc Wilcoxon tests with bonferroni correction: lALT vs mALT: p=1, lALT vs KC: p=0.005268, mALT vs KC: p=0.041760, Fig. 5b). Additionally, KCs showed a pronounced mean transient K^+ current much larger than the persistent K^+ current (Fig. 5a). The ratio of transient K^+ to persistent K^+ currents is significantly larger in KCs than in l- or mALT PNs (Kruskal Wallis test: p=0.005506, post hoc Wilcoxon tests with bonferroni correction: lALT vs mALT: p=0.780300, lALT vs KC: p=0.023862, mALT vs KC: p=0.041760, Fig. 5b).

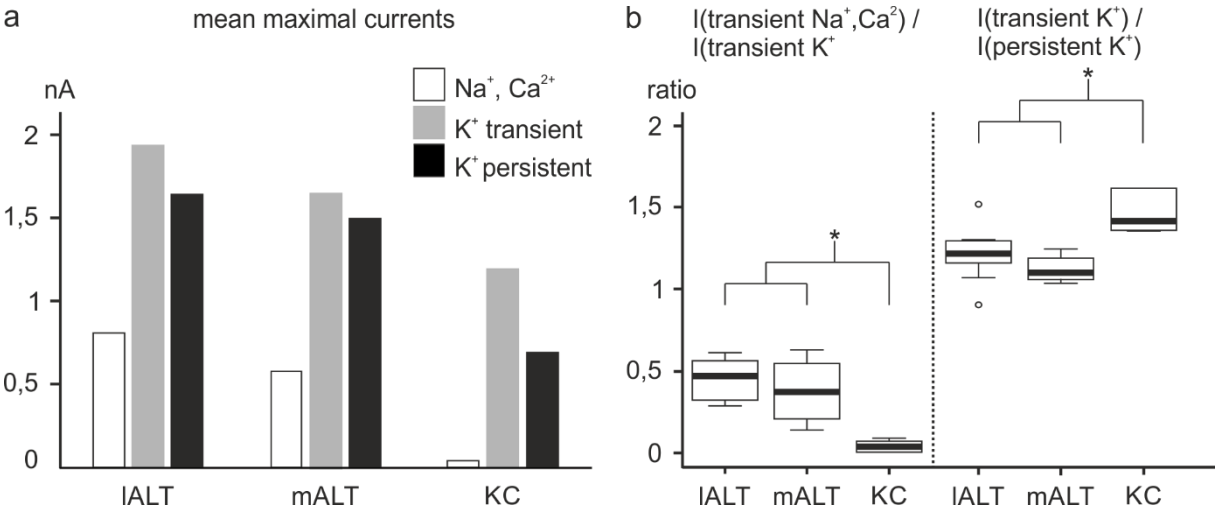

Fig. 5 a Mean maximal currents of lateral and medial antennal-lobe tract (*lALT*/*mALT*) projection neurons (PN) and Kenyon cells (*KC*) (lALT: N=9, mALT: N=4, KC: N=6). **b** The ratios of the transient Na^+, Ca^{2+} currents / transient K^+ currents is significantly smaller in *KCs* than in *lALT* and *mALT* PNs (Kruskal Wallis test: p=0.002526, post hoc Wilcoxon tests with bonferroni correction: lALT vs mALT: p=1, lALT vs KC: p=0.005268, mALT vs KC: p=0.041760). The ratios of transient K^+ currents / persistent K^+ currents is significantly higher in *KCs* than in *PNs* (Kruskal Wallis test: p=0.005506, post hoc Wilcoxon tests with bonferroni correction: lALT vs mALT: p=0.780300, lALT vs KC: p=0.023862, mALT vs KC: p=0.041760, lALT: N=9, mALT: N=4, KC: N=6).

Transient currents

A detailed analysis of the transient K^+ currents revealed that the PN and KC transient K^+ currents do not only differ in their amplitudes, but in their activation and in the time courses (Fig. 6a). To be able to analyze the exact form of the activation of PN and KC currents, we plotted G/Gmax values, which were obtained by using the equilibrium potentials for Na^+ and K^+, although Ca^{2+} and Cl^- currents might also be present under standard conditions (Fig. 6b). As much more Na^+ and K^+ ions are present in the solutions, we assume that this analysis is relatively precise. The activation voltage of the transient K^+ current did not differ between PNs and KCs and was approximately at -40 mV (Fig. 6b). In the conductance analyses, the PN conductance was rising faster than the conductance of KCs. The half-maximal activation of the transient currents was reached at -30mV in lALT PNs, at -15 mV in mALT PNs and at -17 mV in KCs (half-maxima are obtained from Boltzmann fits to the G/Gmax plots of the peak currents, Fig. 6b). Additionally, PN transient K^+ currents were maximal at much lower voltages than KC transient K^+ currents. This indicates that these transient currents are partly Na^+ or Ca^{2+} dependent and partly voltage dependent in PNs, as they do not increase linearly, and, at the same time, do not decrease at higher voltages. In contrast, the relatively linear rising phase in KCs hints at mostly voltage-dependent transient K^+ currents. By looking at an expanded time scale, it becomes obvious that PN transient K^+ currents deactivate much faster than KC transient K^+ currents and appear to activate faster (Fig 6a). To analyze the timing of the activation of the transient K^+ current, we determined its latency, which is significantly shorter in lALT PNs than in KCs (Fig. 6c, Kruskal Wallis test: $p=0.014385$, post hoc Wilcoxon tests with bonferroni correction: lALT vs mALT: $p=0.649200$, lALT vs KC: $p=0.014385$, mALT vs KC: $p=0.598500$). As the transient K^+ currents are likely to be Na^+ or Ca^{2+} dependent, we also analyzed the latency of the inwards currents' maxima. No differences in the latencies to the inwards current maxima (Kruskal Wallis test: $p=0.9523$ Fig. 6d) could be found. We conclude that the difference in the latency of the transient K^+ current does not depend on differences of preceding inward currents, but rather on differences in the types of K^+ currents.

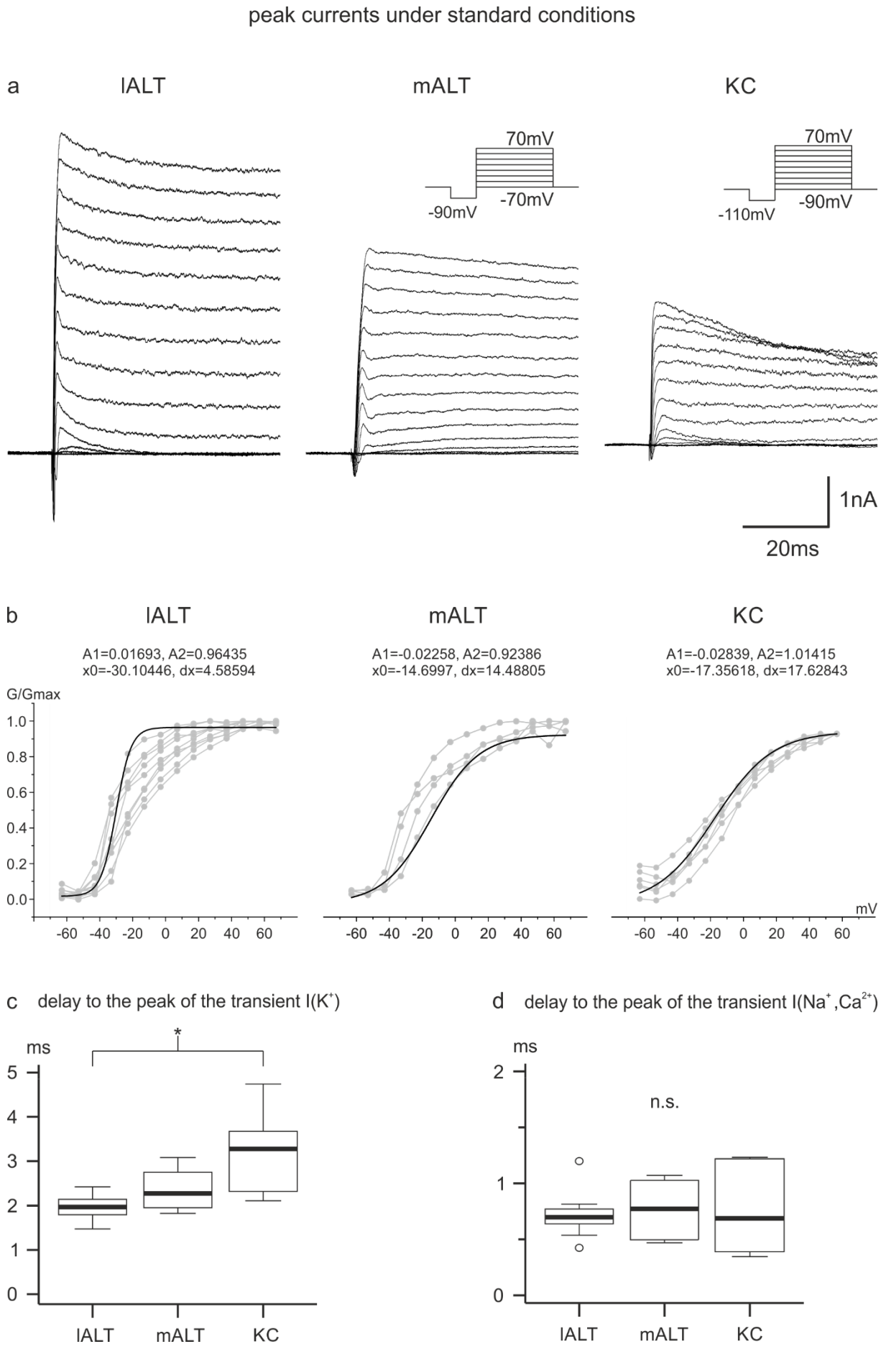
peak currents under standard conditions
a
lALT
mALT
KC
70mV
-90mV
-70mV
70mV
-110mV
-90mV
1nA
20ms
b
lALT
mALT
KC
A1=0.01693, A2=0.96435
x0=-30.10446, dx=4.58594
A1=-0.02258, A2=0.92386
x0=-14.6997, dx=14.48805
A1=-0.02839, A2=1.01415
x0=-17.35618, dx=17.62843
G/Gmax
1.0
0.8
0.6
0.4
0.2
0.0
-60 -40 -20 0 20 40 60
mV
c
delay to the peak of the transient I(K+)
ms
5
4
3
2
1
0
*
lALT
mALT
KC
d
delay to the peak of the transient I(Na+,Ca2+)
ms
2
1
0
n.s.
lALT
mALT
KC

Fig. 6 Transient current analyses under standard conditions. **a** Representative voltage clamp recordings of *lALT* and *mALT* PNs and *KC*. The resolution of the time-axis was adjusted for better visibility of the transient currents. **b** Conductance/maximal conductance (*G/Gmax*) plots for the transient currents of *lALT* and *mALT* PNs and *KCs*. A first-order Boltzman fit was used to model the data, the equations are given above the plots (lALT: N=9, mALT: N=4, KC: N=6). **c** The transient K^+ current activates faster in *lALT* PNs than in *KCs* (Kruskal Wallis test: p=0.014385, post hoc Wilcoxon tests with bonferroni correction: lALT vs mALT: p=0.649200, lALT vs KC: p=0.014385, mALT vs KC: p=0.598500, lALT: N=9, mALT: N=4, KC: N=6). **d** The time delay to the transient Na^+, Ca^{2+} currents is not significantly different for *lALT* and *mALT* PNs and *KCs*. (Kruskal Wallis test: p=0.9523, lALT: N=9, mALT: N=4, KC: N=6).

Pharmacological isolation of currents

In the analysis we conducted so far, the distinction between currents carried by different ions was based only on the distinction of outward and inward currents. This analysis, therefore, mainly helped to identify the predominant currents under standard conditions, but cannot be used to further determine the exact activation thresholds, half-maximal activations, maximal currents, and the conductance of specific ionic currents. As the IV relations we observed under standard conditions indicated Na^+ currents and a variety of K^+ currents in PNs, and Na^+ currents as well as Ca^{2+} sensitive K^+ currents in KCs, we decided to use TTX and CdCl2 as primary pharmacological agents. TTX (10^{-7} mmol), a toxin which is well known from pufferfish, blocks voltage dependent Na^+ channels and Na^+ dependent K^+ channels (Narahashi et al. 1964). $CdCl_2$ ($5x10^{-5}$ mmol) blocks Ca^{2+} channels and, therefore, also Ca^{2+} dependent K^+ channels (Wicher and Penzlin 1997). After pharmacological isolation of currents, we did not observe any obvious differences in the quality of currents between m- and lALT PNs. Therefore, in the following we do not further distinguish the influences of pharmacological blocking separately for m- and lALT. The only slightly varying parameters of mALT and lALT PN currents can be taken from table 1.

Table 1 Parameters of ionic currents of medial antennal-lobe tract and lateral antennal-lobe tract projection neurons (mALT/lALT) obtained from raw data and first-order Boltzman fits of G/Gmax plots.

	Na^+		$K_{Na\,t}$		$K_{Na\,p}$		$K_{Ca\,t}$		$K_{Ca\,p}$	
	mALT	lALT	mALT	lALT	mALT	lALT	mALT	lALT	mALT	lALT
threshold mV	-50	-50	-40	-40	-30	-30	-30	-40	-30	-40
V 0.5act mV	-27.5	-29.0	-32.7	-28.7	9.1	3.7	-25.6	-33.9	-7.4	-22.8
~V max mV	-10	-20	-10	-10	50	60	10	-10	70	70
I max pA	770	1276	930	1536	932	1143	737	1537	555	1160
G max nS	4.9	7.6	7.7	13.8	6.7	8.2	7.1	13.7	3.8	7.8

m-and lALT currents under the influence of TTX and $CdCl_2$

In the I-V plots obtained after adding TTX to the extracellular solution, the fast inward currents were almost completely abolished in PNs (Fig. 7a, Fig 8a). Thus, we conclude that the inwards currents from both types of PNs are dominated by Na^+ inward currents. Additionally, both the transient and the persistent K^+ current were strongly reduced in both PN types after adding TTX, which leads to the conclusion that the outward current partly consists of Na^+ dependent K^+ currents (K_{Na}).

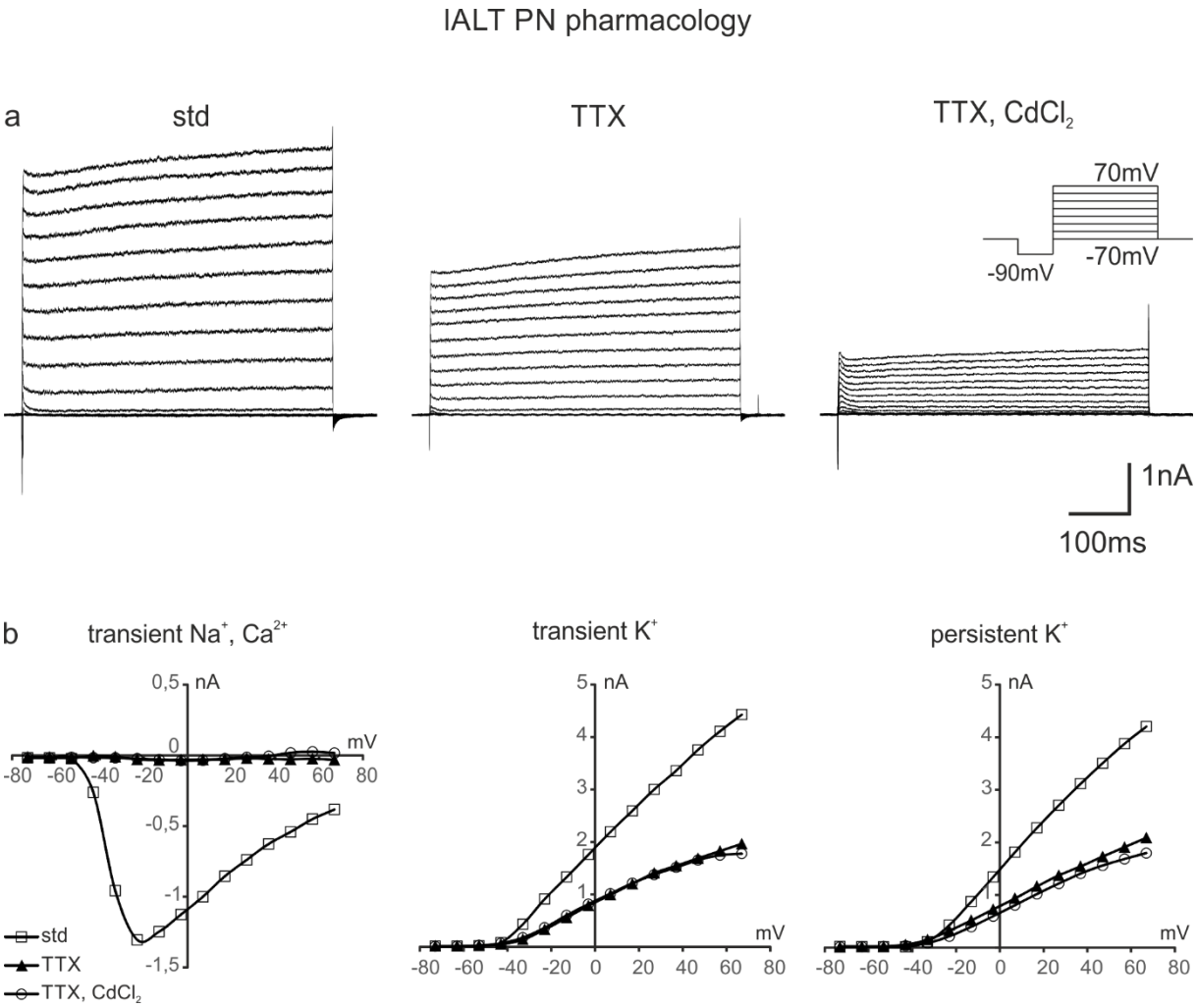

Fig. 7 Pharmacological blocking of Na^+, Ca^{2+}, Na^+ dependent and Ca^{2+} dependent currents in lateral antennal-lobe tract (*lALT*) *PNs*. **a** Representative voltage clamp recordings of *lALT* PNs under standard conditions, TTX and TTX, $CdCl_2$ conditions. Most of the transient inward current is already blocked by TTX, the outward current is also partly blocked. All inward currents are blocked under TTX, $CdCl_2$ conditions, large parts of the outward currents are also blocked. **b** Mean current-voltage (I-V) plots of the lALT PNs. The inward currents are completely blocked with TTX, $CdCl_2$, both small transient as well as small persistent outward currents remain (N=3).

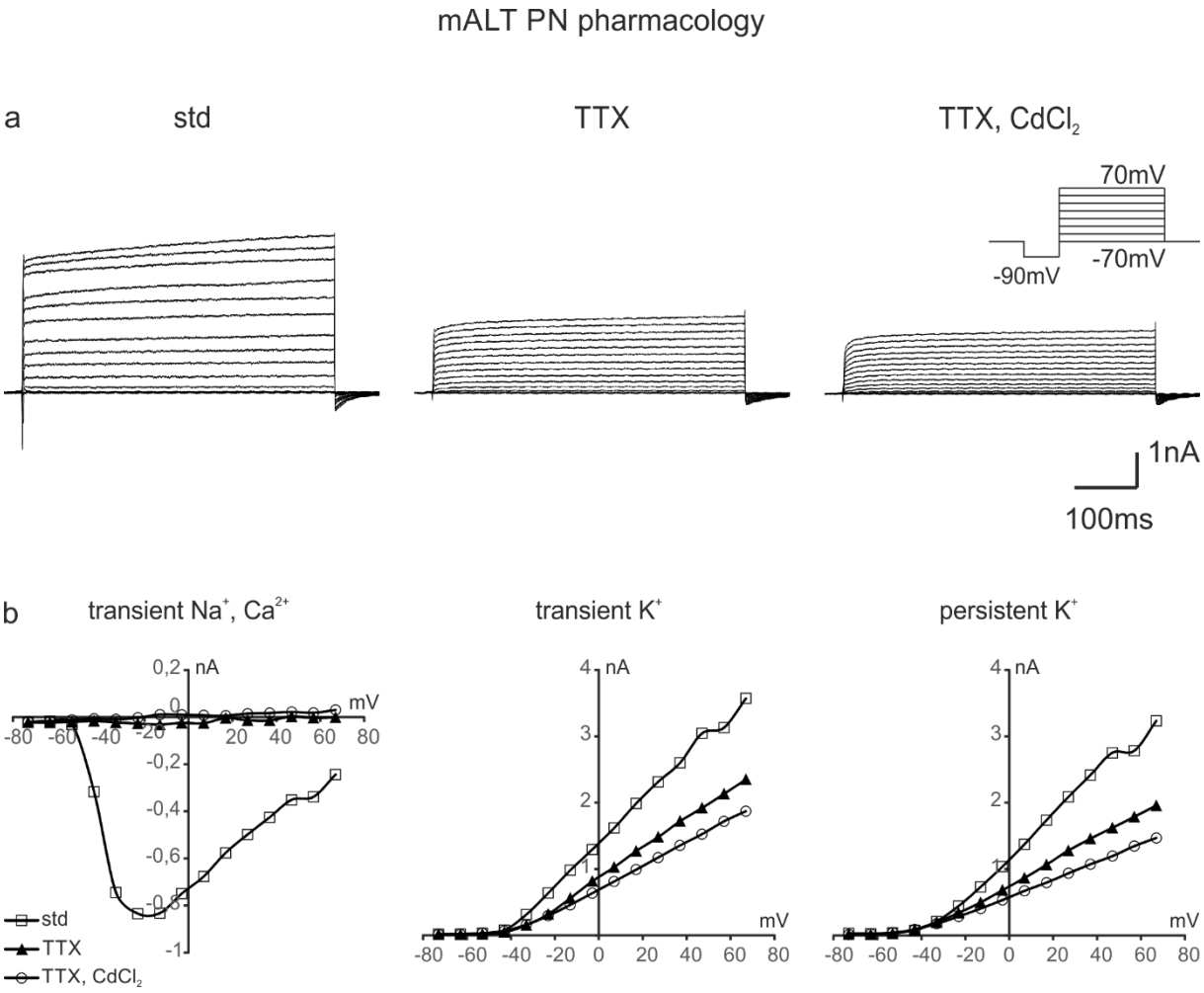

Fig. 8 Pharmacological blocking of Na^+, Ca^{2+}, Na^+ dependent and Ca^{2+} dependent currents in medial antennal-lobe tract (*mALT*) *PNs*. **a** Representative voltage clamp recordings of *mALT* PNs under standard conditions, TTX and TTX, $CdCl_2$ conditions. Most of the transient inward current is already blocked by TTX, the outward current is also partly blocked. All inward currents are blocked under TTX, $CdCl_2$ conditions, large parts of the outward currents are also blocked. **b** Mean current-voltage (I-V) plots of the mALT PNs. The inward currents are completely blocked with TTX, $CdCl_2$, both small transient as well as small persistent outward currents remain (N=3).

Although the amplitude of the K^+ currents was reduced after TTX treatment, the basic shape remained relatively intact, leaving a fast peak outward current and a sustained K^+ current (Fig. 7a, Fig. 8a). Both m- and lALT PNs did not differ significantly in this. In a further step, $CdCl_2$ was added to the extracellular solution in order to block all Ca^{2+} currents and, therefore, also the Ca^{2+} dependent K^+ currents (K_{Ca}). No direct influence on inward currents could be observed, most likely because under standard conditions Ca^{2+} currents were masked by Na^+ and K^+ currents, which have much higher current amplitudes. However, K_{Ca} currents were affected by the block of the Ca^{2+} channels resulting in decreased K^+ currents. Very fast and transient K^+ peak currents were completely abolished (Fig. 7a, Fig 8a). In some cases, a slower K^+ peak

current resembling the A-type current observed in KCs could be observed (Fig. 7a). The onset of the K^+ peak current was significantly slower than under standard conditions (Fig.9, Wilcoxon test, p= 0.009452) and, qualitatively, the deactivation lasted much longer (Fig. 7a, not quantified). Additionally, the amplitude of the sustained K^+ current was reduced. In summary, PNs contain transient Na^+ currents (Na_t), persistent Na+ currents (Na_p), transient Na^+ dependent K^+ currents ($K_{Na\ t}$) and persistent Na^+ dependent K^+ currents ($K_{Na\ p}$), Ca^{2+} currents, transient Ca^{2+} dependent K^+ currents ($K_{Ca\ t}$), persistent Ca^{2+} dependent K^+ currents ($K_{Ca\ p}$), and purely voltage-dependent K^+ currents (K_V).

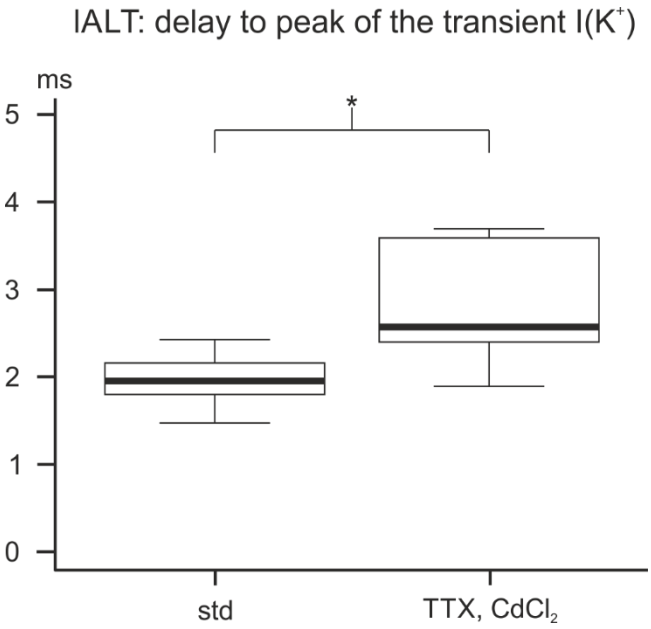

Fig 9 The transient K^+ current ($I(K^+)$) of lateral antennal-lobe tract neurons (*lALT*) is significantly delayed under TTX, $CdCl_2$ conditions (Wilcoxon test, p= 0.009452, N=8).

TTX sensitive currents in m- and lALT PNs

As the amplitude of K^+ currents exceeds the amplitude of Na^+ currents drastically (Fig. 7 A, Fig 8 a), the Na^+ currents are masked by K^+ currents when they are in the same time and voltage frame. To compensate for this and thus be able to identify purely TTX sensitive currents, we subtracted the IV curves obtained with TTX in the extracellular solution as a control from the curves obtained under standard conditions (Fig. 10a, 11a). In both m- and lALT PNs we found a very fast voltage dependent Na^+ current, a sustained Na^+ current, a very fast peak K_{Na} and a sustained K_{Na}. The sustained Na^+ current is relatively small and is also masked by K_{Na} currents, therefore it can only be observed at membrane voltage of -50 to -30mV, as persistent K^+ currents are not pronounced at these low voltages. The two TTX sensitive K^+ currents, the very fast transient and the persistent K^+ current, are both K_{Na} currents which are activated by the fast Na^+

inwards current and the sustained Na^+ current. To analyze these currents in detail, we plotted the conductance/maximal conductance values, fitted them with a first-order Boltzmann fit (Fig.12). With the parameters of the Boltzmann fit and the raw data, we obtained activation thresholds, half-maximal activation values, maximal voltages, maximal currents and the conductance. Both m- and lALT PNs did not differ drastically regarding these parameters (table 1). From these data, it is obvious that the peak K_{Na} exhibits a direct relation to the fast Na^+ current, as it activates at voltages slightly above the Na^+ current and reaches its maximum at approximately -10mV, which is the voltage range where the Na^+ current is maximal (Table 1, Fig. 10b, Fig 11b). The sustained K_{Na} current rises linearly in a voltage-dependent manner and activates at -30mV right after the sustained Na^+ current, which activates at -50mV. Thus, we assume that it is mainly voltage dependent but requires minimal Na^+ ions for activation.

$CdCl_2$ sensitive currents in m- and lALT PNs

Ca^{2+} currents are not only masked by K^+ currents but also by Na^+ currents, therefore Ca^{2+} and Ca^{2+} dependent K^+ (K_{Ca}) currents were analyzed by subtracting the IV traces obtained after adding $CdCl_2$ to the extracellular solution from the traces obtained under standard + TTX conditions (Fig. 10, Fig 11). The current subtraction revealed a slight peak of inward currents between -30 and -20mV indicating the presence of Ca^{2+} currents. Furthermore, two K_{Ca} currents, namely a transient current ($K_{Ca\ t}$) and a persistent current ($K_{Ca\ p}$) can be observed. All parameters concerning theses currents obtained from raw data and the Boltzmann fits (Fig. 12) are summarized in table 1. Both $K_{Ca\ t}$ current and $K_{Ca\ p}$ current activated between -40 and -30mV (table1) and did not deactivate with increasing voltage (Fig. 10, 11), which indicates that both are Ca^{2+} and voltage dependent.

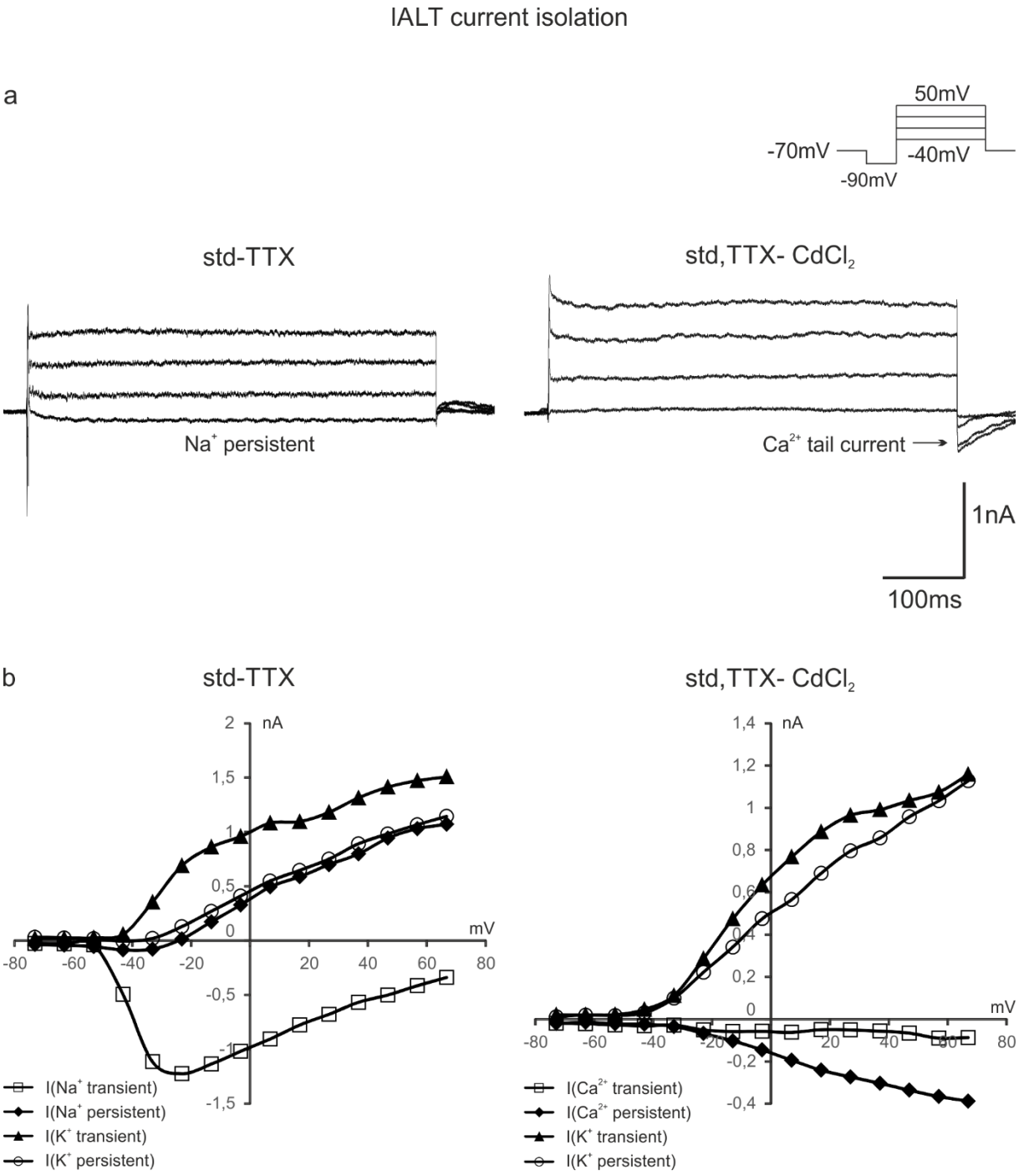

Fig. 10 Isolation of currents in lateral antennal-lobe tract (*lALT*) PNs. **a** TTX (*std-TTX*) (respectively $CdCl_2$ (*std,TTX-CdCl₂*)) sensitive currents were isolated by subtracting the current trace obtained under TTX (respectively $CdCl_2$) conditions from the current trace obtained under standard conditions (respectively TTX conditions). Two representative recordings are shown. For better visibility, the current traces obtained after 30mV difference in membrane voltage are depicted. In the *std-TTX* trace, a persistent Na^+ current can be identified. In the *std,TTX-CdCl₂* trace, Ca^{2+} tail currents can be observed. **b** Mean current-voltage (I-V) plots of the isolated currents. Transient Na^+, Ca^{2+} and K^+ currents as well as persistent Na^+, Ca^{2+} and K^+ currents can be observed (N=3).

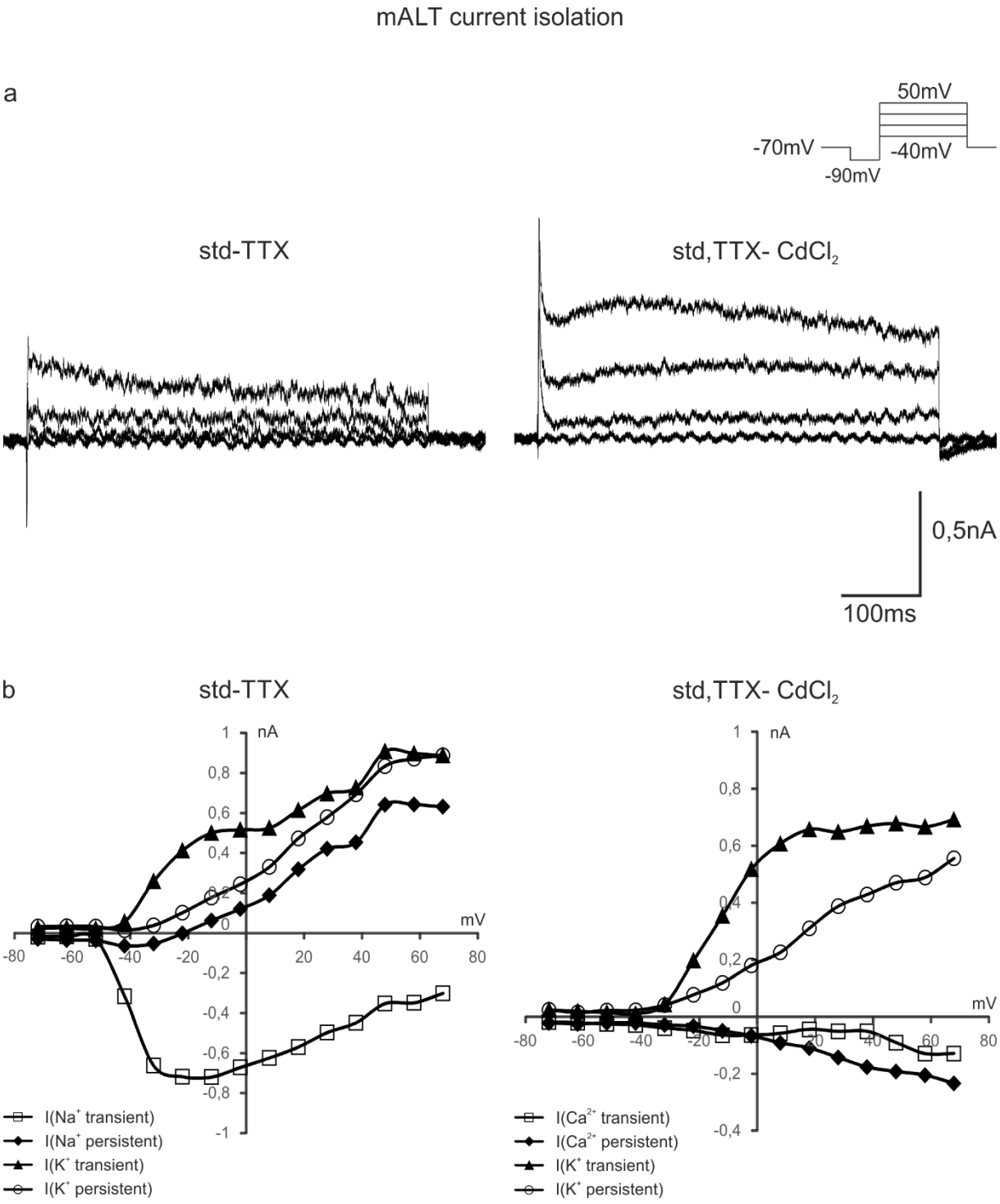

Fig. 11 Isolation of currents in medial antennal-lobe tract (m*ALT*) PNs. **a** TTX (*std-TTX*) (respectively $CdCl_2$ (*std,TTX-CdCl₂*)) sensitive currents were isolated by subtracting the current trace obtained under TTX (respectively $CdCl_2$) conditions from the current trace obtained under standard conditions (respectively TTX conditions). Two representative recordings are shown. For better visibility, the current traces obtained after 30mV difference in membrane voltage are depicted. **b** Mean current-voltage (I-V) plots of the isolated currents. Transient Na^+, Ca^{2+} and K^+ currents as well as persistent Na^+, Ca^{2+} and K^+ currents can be observed (N=3).

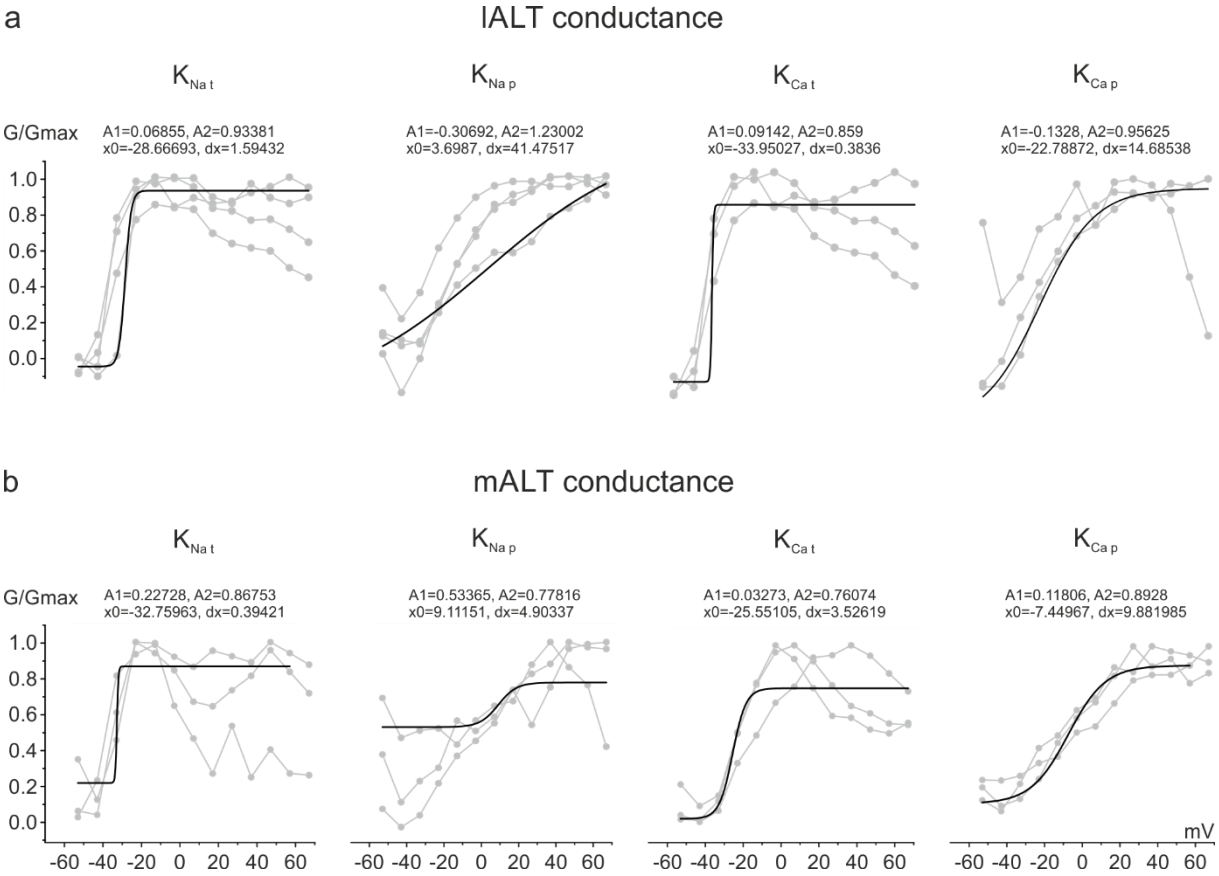

Fig. 12 Conductance/maximal conductance (*G/Gmax*) plots for the transient Na^+ and Ca^{2+} dependent K^+ currents ($K_{Na\,t}$, $K_{Na\,p}$) and persistent Na^+ and Ca^{2+} dependent K^+ currents ($K_{Ca\,t}$, $K_{Ca\,p}$) of several individual lateral antennal-lobe tract (**a**, *lALT*, N=4 for $K_{Na\,t}$, K_{Na}, N=3 for $K_{Ca\,t}$, $K_{Ca\,p}$) and medial antennal-lobe tract (**b**, *mALT*, N=3) projection neurons. A first-order Boltzman fit was used to model the data, the equations are given above the plots.

Pharmacological isolation of currents in KCs

KCs exhibited clearly different ionic current properties compared PNs (Fig. 3, table 2). A single KC was investigated by adding TTX and $CdCl_2$ to the extracellular medium (Fig. 13a). All inward currents were completely abolished, the transient K^+ current was slightly reduced, and the persistent K^+ current was drastically reduced (Fig. 13). The basic shape of the transient K^+ current remained the same, displaying an A-shaped form in the I-V plot. Conversely, the N-form of the persistent K^+ current was completely lost. The subtraction of the TTX plus $CdCl_2$ IV trace from the trace obtained under standard conditions revealed a little TTX and $CdCl_2$ sensitive inward current, a sustained and a peak K^+ current (Fig. 14). The transient K^+ current blocked by TTX and $CdCl_2$ increased linearly in a voltage dependent fashion, whereas the persistent K^+ current increased until 20-30 V and decreased at higher voltages (Fig 14b). This adds evidence to the assumption that this is a purely Ca^{2+} dependent channel, as the reversal potential for Ca^{2+} ions is at 23.1mV with our recording solutions.

Table 2 Parameters of ionic currents of Kenyon cells obtained from raw data and first-order Boltzman fits of G/Gmax plots.

	Na^+	K^+ transient	K^+ persistent
threshold (mV)	-30	-40	-35
V 0.5act (mV)	-21.0	-17.3	-20.8
~V max (mV)	0	60	30
V 0.5 deact (mV)	-	-	37.7
I max (pA)	161	2737	1278
G max (nS)	1.1	20.3	11.5

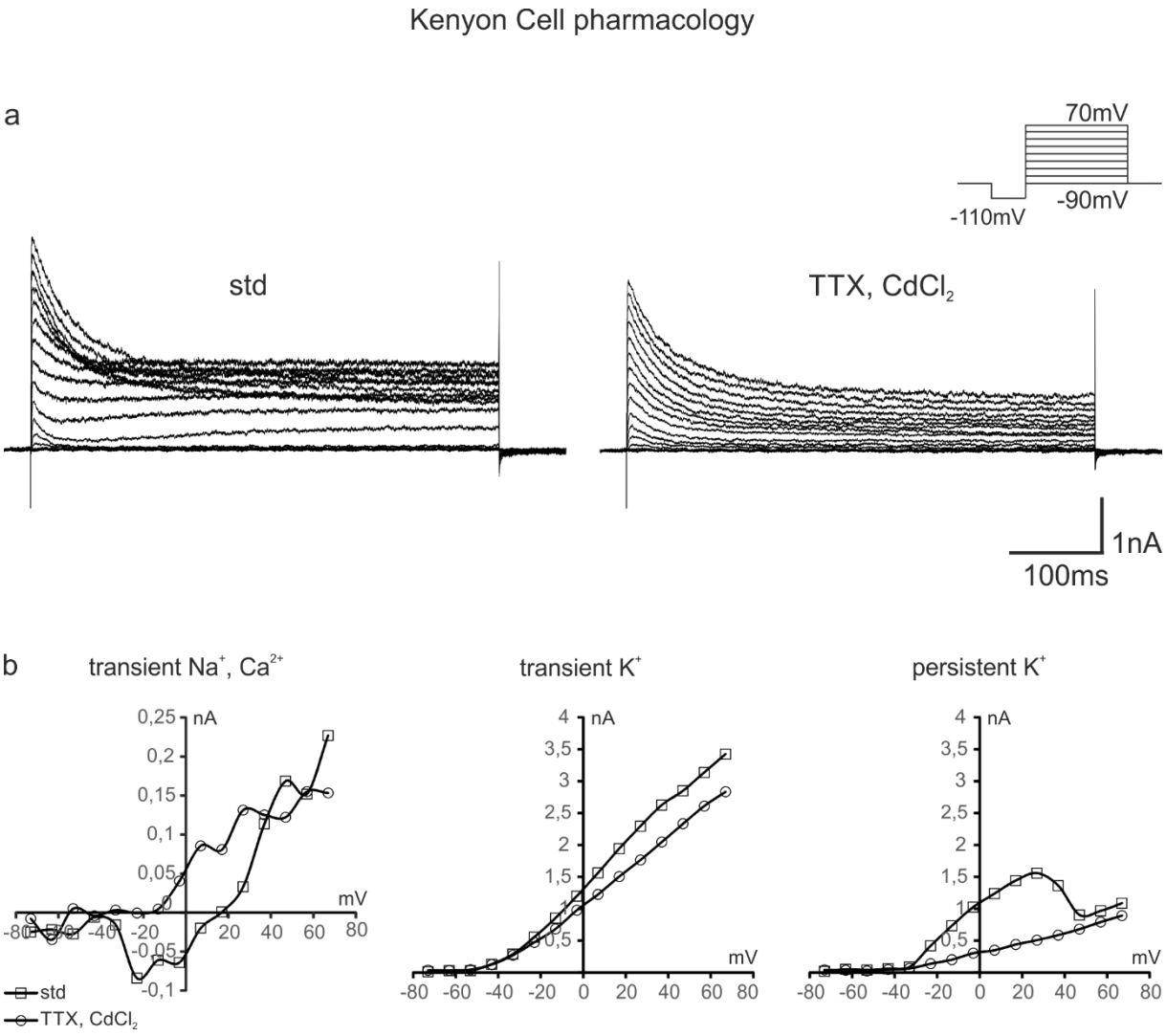

Fig. 13 Pharmacological blocking of Na^+, Ca^{2+}, Na^+ dependent and Ca^{2+} dependent currents in a single Kenyon cell. **a** Exemplary voltage clamp recordings of the Kenyon cell under standard conditions and TTX, $CdCl_2$ conditions. All inward currents are blocked by TTX, $CdCl_2$. The transient outward current remains largely unaffected. One part of the persistent outward current is blocked. **b** Current-voltage (I-V) plots of the mALT PNs. The inward currents are completely blocked with TTX, $CdCl_2$ the transient K^+ current is not affected and the N-form of the persistent K^+ current vanishes.

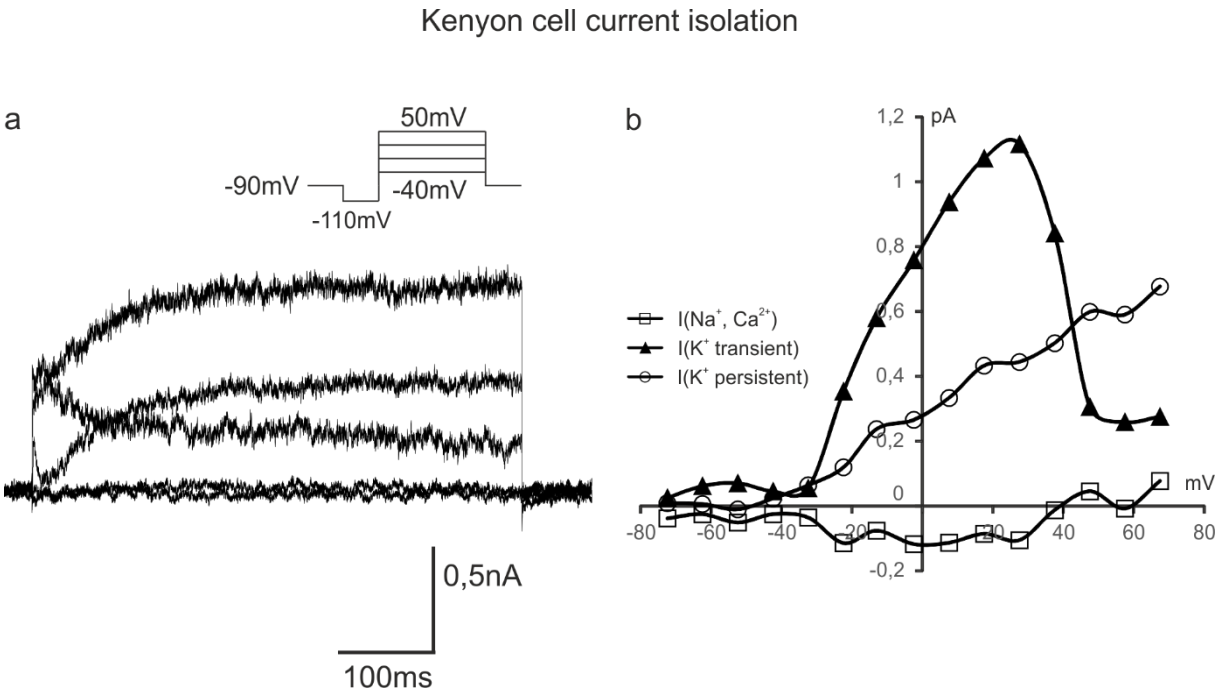

Fig. 14 Isolation of currents in a single Kenyon cell. **a** TTX, $CdCl_2$ sensitive currents were isolated by subtracting the current trace obtained under TTX, $CdCl_2$ conditions from the current trace obtained under standard conditions. For better visibility, the current traces obtained after 30mV difference in membrane voltage are depicted. **b** Current-voltage (I-V) plots of the isolated currents. Transient Na^+, Ca^{2+} currents, a transient K^+ current and a persistent K^+ current deactivating which is maximal at 20-30mV were observed.

Discussion

In this study we selectively recorded *in situ* from KCs, m- and lALT PNs in whole-cell voltage clamp configuration. We were able, for the first time, to distinguish between l- and mALT PNs using a combined staining and recording technique. This revealed no significant differences between m- and lALT PN currents. However, the differences between KCs and both populations of PNs were prominent: PNs exhibit strong transient and small persistent Na^+ currents as well as Na^+ dependent transient and persistent K^+ currents as well as Ca^{2+} dependent transient and persistent K^+ currents. KCs, in contrast, have a relatively small transient Na^+ current, a prominent A-type K^+ current, which is not regulated by Na^+ or Ca^{2+}, and a Ca^{2+} dependent persistent N-shaped K^+ current. Generally, our data fit quite well with whole cell recordings from cultured or isolated brain preparations (Schäfer et al. 1994; Grünewald 2003; Perk and Mercer 2005). Distinct differences between our *in-situ* recordings from adult brains and recordings from pupal neurons in primary cell culture are likely due to differential expression of ion channels in the *in-situ* preparation and in the cell culture situation.

Pre- and post-experimental staining techniques

By staining of PNs in the MBs, we were able to localize and record exclusively AL PNs. We discriminated between m- and lALT PNs by matching their anatomical location with previous reconstructions of the AL with differentially labelled m- and lALT PN cell bodies (Kirschner et al. 2006). By using an upside-down preparation introduced by Ca^{2+} imaging experiments by Carcaud et al. (2012), we were able to selectively access mALT associated PN cell bodies for *in-situ* patch-clamp recordings. The most crucial step here was to remove the SEG. As both *in-situ* Ca^{2+} imaging (Carcaud et al. 2012) and *in-situ* voltage clamp recordings of mALT PNs did not differ drastically from recordings of the lALT PNs, we assume that the recorded neurons were still functionally intact although the microdissection of the brain was more severe compared to mALT PN recordings. Microruby^{TM}, the dye used in our experiments, is a dextran coupled biotin dye and was reported to have no influence on physiological properties of cultured neurons, for example in turtles (Fadool et al. 2001). Micoruby^{TM} was successfully used in several studies to identify neurons prior to in situ recording or in vitro prior to the generation of primary cell cultures (Honeybee AN motoneurons *in situ* and *in vitro*: Kloppenburg et al. 1999; Locust DUM (dorsal unpaired median) neurons *in situ*: Heidel and Pflüger 2006; honeybee PNs in vitro: Grünewald 2003). Therefore, it appears very unlikely that Microruby^{TM}

as an *in-situ* marker prior to voltage clamp recordings of the stained neurons does interfere with current recordings. The standard method used in patch clamp recordings for the anatomical identification of neurons is staining of the neurons with an intracellular marker via the patch pipette. However, unfortunately the success rate of this method is minimal in honeybees. More successful staining experiments via whole-cell patch clamp in honeybees were achieved with antennal nerve motoneurons (Kloppenburg et al. 1999), which could be due to a larger neurite diameter. In cockroaches, staining of AL neurons via the patch pipette is well established (Husch et al. 2009; Fusca et al. 2013). Therefore improving the staining protocol by for example changing the intracellular marker or by pulsed current injection might improve staining efficiency. Consequently, it was not possible to confirm the selective recording of PNs by double labelling of all cells with pre-experimentally injected Microcruby^{TM} and counterstaining with Lucifer Yellow^{TM} (LY) injected via the electrode. However, the distinct localization of m- and lALT cell body clusters did not necessarily require this. Furthermore, the addition of another dye (LY) may as well increase the chance of interference with the neuronal physiology. One difficulty, however, that may hinder staining via the patch clamp electrode might be the occurrence of very thin neuron parts and varicosities in PNs (see Fig. 2d), which can lead to series resistance against the flow of the charged dye molecules.

Electrophysiological properties of PNs

General PN properties

In our recordings, PNs were shown to fire action potentials starting at membrane voltages of around -40mV, and no frequency adaptation was observed. PNs had cell capacitances of about 15pF and a mean membrane resting potential of around -40mV. The capacitances indicate that the cells measured *in situ* are slightly larger than cultured PNs, which were described to have a capacitance of around 11pF (Grünewald 2003). This could also be due to the fact that cultured neurons were from pupal stages. Although the PNs in primary cultures did grow dendritic processes, we assume that the difference is at least partly due to the fact that *in situ* measured PNs have dendritic and axonal arborizations, which are missing in cell culture. A resting membrane potential of -40 mV appears rather depolarized. We assume that the resting potential of PNs is approximately at -50 to -60mV, which resembles the lowest measured resting potentials. The difference is likely due to damage that the cell received either during the preparation, during staining or during rupturing of the cell membrane patch. No significant

differences between m- and lALT PNs regarding their capacitances or their resting membrane potentials were found.

Ionic currents of PNs under standard conditions

PNs were shown to possess prominent Na^+ currents, K_{Na}, K_{Ca} and K_V currents. The I-V relations observed under standard conditions partly resemble the ones recorded in cell culture (Grünewald 2003; Perk and Mercer 2005). Both in *in situ* and *in vitro* studies, PNs exhibit a fast transient Na^+ current, a fast activating and deactivating transient K^+ current and a persistent K^+ current. However, Grünewald (2003) describes a non-linear I-V relation for the persistent K^+ current leading to an N-form of the I-V plot for cultured PNs. Perk and Mercer (2005) recorded two types of cultured AL neurons and one of the two types displays the same shape of I-V relation as in our recordings. The other type does not have a fast transient K^+ current, but has a non-linear N-shaped persistent K^+ current. We conclude from our recordings that the first type measured by Perk and Mercer in 2005 is a PN type, whereas the second type may be a LN type. So far, the only explanation for the differences between our recordings and the PN recordings from Grünewald (2003) are differences between *in situ* and *in vitro* ion channel expression. The basic shape of the I-V plots observed in PN recordings resembles I-V curves in honeybee AN motoneurons (Kloppenburg et al. 1999) and I-V curves in dorsal unpaired median (DUM) neurons recorded in cockroaches (Grolleau and Lapied 1995). The physiology of DUM neurons has been studied extensively, therefore we will compare currents of honeybee PNs with currents measured in DUM neurons to gain knowledge about current identities.

Na^+ currents

The fast Na^+ current is the typical Na^+ current necessary for the fast depolarization during action potential generation (Hille 2001). It activates at -50mV, increases until -10mV, and decreases from there on. This current is sensitive to TTX, which blocks a wide range of Na^+ channels (Hille 2001) and prohibits action potential generation. Additionally, we found a second TTX sensitive current with a low current amplitude representing a persistent Na^+ current that activates around -50mV, but does not deactivate. Due to the very prominent K^+ currents, the persistent Na^+ current can only be observed at membrane voltages below the activation threshold of the persistent K^+ currents. Persistent Na^+ currents have also been described in AN motoneurons (Kloppenburg et al. 1999) and DUM neurons in cockroaches and locusts

(Grolleau and Lapied 1994; Brône et al. 2003). Additionally, persistent Na^+ currents have been investigated in a variety of mammalian neurons, including rat motoneurons (Li and Bennett 2003; Li et al. 2004), rat dorsal root ganglion neurons (Kiernan et al. 2003), rat neostriatum cells (Chao and Alzheimer 1995), human temporal lobe cells (Vreugdenhil et al. 2004) and mouse Purkinje cells (Carter et al. 2012). In all these mammalian cells, the persistent Na^+ currents were activated subthreshold to action potential generation at membrane voltages ranging from -70 to -50mV. The Na^+ currents in insects showed similar activation voltages, yet it is unclear whether the channels are similar. Nevertheless, Crill (1996) presented three hypotheses on the mechanisms for non-inactivating Na^+ channels that could also be valid for insect neurons: the window hypotheses suggests that only a few Na^+ channels are activated and the subset of Na^+ channels keep changing over the time, leading to a non-inactivating Na^+ current which would be consistent with the Hodgkin-Huxley model (Hodgkin and Huxley 1952). The second hypotheses suggests a rare and different type of Na^+ channel as described in Purkinje cells (Llinàs and Sugimori 1980). Finally, it is possible that the same channel displays different inactivation modalities (Alzheimer et al. 1993) and switches between fast and slow inactivation. Whether one of these theories applies for honeybee PNs has to be investigated in further detail. Apart from its still unclear mechanism, the persistent Na^+ current is present in honeybee PNs, AN motoneurons and cockroach DUM neurons leaving room for speculation about its potential functions. In vertebrates, it is thought to contribute slightly to action potential generation and to slightly depolarization of neurons and thus may contribute to subthreshold membrane oscillations (Crill 1996). Furthermore, in olfactory bulb cells of rats, persistent Na^+ currents have been shown to be located in close vicinity to K_{Na} channels to provide the necessary Na^+ ions for the activation of the K^+ channels (Hage and Salkoff 2012). We suggest a similar function in honeybee PNs as we could show that these neurons have $K_{Na\ p}$ currents that open in a mainly voltage-dependent manner, but also require intracellular Na^+. The persistent, yet small Na^+ currents would allow opening of the $K_{Na\ p}$ channels, but the number of opened channels would depend on the membrane voltage.

Na^+ dependent K^+ currents

We observed two types of K_{Na} currents, a fast deactivating transient current and a persistent current. The fast transient current activates at -40mV and increases until -10mV to reach a maximal current plateau. The voltage dependence of this current fits well with its dependence on Na^+. It activates at membrane voltages only slightly above the Na^+ current activation voltage.

Additionally, the plateau value is reached at the voltage level, at which the Na^+ current declines. Whether the $K_{Na\ t}$ current is purely Na^+ dependent or also voltage dependent could not be clarified with our recordings. Therefore, further experiments changing the ion concentrations and thus the reversal potential of Na^+ ions are necessary. $K_{Na\ t}$ currents have been described in DUM neurons in cockroaches (Grolleau and Lapied 1994), and are thought to contribute to the limitation of action potential duration (Grolleau and Lapied 2000). *Manduca sexta* AL neurons (Mercer and Hildebrand 2002) as well as cricket Kenyon cells also possess $K_{Na\ t}$ currents (Aoki et al. 2008). In both *Manduca* and crickets the function of $K_{Na\ t}$ currents is still unclear, yet the most realistic hypothesis so far is that they modulate the shape and duration of APs. Furthermore, these currents have been described in a variety of vertebrate neurons: in bursting neocortical neurons, $K_{Na\ t}$ currents are mainly responsible for the postexcitatory hyperpolarization (Franceschetti et al. 2003), whereas in weakly electric fish $K_{Na\ t}$ currents reduce AP duration and facilitate high spiking frequencies. In honeybee PNs, the $K_{Na\ t}$ currents make up for approximately half of the amplitude of the transient K^+ currents. PNs are known for relatively high firing rates of up to 110Hz (Brill et al. 2013), but do not reach especially high spiking frequencies. Taking this together, we conclude that $K_{Na\ t}$ currents may contribute to postexcitatory hyperpolarization as well as the limitation of AP duration in honeybees. Persistent K_{Na} currents in honeybees are relatively small compared to the transient currents and activate at membrane voltages of about -30mV. In contrast to the transient currents, persistent K_{Na} currents show a linear I-V relation. These currents have also been found in different insect species including cricket KCs (Inoue et al. 2014) and DUM neurons (reviewed in Grolleau and Lapied 2000), yet their functions were not addressed so far. $K_{Na\ p}$ currents in cultured tufted cells of the olfactory bulb of rats are thought to reliably re- or hyperpolarize neurons, as they neither deactivate over time nor with increasing membrane voltage. They seem to achieve the linear I-V relation by close spatial proximity, which allows activation by local Na^+ ion inflow, which is not hindered by the cytosolic Na^+ gradient or the electrical gradient (Budelli et al. 2009). Similar functions can be imagined in the honeybee.

Ca^{2+} currents

In our study Ca^{2+} currents were measured after blocking Na^+ currents with TTX. As K^+ currents were not especially blocked, the full magnitude of the Ca^{2+} currents could not be investigated in our studies. However, it seems that honeybee PNs possess a transient Ca^{2+} current, which appears at -30 to -20mV. Ca^{2+} currents activating at voltages above -30mV are generally

classified as high voltage activated (HVA) Ca^{2+} channels. Yet, we also suppose that Ca^{2+} currents with lower activation thresholds are present in PNs, as K_{Ca} currents were shown to activate already at lower membrane voltages. To determine activation thresholds and dynamics of Ca^{2+} currents, further experiments are necessary. Using tail-current analysis, we could identify a persistent Ca^{2+} current with similar activation voltages. Whether the two observed Ca^{2+} currents are two distinct currents or the inactivation of the transient Ca^{2+} current is just a result of the activation of the Ca^{2+} dependent transient K^+ current remains to be investigated. Ca^{2+} channels are definitely present in PNs, as a lot of Ca^{2+} imaging studies confirm (i.e. Carcaud et al. 2012). Various types of HVA Ca^{2+} channels are expressed in honeybee neurons (reviewed by Quintavalle 2013) and therefore are highly probable to be expressed in PNs. The role of Ca^{2+} channels has been investigated in many species including the honeybee and Ca^{2+} channels are especially important in memory formation (Perisse et al. 2009). Additionally, Ca^{2+} can activate intracellular second messengers (Sah and Faber 2002) and activate a variety of molecules including CAMKinase II (expressed in honeybee cells Pasch et al. 2011) and Ca^{2+} dependent K^+ channels. Modulation of the intracellular Ca^{2+} concentration is one of the most potent way of adjusting neuronal function (see for example Ca^{2+} dependent K^+ channels reviewed by Wicher et al. 2001).

Ca^{2+} dependent K^+ currents

As well as for K_{Na} currents, we did observe a transient and a persistent K_{Ca} current. The transient as well as the persistent K_{Ca} current both activated at membrane voltages between -40 and -30mV. The $K_{Ca\ t}$ current rises after activation and reaches a plateau at around -10 to 10mV membrane voltage. In contrast to the persistent K_{Na} channel conductance, the $K_{Ca\ t}$ channel conductance reaches its half maximal activation value already between -20 and -10mV, which is likely due to the reversal potential of Ca^{2+} at 21.3 mV. Both K_{Ca} currents are not purely Ca^{2+} dependent, but also voltage dependent, as no decrease of the current above 21.3mV was observed. The activation membrane voltage, the existence of a transient and a persistent component as well as the plateau reached by the transient current and the linear I-V relation of the persistent component are all properties of the pSlo subunit of the big K^+ conductance (BK) channel described in cockroach DUM neurons in detail by Derst et al. (2003). A similar current was observed in cultured AL neurons recorded by Perk and Mercer (2006). However, in cultured honeybee PN recordings from Grünewald (2003) no such current was observed. Instead, the K_{Ca} current exhibited a descriptive N-form in the I-V plot (Grünewald (2003),

which is typical for small K^+ conductance (SK) K_{Ca} currents that are purely Ca^{2+} dependent and not voltage-dependent (reviewed by Adelman et al. 2012). We did not observe an N-shape of the K^+ current, therefore we conclude that PNs do not or only at a minimal level express SK currents. Apart from the general difference to the *in-situ* situation we have no comprehensive explanation for these differences with recordings of cell cultured PNs by Grünewald (2003). The transient ($K_{Ca\,t}$) and the persistent ($K_{Ca\,p}$) component indicate the presence of two different BK channel subunits, similar to the α- and β-subunit of human cells (Zeng et al. 2007). To finally determine the nature of the K_{Ca} channels, specific pharmacological blocking with Apamin, a selective SK channel blocker, and Iberiotoxin, a selective BK channel blocker (Sah and Faber 2002), are necessary. Nevertheless, our results suggest that the K_{Ca} current we recorded in honeybee PNs is a BK current. The functional implications of the BK currents have been studied in cockroach DUM neurons in detail. The transient component of the BK current is involved in the shaping of APs, the total time of the AP (Wicher et al. 2006) and the magnitude of the post AP hyperpolarization (Derst et al. 2003). Similar effects of the transient component have been found in different mammalian cells including mouse motoneurons (Lin et al. 2014b) and rat amygdala cells (Faber and Sah 2002). These regulatory tasks of the transient component fit well with our data, as the transient component we recorded is very fast and has a rather large amplitude, which could directly influence these AP properties. The persistent component of the BK current has been reported to influence the interval between two consecutive APs (Wicher et al. 2006).

Purely voltage-dependent K^+ currents

After blocking K_{NA} and K_{Ca} currents with TTX and CdCl2, we still observed voltage dependent outward currents. In most of the neurons, a transient outward current activating between -50 and -40mV, which showed slower activation and inactivation than under standard conditions, could be observed. Furthermore, we found a persistent outward current activating between -40 and -30mV. Both these currents have been observed in cultured AL neurons by Perk and Mercer (2005), although activating at slightly higher membrane voltages. In contrast, in *in-situ* measurements in cockroaches transient and persistent outward currents that activate at slightly lower negative membrane voltages were measured (Grolleau and Lapied 1995). In both studies, the transient outward current was classified as an A-type K^+ current sensitive to 4-Aminopyridin (4-AP), the persistent outward current was sensitive to quinidine (Grolleau and Lapied 1995; Perk and Mercer 2005). We assume that honeybee PNs exhibit similar currents,

although pharmacological blocking with 4-AP and quinidine will be necessary to definitely clarify their presence. The slightly slower activation and inactivation of the transient A-type K^+ current compared to the transient K_{Na} and K_{Ca} currents indicates that it does not play a role in forming the shape or regulating the duration of APs by directly hyperpolarizing the membrane. It is more likely to contribute to re- and hyperpolarization after a longer phase of pronounced depolarization induced by excitatory synaptic input and could therefore regulate the spiking frequency. This function of the A-type K^+ current was also suggested for cockroach DUM neurons (Grolleau and Lapied, 1995). The persistent K_V could be involved in re- and hyperpolarizing the membrane during even more prolonged depolarization, when the A-type current is already inactivated.

Influences of ionic currents on PN functionality

The subset of currents that we observed in PNs is relatively similar to currents observed in cockroach DUM neurons (reviewed by Grolleau and Lapied 2000). The kinetics and activation of all observed currents as well as their probable function was similar to either DUM neuron currents and/or currents known from other animals, including vertebrate neurons and cell cultured neurons. In short: honeybee PNs do have a transient Na^+ current, a persistent Na^+ current, a transient Ca^{2+} current, a persistent Ca^{2+} current, a transient K_{Na} current, a persistent K_{Na} current, a two-phasic BK current, an A-type K^+ current and a persistent K_V current (Fig. 15a). The transient Na^+ current should be responsible for the depolarization phase of the AP, the persistent Na^+ current should counteract extreme hyperpolarization and also keep voltage dependent K_{Na} currents activated. The transient part of the K_{Na} current and the BK current are likely to reduce AP duration and re- and hyperpolarize the membrane. The persistent part of the K_{Na} current and the BK current, the K_{Na} and the persistent KV are likely to hyperpolarize the membrane between APs and to increase the time between two APs. Taken together, this ensemble of properties makes PNs well suited as neurons with relatively high response and spontaneous AP frequencies, which can respond reliably to synaptic input. The phasic-tonic response pattern observed frequently in intracellular and extracellular recordings of PNs (Abel et al. 2001; Müller et al. 2002; Krofczik et al. 2008; Strube-Bloss et al. 2011; 2012; Brill et al. 2013) can be easily explained with this set of ion channels. After odor stimulation, OSNs will excite PNs and cause high AP frequencies, which are supported by transient K_{Na} and K_{Ca} currents decreasing the time of single APS. The excitation will lead to increases in the cytosolic Na^+ and Ca^{2+} levels, persistent K_{Na} and K_{Ca} and K_V channels will open. The K^+ mediated

hyperpolarization will slightly counteract the excitatory input and will thus decrease the phasic odor response to the tonic response. Strong synaptic input will result in a high response AP frequency, which will lead to fast increases in the cytosolic Na^+ and Ca^{2+} levels and thus afterwards a strong hyperpolarization. Pure tonic responses are likely to be caused by either low concentration stimulation or by a low binding probability of the stimulation odor to the receptors on the OSNs, which form synapses with the recorded PN. The AP-burst hyperpolarization response pattern recorded by Müller et al. (2002) can also be explained with the mechanism of hyperpolarization through persistent K_{Na} and K_{Ca} and K_V channels. This pattern was only found in one PN study (Müller et al. 2002), yet most other studies used lower odor concentrations for stimulation (Krofczik et al. 2008; Strube-Bloss et al. 2011; 2012; Brill et al. 2013). After lower concentration stimulation, less persistent excitation will also result in the opening of less K_{Na} and K_{Ca} and no hyperpolarization will be present in the recordings. Similar bursting patterns have been observed in moth after pheromone stimulation (Chaffiol et al. 2012). As moths are extremely sensitive for the pheromone, this fits well with our theory. Strong PN activation will lead to an intrinsic hyperpolarization mechanism, which even causes post-AP –burst inhibition in extreme cases. Although we could show the ionic basis for such a mechanism, LNs may also be the source for the post-burst hyperpolarization. Additional support for the intrinsic hypothesis comes from the fact that some neurons change their spontaneous activity pattern from regular to bursting after stimulation, which indicates elevated Na^+ and Ca^{2+} levels that lead to longer hyperpolarizations and AP frequency oscillations. Nevertheless, a combination of negative feedback via GABAergic LNs and hyperpolarization via K_{Na}, K_{Ca} and K_V currents is most likely. Furthermore, modulation of the firing frequency should be possible on different modulatory channels: both phases of BK currents were shown to be inhibited by dopamine (Perk and Mercer 2006), which could lead to a less pronounced hyperpolarization between two APs and thus higher spiking frequencies (Fig. 15b). Furthermore, AKH1 (adipokinetic hormone) was shown to negatively affect transient Na^+ currents and to positively affect transient and persistent Ca^{2+} channels in cockroach DUM neurons (Wicher et al. 2006). AKH1 modulation of PNs could thus lead to increased spiking frequencies due to shortened AP duration by a more pronounced BK channel activation. If AKH1 influences BK channels and if it is present at all in honeybees remains to be investigated.

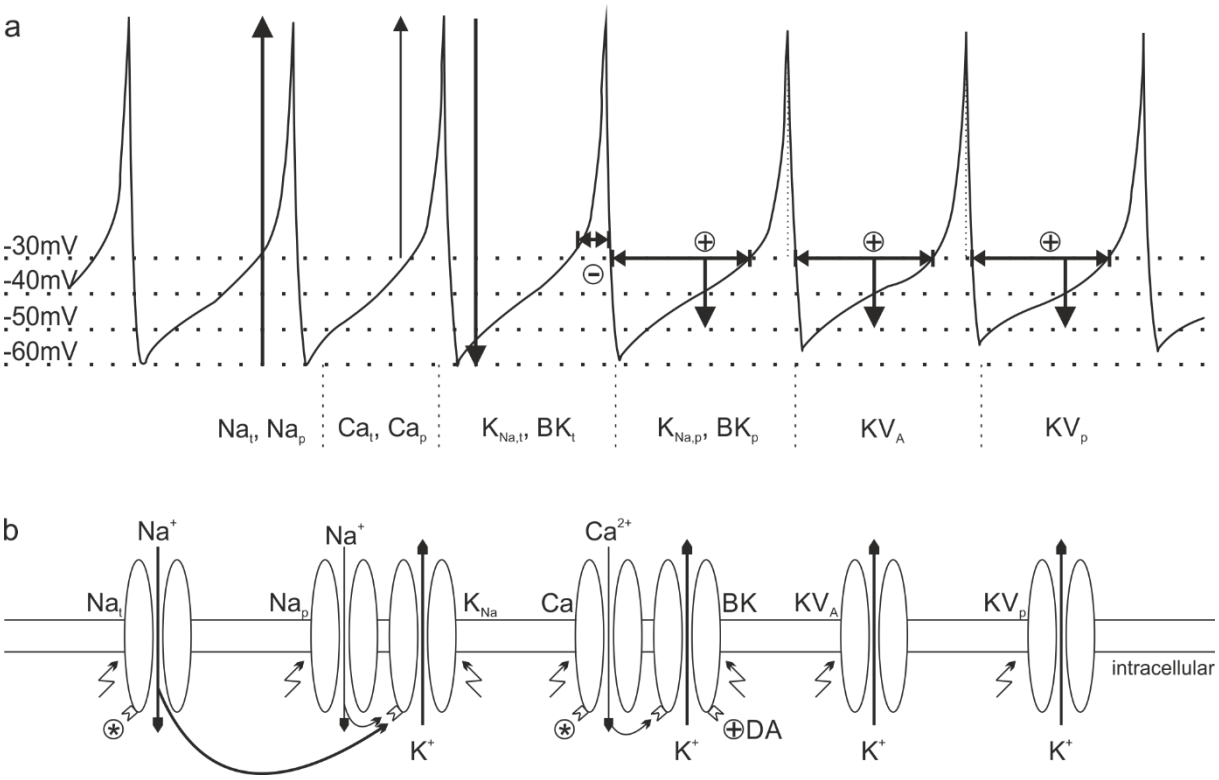

Fig. 15 Comprehensive model of the currents recorded in projection neurons (PN). **a** Action potential trace with membrane voltage levels. The activation voltages and major tasks of the different ionic currents are indicated. Transient (Na_t) and persistent Na^+ (Na_p) currents depolarize the membrane. Transient (Ca_t) and persistent Ca^{2+} (Ca_p) currents also depolarize the membrane, yet are more important for the activation of K^+ currents and modulation. The two fast transient Ca^{2+} dependent K^+ currents ($K_{Na,t}$, BK_t) hyperpolarize the neuron right after activation and reduce action potential (AP) duration. The persistent Ca^{2+} dependent K^+ currents ($K_{Na,p}$, BK_p) generally hyperpolarize the membrane. Voltage-dependent K^+ currents hyperpolarize the membrane and may increase the time between two successive APs. **b** Basis of the activation of the currents implemented in **a**. The lightning symbols mark voltage dependency of a current. The binding pockets show Na^+ dependent or Ca^{2+} dependent activations and possible targets for modulation (*) with, for example dopamine (*DA*,+).

Differences in neuronal coding between m- and lALT

Generally, we did not find major differences concerning the qualitative presence of currents, activation thresholds of currents, resting membrane voltages and cell capacitances between the two tracts. All currents investigated by us are probably non-synaptic currents, as reviewed by Wicher et al. (2001). Both m- and lALT PNs were shown to spontaneously generate APs and to respond with different AP patterns to odor stimulation (Müller et al. 2002; Krofczik et al. 2008; Strube-Bloss et al. 2011; Brill et al. 2013). Therefore, PNs of both tracts do need ion channels, which support rapid de- and hyperpolarization in order to maintain high frequencies and to be able to respond appropriately to synaptic input. The ion channels shown in our

recordings and discussed above seem to be perfectly suited for this task, thus it fits well that these channels are present in PNs of both tracts. In a more detailed analysis of activation thresholds, maximal voltages and the conductance, small differences between the neurons of the two tracts appeared. These differences in the slope of the I-V plots and the G/Gmax plots were most prominent in BK currents: lALT PNs had lower thresholds, lower half maximal activation and lower maximal voltages of K_{Ca} currents. Such BK currents were shown to be negatively affected by dopamine (Perk and Mercer 2005) and were shown to positively affect AP frequency in DUM neurons, as they shorten AP duration (Wicher et al. 2006). Taken this together, dopaminergic modulation of BK channels might decrease BK currents in mALT PNs and thus lead to lower AP frequencies as observed in extracellular recordings (Brill et al. 2013). The explanation of the differences between the two tracts by neuronal modulation instead of basic qualitative differences in ion channels between the two sets of neurons also explains individual neuronal variance. Whether these hypotheses are indeed true, needs to be validated by further experiments, as the quality of the recordings can also affect the different parameters of the observed currents. Additionally, the differences between the two tracts in terms of spontaneous activity and odor response frequencies (Brill et al. 2013) can be due to differences in synaptic connectivity of OSNs, LNs and PNs or due to differences in the synaptic currents. OSNs of a specific type of olfactory sensillum (*Sensillum basiconicum*) were already shown to project preferentially to mALT associated glomeruli. Furthermore, axons of these OSNs seem to be thicker than OSNs from other sensilla (Kropf et al. 2014). This shows that the connectivity of OSNs and PNs may vary between the two tracts. Honeybee LNs vary drastically in their shape and response pattern (Meyer and Galizia 2012) and are thus also likely to affect odor coding in PNs and could lead to differences between the two PN tracts. The hints for differences in wiring together with the fact that we did not find any differences in non-synaptic currents between the two tracts let us assume that the differences between the two tracts are most likely due to differences in the neuronal wiring and to neuronal modulation via LNs.

Electrophysiological properties of KCs

General KC properties

The KCs in our experiments had mean membrane resting potentials ranging from -42 to -58mV and a mean capacitance of 6.5pF. As in PNs, we suppose that the membrane potential will be lower when the neuron is not injured, thus we expect membrane potentials of -60 to -65mV, which would be consistent with the mean potential (-62.1mV) in other *in situ* recordings of honeybee KCs (Palmer et al. 2013). Several *in vitro* studies with primary cultures of honeybee KCs were conducted so far. The mean membrane resting potential was only published once with a value of -84.7mV (Wüstenberg et al. 2004), mean capacitances ranged from 2.6 to 4.1pF (Schäfer et al. 1994; Grünewald 2003; Wüstenberg et al. 2004). The capacitance measured in situ by Palmer et al. (2013) amounted 3.2pf. So far, we have no satisfying explanations for the differences in cell capacitance.

Ionic currents of KCs

Under standard conditions, KCs exhibit a fast inward current, which is likely to be a Na^+ current. The outward currents can be roughly divided in a transient K^+ current with an A-shaped form and a persistent current which has a non-linear I-V relation leading to an N-shaped form of the I-V plot. The A-type K^+ current activates at -45mV, the Na^+ and the persistent K^+ current activate at approximately -40mV. The activation voltages of the currents as well as the basic shape of the I-V plots is consistent with the I-V plots obtained from KCs in cell culture (Schäfer et al. 1994; Pelz et al. 1999; Grünewald 2003) and *in situ* in isolated brain preparations (Palmer et al. 2013). The only prominent difference is that no N-shape was observed in cell cultured KCs by Grünewald (2003).

A-type K^+ current in KCs

The most prominent current observed in the KC recordings was the transient A-type K^+ current. This current activates at approximately -45mV and increases linearly in a voltage dependent manner. It remains almost unaffected by blocking of Na^+ channels with TTX and blocking of Ca^{2+} channels with $CdCl_2$. Under standard conditions, this current is about twice as large as the persistent K^+ current and about 20x larger than the Na^+ current. The A-type K^+ current was investigated in great detail in cell cultured honeybee PNs (Pelz et al. 1999). The activation

threshold as well as the dynamics of the A-type current are relatively similar in all studies on primary KC cultures (Schäfer et al. 1994; Pelz et al. 1999; Grünewald 2003) and fit well with our data. Although the A-type current is a fast transient activating current in honeybees, its activation is marginally slower than the activation of the Na^+ and Ca^{2+} dependent transient currents in PNs. Especially the deactivation lasts much longer than the deactivation of the transient currents in PNs. With its slightly slower kinetics compared to PN transient K^+ currents, we think that the A-type current does not contribute as much to AP shaping but rather inhibits the neuron after synaptic input and thus contributes to the sparse information coding in the MBs.

Na^+ and Ca^{2+} sensitive currents in KCs

After blocking Na^+ and Ca^{2+} currents, no inward current was present anymore. The transient K^+ current was slightly reduced, yet the dynamics of the transient current were not affected. Thus, we conclude that the transient current is carried only to a minor degree by either Ca^{2+} or Na^+ sensitive K^+ channels. Furthermore, the persistent outward current was drastically reduced in amplitude and did not display the typical N-shaped form in the I-V plot anymore. The N-shape is normally caused by voltage independent K_{Ca} currents channels (Hirschberg et al. 1998), which are mostly termed SK channels (Adelman et al. 2012). The Ca^{2+} influx after depolarization ends when the equilibrium potential for Ca^{2+} ions is reached. Above this membrane potential, the K_{Ca} current will also decrease, which will lead to an N-form in the I-V plot. This typical shape has been reported both in honeybee KC primary cultures (Schäfer et al. 1994) as well as *in situ* isolated brain preparations (Palmer et al. 2013). Although this shape did not appear in cultured KCs (Grünewald 2003), we assume that it is an important current in honeybee KCs. SK channels have been studied in various species so far, yet their clear functions remain uncertain (reviewed by Adelman et al. 2012). Similar K_{Ca} currents were found in cockroaches, yet their amplitude was about twice as large as the amplitude of the A-type K^+ current (Demmer and Kloppenburg 2009). Because of the huge Ca^{2+} currents and the rather large K_{Ca} currents they found, Demmer and Kloppenburg (2009) argue that the K_{Ca} channels are likely to contribute to sparse odor coding in cockroach KCs. As the A-type K^+ current is almost twice as large as the persistent K_{Ca} in honeybees, we suppose that in honeybees sparse odor coding is more likely to be influenced by the A-type K^+ current. Other functions of SK channels have been described in vertebrates: although the mechanism is unclear, SK channels were shown to be inhibited after muscarinic acetylcholine receptor activation (Buchanan et al.

2010; Giessel and Sabatini 2010). The block of the SK channels was followed by an increase of the amplitude of synaptic potentials and therefore facilitated long term potentiation (LTP) (Giesel and Sabatini 2010). KCs are the cell type, which is mainly associated with learning and memory in insects (reviewed by Heisenberg 2003). Together with the modulation of muscarinic acetylcholine receptors, which leads to more dendritic arborizations in honeybees (Dobrin et al. 2011), this gives support to the hypothesis that muscarinic modulated SK channels in honeybee KCs mediate LTP and thus also synaptic plasticity.

Impact of ionic currents on KC functionality

Generally, KCs in insects are thought to act as coincidence detectors exhibiting synaptic plasticity after simultaneous input from PNs, which may even convey information from different sensory modalities (Perez-Orive et al. 2004; Gupta and Stopfer 2011; Dubnau 2012; Rössler and Brill 2014). To achieve good coincidence detection properties and a pronounced spatial separation of information, neurons need to encode information in a spatially and temporally sparse fashion. After the integration of information from different sensory modalities, specific synaptic connections can be strengthened, which than lead to the establishment of long-term memory traces. The MBs are well known for synaptic plasticity (Hourcade et al. 2010; Stieb et al. 2010) and therefore likely to be the major center of learning and the formation of long-term memory.

Sparse coding

The huge A-type K^+ current observed in honeybees can serve perfectly for the generation of sparse stimulus representations ending already shortly after stimulus onset (Fig. 16). KCs in honeybees have been shown to respond only to the stimulus onset (Szyszka et al. 2005, Froese et al. 2014), even though the odor responses of PN axonal boutons lasted during the whole odor stimulation (Szyszka et al. 2005). This change in stimulus representation can be caused by the huge voltage dependent A-type currents in KCs. Additionally, KCs are inhibited by SK channels. Yet SK channels have much slower activation kinetics than the A-type current, therefore they are less likely to cause the shortening of stimulus responses. Instead, they might contribute to the hyperpolarization at times when no APs are generated and might impede the generation of new APs. Honeybee KCs also receive GABAergic input in the MBs, which could also lead to self-inhibition after odor stimulation (Palmer and Harvey 2014). Yet Froese et al.

(2014) could show that blocking of the fast ionotropic part of the GABA response did not affect the fast termination of odor responses. Whether dominant A-type currents generally promote sparse coding remains to be investigated. In at least one type of *Drosophila* KCs, the A-type K^+ current is also the most prominent current (Gasque et al. 2005). In Ca^{2+} imaging experiments, *Drosophila* KCs do seem to respond less sparse than honeybee KCs (Lei et al. 2013; Li et al. 2013). Yet in whole cell patch clamp studies *Drosophila* KCs also exhibit temporally sparse and fast odor responses (Turner et al. 2008; Murthy and Turner 2013). One reason for this difference might be that the Ca^{2+} sensor, G-CaMP, was genetically expressed (Lei et al. 2013; Li et al. 2013) and might be too abundant in the cells, which could lead to artificially prolonged odor responses. We therefore conclude that *Drosophila* KCs may also employ temporal sparse coding, which is at least partly achieved by a prominent A-type current similar to honeybees. The whole cell currents of a few other insects have been studied (cockroaches: Demmer and Kloppenburg 2009; crickets: Terazima and Yoshino 2010; Inoue et al. 2014; silkmoths: Tabuchi et al. 2012). Although only cockroach KCs have been shown to employ sparse odor coding, it is highly likely that KCs of other insects also encode information in a sparse fashion. Besides *Drosophila*, none of the other species with identified KC currents exhibits similar current-ratios of transient K^+ currents to persistent K^+ currents to the honeybee. Under standard conditions, the current set of cricket KCs (Terazima and Yoshino 2010; Inoue et al. 2014) resembles the currents of honeybee PNs or cockroach DUM neurons (reviewed by Grolleau and Lapied 2000). Silkmoth KCs do, under standard conditions, not exhibit prominent transient K^+ currents at all (Tabuchi et al. 2012). In cockroaches, A-type K^+ currents were observed, yet they do not dominate the I-V plots comparable to the situation in the honeybee. Instead, cockroaches display large SK currents in KCs, which could serve the generation of a sparse code (Demmer and Kloppenburg 2009). Nevertheless, no physiological data after odor stimulation is available for silkmoth or cricket KCs, therefore we cannot be sure whether these insects really exhibit such a sparse temporal code as it is the case in the honeybee. We finally conclude that honeybee KCs and *Drosophila* KCs employ sparse odor coding and thus need a pronounced A-type current, which directly hyperpolarizes the membrane after stimulation. We expect a similar current profile in locusts, as their KCs also generate APs in an extremely sparse fashion. Whether the other species, which do not employ such a dominant A-type current, exhibit extremely sparse odor responses remains to be investigated. The example of sparse coding in cockroach KCs shows that there are at least two mechanism to generate sparse coding with intrinsic neuronal properties (Demmer and Kloppenburg 2009). The different ionic currents

observed in crickets (Terazima and Yoshino 2010; Inoue et al. 2014) and silkmoths (Tabuchi et al. 2012) imply that even more mechanisms might be possible.

Additionally to the temporal sparseness of stimulus representation, the spatial sparseness, which is a measure for the number of KCs, which respond to the same stimulus, is also important. Honeybee KCs were shown to receive GABAergic input (Palmer and Harvey 2014) via feedback neurons. In *Drosophila*, blocking of feedback neurons in the MBs led to a less sparse spatial coding in the MBs (Lin et al. 2014a). Different types of feedback neurons have been morphologically described in the honeybee and were shown to branch over the whole calyx (Grünewald 1999). Taking this together, we conclude that feedback neurons inhibit KCs in a negative feedback loop and are thus responsible for creating a potentially spatially sparse representation of stimuli in the MBs, whereas the temporally sparse code is caused by intrinsic neuronal properties.

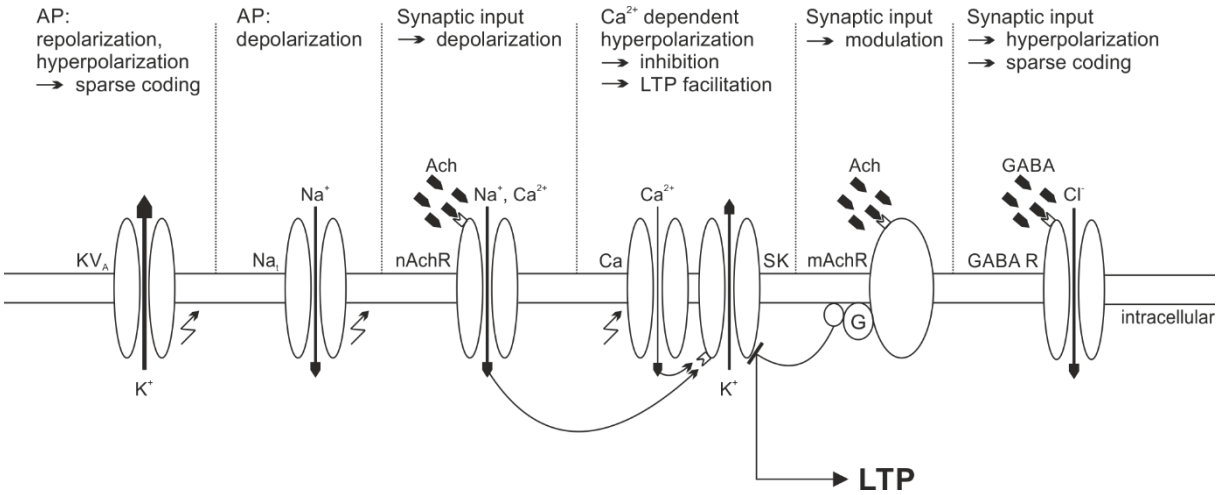

Fig. 16 Comprehensive model of the potential influence of currents recorded in Kenyon cells on information coding and learning and memory. The lightning symbol marks voltage dependencies of a current, the intracellular binding pockets show Ca^{2+} dependent activations. The extracellular binding pockets indicate neurotransmitter receptors. Synaptic input will depolarize the neuron through nicotinic acetylcholine receptors (*nAchR*), action potentials (*AP*) are potentially generated by Na^+ channels. Voltage-dependent, transient K^+ currents (KV_A) hyperpolarize the neuron immediately and ensure the temporally sparse code. Ca^{2+} dependent K^+ channels (*SK*) hyperpolarize the neuron after the transient K^+ currents and prevent excitation. Acetylcholine (*Ach*) may bind to muscarinic acetylcholine receptors (*mAchR*), which inhibit SK channels via a G-protein coupled cascade. This allows follow-up excitation and therefore may promote long term potentiation (*LTP*). GABAergic activation of GABA receptors (*GABA R*) will hyperpolarize the cell and regulate its excitability to regulate spatially sparse coding.

Ion channels and learning and memory

The most important role of the MBs according to insect literature is the formation of memory (for example: Gerber et al. 2004; Davis 2005; Giurfa 2007; Hourcade et al. 2010; Cervantes-Sandoval et al. 2013). The knowledge about the exact neuronal mechanisms of learning and memory is mainly fragmental, yet it is highly likely that sufficient neuronal activation leads to increases in the cytosolic Ca^{2+} level, which than triggers Ca^{2+} dependent kinases that activate protein synthesis (for a broad overview of potential mechanisms see Kandel et al. 2014). Strong simultaneous input from neurons transmitting information about different modalities should depolarize the neuron sufficiently. But, as honeybee KCs possess A-type K^+ channels, SK channels and GABAergic feedback neurons, which hyperpolarize the membrane, sufficient depolarization for the induction of synaptic plasticity is probably rare. Synaptic excitatory input to the KCs is mediated by acetylcholine and several nicotinic acetylcholine receptor subunits are expressed in the honeybee MBs (Dupuis et al. 2011). Nevertheless, modulation of muscarinic acetylcholine receptors has been shown to affect the volume changes in the MBs in honeybees (Ismail et al. 2006). Furthermore, Dobrin et al. (2011) could also show that activation or inhibition of the muscarinic acetylcholine receptor influences the dendritic growth of KCs, which indicates that muscarinic actylcholine receptors are also involved in learning and memory processes. In vertebrates, muscarinic acetylcholine receptors have been shown to inhibit SK channels via a G-protein coupled cascade (Buchanan et al. 2010; Giessel and Sabatini 2010). Inhibition of SK channels leads to LTP and can therefore help rising Ca^{2+} levels over a prolonged time which will finally lead to an increase of the dendritic arborizations. As the dendrites of honeybee KCs have been shown to grow after activation of muscarinic acetylcholine receptors (Dobrin et al. 2011) and we could show the presence of SK channels in KCs, we suppose a mechanism similar to the one in vertebrates. This would also fit well with data from cultured honeybee KCs, which did not exhibit ionic currents induced by muscarinic agonists (Wüstenberg and Grünewald 2004), as the mAchR-SK coupling hypotheses does not involve muscarinic activation of ion channels (Fig. 16).

Conclusion

Finally, we conclude that PNs of both the m- and the lALT do not differ in the quality of their ionic currents, which support their properties as spiking neurons (Fig. 15). Whether the differences between m- and lALT PNs are due to modulation or due to synaptic input or even both remains to be investigated. The currents observed in KCs support sparse coding and might provide a basis for processes involved in learning and memory (Fig. 16). To clarify these processes, further experiments are necessary.

References

Abel R, Rybak J, Menzel R (2001) Structure and response patterns of olfactory interneurons in the honeybee, *Apis mellifera*. J Comp Neurol 437:363–383

Ache BW, Young JM (2005) Olfaction: diverse species, conserved principles. Neuron 48:417–430

Adelman JP, Maylie J, Sah P (2012) Small-Conductance Ca(2+)-Activated K(+) Channels: Form and Function. Annu Rev Physiol 74:245-269

Alzheimer C, Schwindt PC, Crill WE (1993) Modal gating of Na+ channels as a mechanism of persistent Na+ current in pyramidal neurons from rat and cat sensorimotor cortex. J Neurosci 13:660–673

Aoki K, Kosakai K, Yoshino M (2008) Monoaminergic modulation of the Na+-activated K+ channel in Kenyon cells isolated from the mushroom body of the cricket (*Gryllus bimaculatus*) brain. J Neurophysiol 100:1211–1222

Brill MF, Rosenbaum T, Reus I, Kleineidam CJ, Nawrot MP, Rössler W (2013) Parallel Processing via a Dual Olfactory Pathway in the Honeybee. J Neurosci 33:2443–2456

Brône B, Tytgat J, Wang D-C, Van Kerkhove E (2003) Characterization of Na+ currents in isolated dorsal unpaired median neurons of *Locusta migratoria* and effect of the alpha-like scorpion toxin BmK M1. J Insect Physiol 49:171–182

Buchanan KA, Petrovic MM, Chamberlain SEL, Marrion, NV, Mellor, JR (2010) Facilitation of long-term potentiation by muscarinic M(1) receptors is mediated by inhibition of SK channels. Neuron 68:948–963

Budelli G, Hage TS, Wei A, Rojas P, Yuh-Jiin IJ, O'Malley K, Salkoff L (2009) Na+-activated K+ channels express a large delayed outward current in neurons during normal physiology. Nat Neurosci 12:745–50

Carcaud J, Hill T, Giurfa M, Sandoz JC (2012) Differential coding by two olfactory subsystems in the honeybee brain. J Neurophysiol 108:1106–1221

Carter BC, Giessel AJ, Sabatini BL, Bean BP (2012) Transient sodium current at subthreshold voltages: activation by EPSP waveforms. Neuron 75:1081–93

Cervantes-Sandoval I, Martin-Peña A, Berry JA, Davis RL (2013) System-like consolidation of olfactory memories in *Drosophila*. J Neurosci 33:9846–54

Chaffiol A, Kropf J, Barrozo RB, Gadenne CG, Rospars JP, Anton S (2012) Plant odour stimuli reshape pheromonal representation in neurons of the antennal lobe macroglomerular complex of a male moth. J Exp Biol 215:1670–1680

Chao TI, Alzheimer C (1995) Do neurons from rat neostriatum express both a TTX-sensitive and a TTX-insensitive slow Na+ current? J Neurophysiol 74:934–941.

Crill WE (1996) Persistent sodium current in mammalian central neurons. Annu Rev Physiol 58:349–362.

Davis RL (2005) Olfactory memory formation in *Drosophila*: from molecular to systems neuroscience. Annu Rev Neurosci 28:275–302

Deisig N, Giurfa M, Sandoz JC (2010) Antennal lobe processing increases separability of odor mixture representations in the honeybee. J Neurophysiol 2185–2194

Demmer H, Kloppenburg P (2009) Intrinsic membrane properties and inhibitory synaptic input of kenyon cells as mechanisms for sparse coding? J Neurophysiol 102:1538–1550

Derst C, Messutat S, Walther C, Eckert M, Heinemann SH, Wicher D (2003) The large conductance Ca2+-activated potassium channel (pSlo) of the cockroach *Periplaneta americana*: structure, localization in neurons and electrophysiology. Eur J Neurosci 17:1197–1212

Dobrin SE, Herlihy JD, Robinson GE, Fahrbach SE (2011) Muscarinic regulation of Kenyon cell dendritic arborizations in adult worker honey bees. Arthropod Struct Dev 40:409–419

Dubnau J (2012) Ode to the Mushroom Bodies. Science 335:664–665

Dupuis JP, Gauthier M, Raymond-Delpech V (2011) Expression patterns of nicotinic subunits α2, α7, α8, and β1 affect the kinetics and pharmacology of ACh-induced currents in adult bee olfactory neuropiles. J Neurophysiol 106:1604–13

Esslen J, Kaissling K (1976) Zahl und Verteilung antennaler Sensillen bei der Honigbiene *Apis mellifera* L. Zoomorphologie 83:227–251

Faber ESL, Sah P (2002) Physiological role of calcium-activated potassium currents in the rat lateral amygdala. J Neurosci 22:1618–1628

Fadool DA, Wachowiak M, Brann JH (2001) Patch-clamp analysis of voltage-activated and chemically activated currents in the vomeronasal organ of *Sternotherus odoratus* (stinkpot/musk turtle). J Exp Biol 204:4199–4212

Franceschetti S, Lavazza T, Curia G, Aracri P, Panzica F, Sancini G, Avanzini G, Magistretti J (2003) Na+-activated K+ current contributes to postexcitatory hyperpolarization in neocortical intrinsically bursting neurons. J Neurophysiol 89:2101–11

Froese A, Szyszka P, Menzel R (2014) Effect of GABAergic inhibition on odorant concentration coding in mushroom body intrinsic neurons of the honeybee. J Comp Physiol A 200:183–195

Fusca D, Husch A, Baumann A, Kloppenburg P (2013) Choline acetyltransferase-like immunoreactivity in a physiologically distinct subtype of olfactory nonspiking local interneurons in the cockroach (*Periplaneta americana*). J Comp Neurol 521:3556–3569

Galizia CG, Franke T, Menzel R, Sandoz JC (2012) Optical imaging of concealed brain activity using a gold mirror in honeybees. J Insect Physiol 58:743–749

Galizia CG, Kimmerle B (2004) Physiological and morphological characterization of honeybee olfactory neurons combining electrophysiology, calcium imaging and confocal microscopy. J Comp Physiol A 190:21–38

Galizia CG, Kreissl S (2012) Neuropeptides in Honey Bees. In: Galizia CG, Eisenhardt D, Giurfa M (eds) Honeybee neurobiology and behavior— a tribute to Randolf Menzel. Springer, The Netherlands, pp 211–226

Galizia CG, McIlwrath SL, Menzel R (1999) A digital three-dimensional atlas of the honeybee antennal lobe based on optical sections acquired by confocal microscopy. Cell Tissue Res 295:383–394

Galizia CG, Rössler W (2010) Parallel olfactory systems in insects: anatomy and function. Annu Rev Entomol 55:399–420

Gao Q, Yuan B, Chess A (2000) Convergent projections of *Drosophila* olfactory neurons to specific glomeruli in the antennal lobe. Nat Neurosci 3:780–785

Gasque G, Labarca P, Reynaud E, Darszon A (2005) Shal and shaker differential contribution to the K+ currents in the *Drosophila* mushroom body neurons. J Neurosci 25:2348–2358

Gerber B, Tanimoto H, Heisenberg M (2004) An engram found? Evaluating the evidence from fruit flies. Curr Opin Neurobiol 14:737–744

Giessel AJ, Sabatini BL (2010) M1 muscarinic receptors boost synaptic potentials and calcium influx in dendritic spines by inhibiting postsynaptic SK channels. Neuron 68:936–947

Giurfa M (2007) Behavioral and neural analysis of associative learning in the honeybee: a taste from the magic well. J Comp Physiol A 193:801–824

Groh C, Tautz J, Rössler W (2004) Synaptic organization in the adult honey bee brain is influenced by brood-temperature control during pupal development. Proc Natl Acad Sci U S A 101:4268–4273

Grolleau F, Lapied B (1995) Separation and identification of multiple potassium currents regulating the pacemaker activity of insect neurosecretory cells (DUM neurons). J Neurophysiol 73:160–71

Grolleau F, Lapied B (1994) Transient Na(+)-activated K+ current in beating pacemaker-isolated adult insect neurosecretory cells (dum neurones). Neurosci Lett 167:46–50

Grolleau F, Lapied B (2000) Dorsal unpaired median neurones in the insect central nervous system: towards a better understanding of the ionic mechanisms underlying spontaneous electrical activity. J Exp Biol 203:1633–48

Grünewald B (1999) Morphology of feedback neurons in the mushroom body of the honeybee, Apis mellifera. J Comp Neurol 404:114–26

Grünewald B (2003) Differential expression of voltage-sensitive K+ and Ca2+ currents in neurons of the honeybee olfactory pathway. J Exp Biol 206:117–129

Gupta N, Stopfer M (2011) Insect olfactory coding and memory at multiple timescales. Curr Opin Neurobiol 21:768–773

Hage TA, Salkoff L (2012) Sodium-activated potassium channels are functionally coupled to persistent sodium currents. J Neurosci 32:2714–2721

Heidel E, Pflüger HJ (2006) Ion currents and spiking properties of identified subtypes of locust octopaminergic dorsal unpaired median neurons. Eur J Neurosci 23:1189–1206

Heisenberg M (2003) Mushroom body memoir: from maps to models. Nat Rev Neurosci 4:266–275

Hildebrand JG, Shepherd GM (1997) Mechanisms of olfactory discrimination: converging evidence for common principles across phyla. Annu Rev Neurosci 20:595–631.

Hille B (2001) The Superfamily of Voltage-Gated Channels. In Hille (ed) Ion Channels of Excitable Membranes, 3rd ed. Sinauer Associates Inc, Sunderland, U S A, pp 61-93

Hirschberg B, Maylie J, Adelman JP, Marrion N V (1998) Gating of recombinant small-conductance Ca-activated K+ channels by calcium. J Gen Physiol 111:565–581

Hodgkin AL, Huxley AF (1952) A quantitative description of membrane current and its application to conduction and excitation in nerve. Bull Math Biol 117:25–71

Homberg U, Christensen TA, Hildebrand JG (1989) Structure and function of the deutocerebrum in insects. Annu Rev Entomol 34:477–501

Homberg U, Montague RA a, Hildebrand JGG (1988) Anatomy of antenno-cerebral pathways in the brain of the sphinx moth *Manduca sexta*. Cell Tissue Res 254:255–821

Hourcade B, Muenz TS, Sandoz JC, Rössler W, Devaud JM (2010) Long-term memory leads to synaptic reorganization in the mushroom bodies: a memory trace in the insect brain? J Neurosci 30:6461–6465

Husch A, Paehler M, Fusca D, Paeger L, Kloppenburg P (2009) Distinct electrophysiological properties in subtypes of nonspiking olfactory local interneurons correlate with their cell type-specific Ca2+ current profiles. J Neurophysiol 102:2834–2845

Inoue S, Murata K, Tanaka A, Kakuta E, Tanemura S, Hatakeyama S, Nakamura A, Yamamoto C, Kosakai K, Yoshino M (2014) Ionic channel mechanisms mediating the intrinsic excitability of Kenyon cells in the mushroom body of the cricket brain. J Insect Physiol 68:44-57

Ismail N, Robinson GE, Fahrbach SE (2006) Stimulation of muscarinic receptors mimics experience-dependent plasticity in the honey bee brain. Proc Natl Acad Sci U S A 103:207–211

Ito K, Shinomiya K, Ito M, Armstrong JD, Boyan G, Hartenstein V, Harzsch S, Heisenberg M, Homberg U, Jenett A, Keshishian H, Restifo LL, Rössler W, Simpson JH, Strausfeld NJ,

Strauss R, Vosshall LB, Insect Brain Name Working Group (2014) A systematic nomenclature for the insect brain. Neuron 81:755–765

Kandel ER, Dudai Y, Mayford MR (2014) The molecular and systems biology of memory. Cell 157:163–186

Kiernan MC, Baker MD, Bostock H (2003) Characteristics of late Na(+) current in adult rat small sensory neurons. Neuroscience 119:653–660

Kirschner S, Kleineidam CJ, Zube C, Rybak J, Grünewald B, Rössler W (2006) Dual olfactory pathway in the honeybee, *Apis mellifera*. J Comp Neurol 499:933–952

Kloppenburg P, Kirchhof BS, Mercer AR (1999) Voltage-activated currents from adult honeybee (*Apis mellifera*) antennal motor neurons recorded in vitro and in situ. J Neurophysiol 81:39–48

Krofczik S, Menzel R, Nawrot MP (2008) Rapid odor processing in the honeybee antennal lobe network. Front Comput Neurosci 2:9

Kropf J, Kelber C, Bieringer K, Rössler W (2014) Olfactory subsystems in the honeybee: sensory supply and sex specificity. Cell Tissue Res 357:583–595

Lei Z, Chen K, Li H, Liu H, Guo A. (2013) The GABA system regulates the sparse coding of odors in the mushroom bodies of *Drosophila*. Biochem Biophys Res Commun 436:35–40

Li H, Li Y, Lei Z, Wang K, Guo A (2013) Transformation of odor selectivity from projection neurons to single mushroom body neurons mapped with dual-color calcium imaging. Proc Natl Acad Sci U S A 110:12084–12089

Li Y, Bennett DJ (2003) Persistent sodium and calcium currents cause plateau potentials in motoneurons of chronic spinal rats. J Neurophysiol 90:857–69

Li Y, Gorassini MA, Bennett DJ (2004) Role of persistent sodium and calcium currents in motoneuron firing and spasticity in chronic spinal rats. J Neurophysiol 91:767–83

Lin AC, Bygrave AM, de Calignon A, Lee T, Miesenböck G (2014a) Sparse, decorrelated odor coding in the mushroom body enhances learned odor discrimination. Nat Neurosci 17:559–568

Lin M, Hatcher JT, Wurster RD, Chen QH, Cheng ZJ (2014b) Characteristics of single large-conductance Ca2+-activated K+ channels and their regulation of action potentials and excitability in parasympathetic cardiac motoneurons in the nucleus ambiguus. Am J Physiol Cell Physiol 306:C152–166

LLinás R, Sugimori M (1980) Electrophysiological properties of in vitro purkinje cell dendrites in mammalian cerebellar slices. J Physiol 197–213

Mercer AR, Hildebrand JG (2002) Developmental changes in the density of ionic currents in antennal-lobe neurons of the sphinx moth, *Manduca sexta*. J Neurophysiol 87:2664–2675

Meyer A, Galizia CG (2012) Elemental and configural olfactory coding by antennal lobe neurons of the honeybee (*Apis mellifera*). J Comp Physiol A 198:159–171

Meyer A, Galizia CG, Nawrot MP (2013) Local interneurons and projection neurons in the antennal lobe from a spiking point of view. J Neurophysiol 110:2465–2474

Müller D, Abel R, Brandt R Zöckler M, Menzel R (2002) Differential parallel processing of olfactory information in the honeybee, *Apis mellifera* L. J Comp Physiol A 188:359–370

Murthy M, Turner G (2013) Dissection of the head cuticle and sheath of living flies for whole-cell patch-clamp recordings in the brain. Cold Spring Harb Protoc 2013:134–139

Narahashi T, Moore JW, Scott WR (1964) Tetrodotoxin Blockage of Sodium Conductance Increase in Lobster Giant Axons. J Gen Physiol 47:965–974

Palmer MJ, Harvey J (2014) Honeybee Kenyon cells are regulated by a tonic GABA receptor conductance. J Neurophysiol doi: 10.1152/jn.00180.2014

Palmer MJ, Moffat C, Saranzewa N, Harvey J, Wright GA, Connolly CN (2013) Cholinergic pesticides cause mushroom body neuronal inactivation in honeybees. Nat Commun 4:1634

Pasch E, Muenz TS, Rössler W (2011) CaMKII is differentially localized in synaptic regions of Kenyon cells within the mushroom bodies of the honeybee brain. J Comp Neurol 3712:3700–3712

Pelz C, Jander J, Rosenboom H, Hammer M, Menzel R (1999) IA in Kenyon cells of the mushroom body of honeybees resembles shaker currents: kinetics, modulation by K+, and simulation. J Neurophysiol 81:1749–1759

Perez-Orive J, Bazhenov M, Laurent G (2004) Intrinsic and circuit properties favor coincidence detection for decoding oscillatory input. J Neurosci 24:6037–6047

Perisse E, Raymond-Delpech V, Néant I, Matsumoto Y, Leclerc C, Moreau M, Sandoz, JC (2009) Early calcium increase triggers the formation of olfactory long-term memory in honeybees. BMC Biol 7:30

Perk CG, Mercer AR (2006) Dopamine modulation of honey bee (*Apis mellifera*) antennal-lobe neurons. J Neurophysiol 95:1147–1157

Quintavalle A (2013) Voltage-Gated Calcium Channels in Honey Bees : Physiological Roles and Potential Targets for Insecticides. Biosci Master Rev 1–11

Robertson HM, Wanner KW (2006) The chemoreceptor superfamily in the honey bee, *Apis mellifera*: expansion of the odorant, but not gustatory, receptor family. Genome Res 16:1395–1403

Rössler W, Brill MF (2013) Parallel processing in the honeybee olfactory pathway: structure, function, and evolution J Comp Physiol A 199:981–996

Rössler W, Zube C (2011) Dual olfactory pathway in Hymenoptera: evolutionary insights from comparative studies. Arthropod Struct Dev 40:349–357

Rybak J (2012) The Digital Honey Bee Brain Atlas. In: Galizia CG, Eisenhardt D, Giurfa M (eds) Honeybee neurobiology and behavior— a tribute to Randolf Menzel. Springer, The Netherlands, pp 125–140

Rybak J, Menzel R (1993) Anatomy of the mushroom bodies in the honey bee brain: the neuronal connections of the alpha-lobe. J Comp Neurol 334:444–465

Sachse S, Rappert A, Galizia CG (1999) The spatial representation of chemical structures in the antennal lobe of honeybees: steps towards the olfactory code. Eur J Neurosci 11:3970–3982

Sah P, Faber ESL (2002) Channels underlying neuronal calcium-activated potassium currents. Prog Neurobiol 66:345–353

Sandoz JC (2011) Behavioral and Neurophysiological Study of Olfactory Perception and Learning in Honeybees. Front Syst Neurosci 5:1–20

Schäfer S, Rosenboom H, Menzel R (1994) Ionic currents of Kenyon cells from the mushroom body of the honeybee. J Neurosci 14:4600–4612

Slessor KN, Winston ML, Le Conte Y (2005) Pheromone communication in the honeybee (*Apis mellifera* L.). J Chem Ecol 31:2731–2745

Stieb SM, Muenz TS, Wehner R, Rössler W (2010) Visual experience and age affect synaptic organization in the mushroom bodies of the desert ant *Cataglyphis fortis*. Dev Neurobiol 70:408–423

Strausfeld NJ (2002) Organization of the honey bee mushroom body: representation of the calyx within the vertical and gamma lobes. J Comp Neurol 450:4–33

Strube-Bloss MF, Herrera-Valdez MA, Smith BH (2012) Ensemble Response in Mushroom Body Output Neurons of the Honey Bee Outpaces Spatiotemporal Odor Processing Two Synapses Earlier in the Antennal Lobe. PLoS One 7:e50322

Strube-Bloss MF, Nawrot MP, Menzel R (2011) Mushroom body output neurons encode odor-reward associations. J Neurosci 31:3129–3140

Szyszka P, Ditzen M, Galkin A, Galizia CG, Menzel R (2005) Sparsening and temporal sharpening of olfactory representations in the honeybee mushroom bodies. J Neurophysiol 94:3303–3313

Tabuchi M, Inoue S, Kanzaki R, Nakatani K (2012) Whole-cell recording from Kenyon cells in silkmoths. Neurosci Lett 6–11

Tanaka NK, Suzuki E, Dye L, Ejima A, Stopfer M (2012) Dye fills reveal additional olfactory tracts in the protocerebrum of wild-type *Drosophila*. J Comp Neurol 520:4131–4140

Terazima E, Yoshino M (2010) Modulatory action of acetylcholine on the Na+-dependent action potentials in Kenyon cells isolated from the mushroom body of the cricket brain. J Insect Physiol 56:1746–1754

Turner GC, Bazhenov M, Laurent G (2008) Olfactory representations by *Drosophila* mushroom body neurons. J Neurophysiol 99:734–746

Vosshall LB, Wong AM, Axel R (2000) An olfactory sensory map in the fly brain. Cell 102:147–59

Vreugdenhil M, Hoogland G, van Veelen CWM, Wadman WJ (2004) Persistent sodium current in subicular neurons isolated from patients with temporal lobe epilepsy. Eur J Neurosci 19:2769–2778

Wicher D, Berlau J, Walther C, Borst A (2006) Peptidergic counter-regulation of Ca(2+)- and Na(+)-dependent K(+) currents modulates the shape of action potentials in neurosecretory insect neurons. J Neurophysiol 95:311–322

Wicher D, Penzlin H (1997) Ca2+ currents in central insect neurons: electrophysiological and pharmacological properties. J Neurophysiol 77:186–199

Wicher D, Walther C, Wicher C (2001) Non-synaptic ion channels in insects--basic properties of currents and their modulation in neurons and skeletal muscles. Prog Neurobiol 64:431–525

Witthöft W (1967) Absolute Anzahl und Verteilung der Zellen im Hirn der Honigbiene. Zeitschrift für Morphol der Tiere 61:160–184

Wüstenberg DG, Boytcheva M, Grünewald B, Byrne JH, Menzel R, Baxter DA (2004) Current- and voltage-clamp recordings and computer simulations of Kenyon cells in the honeybee. J Neurophysiol 92:2589–2603

Wüstenberg DG, Grünewald B (2004) Pharmacology of the neuronal nicotinic acetylcholine receptor of cultured Kenyon cells of the honeybee, *Apis mellifera*. J Comp Physiol A 190:807–821

Zeng XH, Benzinger GR, Xia XM, Lingle CJ (2007) BK channels with beta3a subunits generate use-dependent slow afterhyperpolarizing currents by an inactivation-coupled mechanism. J Neurosci 27:4707–4715

Additional material and methods

One major part of my PhD project was the establishment of a preparation suitable for *in situ* patch clamp recordings of m- and lALT PNs and KCs. The major points for this procedure will be explained in this short material and methods paragraph. I will not describe tract staining with Microruby^{TM} in detail, as this method is well established (Kirschner et al. 2006; Zube et al. 2008).

For the success of the *in situ* preparation, three major goals should be pointed out:

1. accessibility of the desired cell bodies
2. stability of the preparation
3. survival rate of the preparation

1. A clear path of the patch clamp electrode to the goal cell bodies is necessary. By simply opening the cuticle from above, it is fairly easy to approach lALT and KC cell bodies (Fig. 1a, b). However, mALT cell bodies are located in two clusters at the dorsal side of the AL: To access these, the preparation needed to be turned upside down (Fig. 1c), similar as it was done in imaging experiments by Carcaud et al. (2012). The proboscis and the cuticle beneath the brain were removed using microscissors. Glands, muscles and tracheae covering the brain were gently removed. Additionally, the subesophageal ganglion (SEG) was removed by pushing it in the direction of the MBs (Fig. 1c, d). Removing of the SEG turned out to be the most critical step. After carefully cutting away the proboscis and the surrounding cuticle, the nerves containing gustatory sensory neurons became visible. By grabbing those with foreceps, it became possible to slightly pull the SEG in the direction of the MBs. At some point, pulling of the SEG became no more feasible. I then closed the forceps and pushed the SEG further away from the AL. To confirm the progress of the dissection, the brain was sometimes viewed under the fluorescent microscope with 400x magnification. As the mALT PN cell bodies are situated in two large clusters, they are relatively easy to identify. If these two clusters were not visible, more of the SEG had to be removed. The SEG in the honeybee is a relatively large structure and needs to be removed in a rather drastic fashion, which sometimes leads to severing the antennal nerve. I discarded preparations with severed antennal nerves, as the nerve keeps the AL in place which is necessary for correct identification of the PN cell bodies.

2. Patch clamp recording demands a preparation which is even more stable than the preparation for intracellular recordings or for Ca^{2+} imaging, as even little movements will disrupt giga seal formation. Therefore, the mandibles were put into gently heated dental wax (Flexaponal white, Dentaurum, Ispringen, Germany) in an upright fashion to avoid movements. I used a soldering iron with a fine soldering head controlled with an adjustable power source (ouput: ~3.2 V, 1.5A, Voltcraft PS-1152A, Conrad Electronics, Hirschau, Germany) to melt the dental wax. Once the mandibles were covered with wax, the preparation was put in a refrigerator for approximately 10 seconds to harden the dental wax. All of the cuticle covering the ALs and the MBs was removed. The cuticle below the brain as well as the eyes were left intact to stabilize the brain. All glands and trachea covering the brain were manually removed using fine forceps. Then, the heads were severed from the thorax. The brain was fixed in the recording chamber (RC-22C, Warner Instruments, LLC, Hamden, Connecticut, USA) by pressing the hardened dental wax surrounding the mandibles into slightly softer peripheral wax (Surgident, Heraeus Kulzer GmbH, Hanau, Germany) in the recording chamber. The cuticle around the eyes and beneath the brain was left intact to stabilize the brain. In contrast, Palmer et al. (2013) isolated the brain and used a harp to keep it in place. For stabilization purposes, both methods work. One advantage of my method is that theoretically an olfactory stimulus device could be added and the brain is still connected to major sensory and motor nerves.

3. The survival rate of the neuronal cell bodies directly depends on the amount of damage they received during dissection. Therefore, fine and, most importantly, firmly closing dissecting forceps are necessary for the preparation. Additionally, a high quality dissection microscope (maximal magnification 60x multiplied with for example 2.5x oculars) should be used. No stabilization tools or micromanipulators are needed for the dissection. To be able to record from the cell bodies, the glia sheath covering them has to be removed. In my hands, manually removing it without enzymatic treatment worked best. A thick layer of tracheae covers the honeybee brain, which was removed in a first step. After this, fine tracheae, which may not be visible, still remained over the brain. To remove the glia sheath, these tracheae were carefully grabbed, distant from the target tissue. Once a secure hold on one of these tracheae was achieved, they were pulled in direction of the target tissue and the glia sheath was slightly elevated with the tracheae. After the glia sheath was slightly elevated from the tissue, it was directly grabbed and removed. If the brain was still covered with the glial sheath, the procedure was repeated. The surface of the cells was then carefully examined with the microscope and blown up or shriveled cells were excluded from recording.

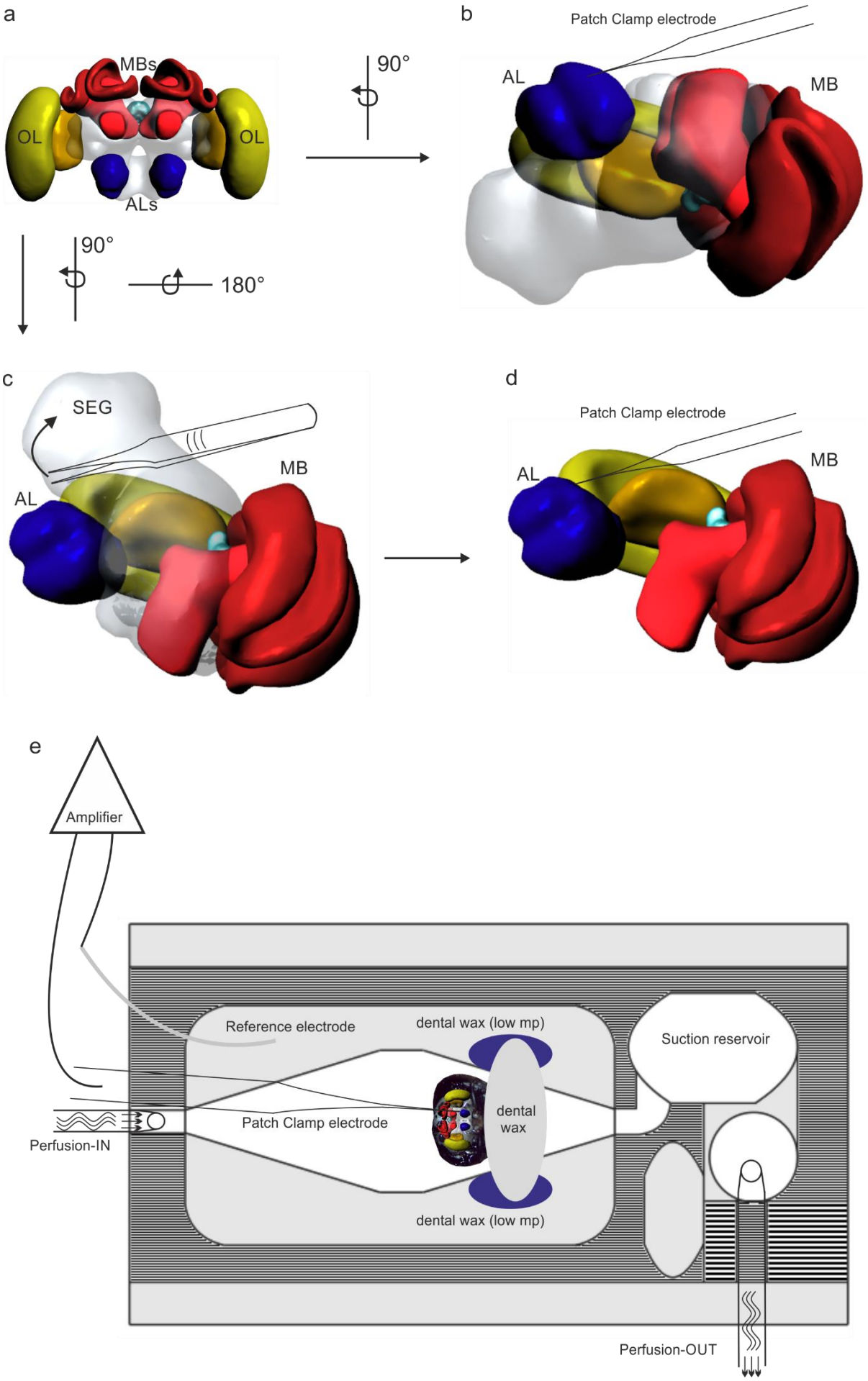
a
MBs
OL
OL
ALs
90°
90°
180°
b
Patch Clamp electrode
AL
MB
c
SEG
AL
MB
d
Patch Clamp electrode
AL
MB
e
Amplifier
Reference electrode
dental wax (low mp)
Suction reservoir
Patch Clamp electrode
dental wax
Perfusion-IN
dental wax (low mp)
Perfusion-OUT

Fig. 1 Schematic drawing of the preparation of the honeybee brain for patch clamp recording **a** Top view at a reconstruction of a honeybee brain. The optic lobes (*OL*), the mushroom bodies (*MBs*) as well as the antennal lobes (*ALs*) are visible. Adapted from Rybak et al. 2010. **b** Side view of the reconstruction under the conditions of lateral antennal-lobe tract recording or Kenyon cell recording. Both the *AL* and the *MB* are easily accessible with the patch clamp electrode. **c** Side view of the reconstruction under the conditions of medial antennal-lobe tract recording. The preparation is already turned around. The subesophageal ganglion (*SEG*) hinders access to the *AL* and has to be removed. **d** Side view of the reconstruction under the conditions of medial antennal-lobe tract recording with the *SEG* already removed. The *AL* then is easily accessible for patch-clamp recordings. **e** Schematic drawing of the honeybee brain in the recording and perfusion chamber. All structures with the same color or pattern are at the same horizontal level. The mandibles are fixed in dental wax, and the dental wax is secured in the chamber with additional dental wax with a lower melting point (*mp*). The patch-clamp electrode is connected to an AL projection neuron. The reference electrode is in the bath solution. Perfusion-IN and OUT as well as the suction reservoir are shown.

General discussion

In my doctoral thesis I investigated the olfactory pathway of the honeybee, an important model system for olfactory processing and behavior. The main focus was on identifying the origins of differences in odor coding between several components of the olfactory system, projection neurons of the medial and lateral antennal lobe output tracts (m/ALT PNs) and downstream intrinsic neurons of the mushroom bodies, the KCs. By means of neuroanatomical tracing and quantification by 3D confocal imaging, a female specific subsystem comprising *S. basiconica* and mALT associated glomeruli could be identified. Furthermore, I investigated the ion channel composition of mALT PNs, lALT PNs and KCs. Some of these ionic currents were already recorded from the respective honeybee neuronal populations with the neurons maintained in primary cell cultures (for example Schäfer et al. 1994; Grünewald 2003; Perk and Mercer 2006). My approach is the first to investigate the whole cell currents of these neuronal populations *in situ*, being able to distinguish between m/l ALT PNs and to record from intact KCs.
Using these experimental approaches, I set out to answer two major questions:
1. What are the differences in the connectivity of sensory input that may promote differences in the m- and lALT PNs?
2. Do the intrinsic electrical neuronal properties of the different neuronal classes (l/mALT PNs, KCs) differ, and how may differences in these properties affect neuronal coding?
I will start briefly outlining my results, then discuss their general impact in relation to recent research to finally suggest future research approaches.

Differences in sensory input and neuronal connectivity in the AL: reasons and consequences

Dealing with the first question, we found out that in the female AL OSNs from *S. basiconica* mainly project to glomeruli, which are associated with the mALT. These glomeruli, as well as the respective mALT PNs are missing in (male) honeybee drones (for an exact description of the female specific subsystem, see manuscript I: Olfactory subsystems in the honeybee: sensory supply and sex specificity). The sex specificity and the preference of *S. basiconica* for a certain glomerulus cluster is a phenomenon well known from ants (Zube and Rössler 2008; Kelber et al. 2010; Nakanishi et al. 2010; Rössler and Zube 2011). This olfactory subsystem was discussed to be involved in nest-mate recognition in these ants. Similar functions, which are exclusive to workers could also be imagined for the T3 and mALT associated AL subsystem in

honeybees. One distinction to bees, however, is that all foraging ants have contact with ants from other colonies and respond aggressively to ants belonging to other colonies (Carlin and Hölldobler 1983). The important cues are cuticular hydrocarbons that are sensed and mediated by the olfactory system (Lahav et al. 1999; Wagner et al. 2000; Howard and Blomquist 2005; Brandstaetter et al. 2008). In contrast to ants, nest-mate recognition in honeybees is a feature mainly restricted to guard bees (Downs and Ratnieks 2000). In a typical honeybee colony, only few workers perform guard duties and some workers are even genetically prone to do less guarding than others. All other duties performed by honeybee workers also change over their lifetime, as honeybees exhibit an age-related division of labor (reviewed by Robinson 1992). Taken these points together, it would be relatively pointless to have an olfactory subsystem comprising up to 20% of all AL glomeruli merely specialized for nest-mate recognition. Although tasks such as cooperative brood care, communication with other bees and foraging might be more abundant during the life time of a single honeybee, still a few honeybees might not profit from a subsystem specialized for one of these tasks. This makes it unlikely that the female specific subsystem observed in our experiments is specialized only for a certain subset of odors.

This aspect is largely supported by the fact that recent physiological studies using multi-unit recordings and Ca^{2+} imaging of m/lALT PNs show that all tested odorants were transferred by PNs of both tracts. Three recent studies challenged this question of odor coding in mALT glomeruli and PNs. All three studies showed that all individual odorants and odorant mixtures tested were encoded in both the m- and the lALT (Ca^{2+} imaging: Carcaud et al. 2012; Galizia et al. 2012; extracellular recordings: Brill et al. 2013). Yet one intriguing feature of the mALT is that the single neurons of it respond more odorant specific than the lALT neurons (Brill et al. 2013; Rössler and Brill 2013). Transferring this information on the sensory input of the AL may imply that OSNs arborizing in the mALT region may mediate this higher odorant specificity. As the majority of *S. basiconica* housed OSNs is associated with the mALT glomeruli, we conclude that *S. basiconica* OSNs may either be more odor specific than OSNs from the other olfactory sensilla or they may exclusively transmit information about odorants that, so far, have not been tested in all studies conducted so far. Although this hypothesis needs to be validated, it fits well with the recordings from *S. basiconica* (Lacher 1964), in which it was possible to record APs, yet no odor responses were observed. Taken potentially highly odor specific OSNs together with a sensillum that contains multiple OSNs, the probability of identifying odor responses, which are masked by the spontaneous activity of non-responding OSNs, appears very unlikely. Additionally, (male) drones lack *S. basiconica* but have a

drastically increased number of *S. placodea* (Esslen and Kaissling 1976). *S. placodea* process the sex pheromone information in drones (Kaissling and Renner 1968), thus the loss of *S. basiconica* might be a compromise allowing improved pheromone detection. In the case that *S. basiconica* were specialized for a certain set of odorants, the detection of especially this set would be drastically impaired in drones. This might affect drone survival, whereas an overall lack of sensitivity for a broad range of odors should not interfere with general olfactory tasks of the drones.

The hypothesis described above goes in line with the hypothesis of combinatorial odor coding (Malnic et al. 1999). A recent study shows that the AL of *Drosophila* is functionally divided into glomeruli sensitive for pleasant and non-pleasant odors (Knaden et al. 2012). This division of the AL according to odor valence has not been investigated in other insects so far. However, mice do not exhibit a clear separation of glomeruli encoding pleasant and unpleasant odors (reviewed by Knaden and Hansson 2013). Along with the AL division, a "labeled-line" avoidance system through the brain of *Drosophila* was suggested (Stensmyr et al. 2012). This avoidance system as well as the glomerular clusters sensitive for pleasant and non-pleasant odors show characteristics similar to the pheromone detection system of moths. These systems generally consist of specialized sensilla and enlarged glomeruli, so-called macroglomeruli (reviewed for example by Stengl 2010; Hansson and Stensmyr 2011). Within these glomeruli pheromone coding takes place and is only slightly affected by other odorants (see for example Chaffiol et al. 2012). Such a pheromone coding system is also present in honeybee drones (Sandoz 2006). In honeybee workers, neither a specialized pheromone coding system nor a valence based organization of the AL was described so far (for example, reviewed in Galizia and Rössler 2010). On the one hand, the behavioral ecology and behavioral repertoires of honeybees are significantly different and more complex compared with *Drosophila*. Honeybees need to cope with high numbers of social odors in addition to environmental and food-related odors, in particular especially floral odors need to be learned and memorized (for references of the multiple olfactory tasks, see: general introduction - the olfactory world of the honeybee). The age-related division of labor performed by honeybees demands flexible responses to changing tasks/environments (reviewed by Robinson 1992). Therefore "labeled-lines" and a valence based organization of the AL in honeybees might be even counterproductive and would prevent plasticity of the olfactory system. Additionally, the enormous complexity of the local neurons (LN) population in the honeybee AL (Meyer and Galizia 2012; Girardin et al. 2013) may allow much more interaction between glomeruli than in fruit flies or moth. Thus, we suspect a combinatorial and more plastic coding system in honeybees. Nevertheless, special

odors, such as the sex pheromone are more likely to be encoded in a "labeled-line" like fashion. However, even responses to social pheromone are context dependent. One component of the alarm pheromone, 2-heptanone, induces aggressive/attacking behavior in guard bees (Shearer and Boch 1965) and avoidance behavior in foragers (Giurfa and Nunez 1992). This predicts interaction with other odorant information making a pure labeled line system extreme unlikely. Even in moth, which were long thought to use a "labeled-line" system in pheromone coding, more and more studies showing interaction of pheromones and plant odors appear (see for example Party et al. 2009; Rouyar et al. 2011; Chaffiol et al. 2012; Deisig et al. 2012; Pregitzer et al. 2012). The lifestyle of *Drosophila* might not require so much interaction between different olfactory channels. An odorant that signals harmful microbes should always overwrite fruit odors (Stensmyr et al. 2012). Conversely in honeybees, a wide variety of social pheromones (reviewed by Sandoz et al. 2007) may be present at the same time in the hive. For a single worker, it is then necessary to correctly identify and evaluate the individual components out of this variety to be able to behave adequately. Regarding the fact that honeybees react differently to these components in an age-related fashion, a "labeled-line" system may have problems with extracting all necessary information. The differences in lifestyle between fruit flies and eusocial honeybees are likely to have promoted selection of differences in odor coding. One indication for this may be the prominence of a dual olfactory pathway (Galizia and Rössler 2010; Rössler and Zube 2011; Rössler and Brill 2013).

I finally conclude that m- and lALT PNs both transmit information about a similar set of odorants, and the female specific mALT subsystem does not appear to be specialized for a certain class of odors. Nevertheless, given the large odor space, we cannot exclude that particular odorants may only be processed in one of the two subsystems. The difference in odor selectivity between m- and lALT PNs is likely due to the different sensory supply with OSNs. *S. basiconica* associated OSNs are thus likely to be more odorant specific than OSNs from the two other types of sensilla. This hypothesis remains to be investigated with single sensillum recordings from *S. basiconica* and in comparison with recordings from the two other types of sensilla under similar stimulation conditions.

Ion channel composition of m- and lALT PNs

The ionic currents observed in whole-cell voltage-clamp recordings did not differ significantly between m- and lALT PNs, meaning that both PN classes seem to express similar sets of ion channels. Both PN classes possess ion channels typical for neurons that spontaneously generate

APs (Wicher et al. 2006) (for an exact description and discussion of the recorded ionic currents, see manuscript II: Complex and sparse coding along the honeybee's olfactory pathway: potential contribution of ionic currents of medial and lateral projection neurons and Kenyon cells). The extracellular recordings of the two tracts revealed that mALT PNs, generally, have lower AP frequencies than lALT PNs, both during spontaneous activity and odor responses (Brill et al. 2013). From my patch-clamp recordings I can conclude that differences between m- and lALT AP frequencies are likely due to different synaptic input to different modulation of the currents in PNs of both tracts.

One potential target of neuronal modulation leading to differences in AP frequencies is the big K^+ conductance (BK) channel, a Ca^{2+} and voltage dependent K^+ channel. This channel was already observed in cultured honeybee AL neurons and shown to be positively modulated by dopamine (Perk and Mercer 2006). In our recordings, this channel activates slightly earlier in lALT neurons compared to mALT neurons, which gives a good hint that this may result in generally higher activity levels in lALT PNs. BK currents hyperpolarize neurons, thus a positive modulation of it leading to an increased AP frequency seems counterintuitive at a first glance. Yet, BK channels were shown to decrease the duration of a single AP by fast hyperpolarization of the neuron (Wicher et al. 2006). Therefore, the next AP can be generated faster and, in consequence, higher AP frequencies are possible. In the cockroach DUM (dorsal unpaired median) neurons AKH I, a neuropeptide, was shown to affect Na^+ and Ca^{2+} currents. The modulation also reduced AP duration leading to increased AP frequencies (Wicher et al. 2006). A similar mechanism can also be imagined in the honeybee. This hypothesis needs to be tested by evaluating the influence of dopamine and various neuropeptides on ionic currents in voltage-clamp mode and on AP duration and frequency in current-clamp mode.

In conclusion, both m- and lALT PNs have a similar current repertoire and only differ in the modulation of it. This is also in accordance with the fact that individual mALT PNs may in some cases have higher AP frequencies than individual lALT PNs (Brill et al. 2013). The dopaminergic modulation of cell cultured AL neurons (Perk and Mercer 2006) is likely to be also present *in vivo*, as dopaminergic neurons arborizing in the AL were identified by Schäfer and Rehder (1989). As a matter of fact, no data on potentially different innervation of the m- and lALT proportion of the AL is available (Schäfer and Rehder 1989). Besides dopamine, octopamine was shown to affect activity of the AL network (Rein et al. 2013) and might thus also affect PN activity. Furthermore, four neuropeptides have been identified in the honeybee AL (reviewed by Galizia and Kreissl 2012), which might influence PN activity. However no data on their function are available to date.

Ionic currents of KCs and their potential impact on sparse coding

In contrast to both m- and lALT PNs, the *in-situ* patch-clamp analyses show that KCs have a completely different set of currents. The most prominent currents observed in KCs under standard conditions are a transient A-type like voltage-dependent K^+ current and a persistent Ca^{2+} dependent K^+ current. The transient K^+ current is likely to be responsible for the generation of the very temporally sparse odor responses in KCs observed in Ca2+ imaging experiments (Szyszka et al. 2005). As it is purely voltage dependent, is will hyperpolarize KCs drastically right after activation. This generates a short circuit of self-inhibition of KCs which will sharpen the responses to synaptic input. In a slightly prolonged fashion, Ca^{2+} dependent K^+ currents will hyperpolarize KCs even after the voltage-dependent transient K^+ currents are already closed. This mechanism can ensure that KCs are silent for a short time after activation. Similar dominant currents were found in *Drosophila* KCs (Gasque et al. 2005), yet cockroach (Demmer and Kloppenburg 2009), silkmoth (Tabuchi et al. 2012) and cricket KCs (Inoue et al. 2014) exhibit different currents under standard conditions that may serve a similar function. The only insects besides the honeybee, which were shown to employ sparse coding for odor representation are fruit flies (Turner et al. 2008) and cockroaches (Demmer and Kloppenburg 2009). Nevertheless, insect KCs are generally thought of as sparse coding neurons (Perez-Orive et al. 2002; Farkhooi et al. 2013; Lin et al. 2014). Combining our data with the fruit fly and cockroach data shows that sparse coding in different insect species may be promoted by different intrinsic mechanisms of KCs. In addition to the intrinsic generation of sparse coding properties, GABAergic feedback neurons in the MBs are present (Bicker et al. 1985). The feedback neurons were shown to have several subclasses that span over wide parts of the MB (Grünewald 1999). As the whole MB is innervated, the overall excitability of KCs may be regulated by them (Palmer and Harvey 2014). In this context, GABAergic feedback neurons could also serve a gain-control mechanism, which helps KCs to respond adequately to high concentration stimulation (Froese et al. 2014). Furthermore, these neurons could, over inhibitory synapses, participate in sharpening the responses over a negative feedback circuit. However, the intrinsic ion channels can produce a much faster negative feedback and blocking of GABA receptors increased response intensity of KCs yet did not change the temporal pattern in Ca^{2+} imaging recordings (Froese et al. 2014). Taken these points together, it is likely that the GABAergic input to KCs observed in honeybees (Palmer and Harvey 2014) rather regulates general excitability of KCs and promotes the spatially sparse representation of stimuli in KCs.

To achieve a spatially sparse representation of information in the MBs, the first KC responding with APs would activate a GABAergic neuron, which would in turn inhibit other KCs. This is supported by the fact that GABAergig feedback neurons have wide arborizations in the MB calyx (Bicker et al. 1985; Grünewald 1999). In summary, GABAergic feedback appears more likely to contribute to general excitability and spatial sparsenesss rather than to temporal sparseness.

For the KCs, I conclude that in the honeybee they employ a temporally and spatially sparse way of coding odor information. The temporal sparseness is promoted by intrinsic neuronal properties, whereas the spatial sparseness may additionally require inhibitory synaptic GABAergic input. The especially high number of the KC neuronal population in the honeybee (Groh and Rössler 2011) makes it a very likely mechanism. Sparse coding in KCs is likely a general mechanism employed in insects. Conversely, the mechanism behind sparse coding may be different between different insect species. Nevertheless, clear differences in the ion channel composition between neurons that are spontaneously active and between sparse neurons were observed. In this context, the possibility of predicting AP patterns of any neuron based on its intrinsic neuronal properties (and vice versa) emerges as an intriguing idea. This would support the generation of models of neural circuits as presented by Farkhooi et al. (2013). To be finally able to draw comprehensive conclusions about the consequences of the ion channel composition on the spiking pattern of a neuron, however, more data on both AP frequencies and ion channels of different neurons along the olfactory pathway are necessary. In a next step, it would be most interesting to record from MB extrinsic neurons (ENs) in voltage-clamp mode. Based on their AP frequencies (see Strube-Bloss et al. 2011; 12), ENs should resemble PNs more in terms of ionic currents compared to KCs.

Consequences of ion channel properties mediating sparse coding on learning and memory

Because of their sparse coding properties, KCs are ideal coincidence detectors. Coincidences could potentially be detected between PNs within and across both tracts, and even between PNs conveying information from different sensual modalities. Morphological studies of KCs have shown different morphologies in different KC subpopulations (Mobbs 1982; Strausfeld 2002), which are likely to provide the morphological substrate for these different levels of coincidence coding. Two major classes of KCs have been identified so far: class I (spiny) KCs and class II (clawed) KCs. Spiny KCs have a prominent dendritic branching pattern restricted to specific

MB regions and the PNs connecting to them are restricted to one PN tract. In contrast, clawed KCs receive input from both m- and lALT (Kirschner et al. 2006) and are therefore potential detectors of coincidence between the m- and the lALT. Therefore, I only recorded from clawed KCs. Coincidence detection, which potentially leads to learning of this coincidence, requires exact timing of synaptic input. Just recently, Gupta and Stopfer (2014) analyzed the influence of disruptions of the AP pattern of KCs on following neurons, namely ENs, in locusts. Even small manipulations had a huge impact on the AP pattern recorded in ENs (Gupta and Stopfer 2014), which implies that the temporal pattern of KCs is of great importance for learning and memory tasks.

The aspects of honeybee olfactory associative learning have been intensively studied with the proboscis extension response to date (for a detailed description see Matsumoto et al. 2012). In this classical conditioning paradigm, honeybees form an association between an odor and a sucrose reward (Bitterman et al. 1983). The MB is the first brain station in which olfactory and gustatory information converge (olfactory: for example Kirschner et al. 2006; gustatory: Farris 2008). In a potential cellular mechanism for associative learning, olfactory and gustatory PNs converge on the same KC, which in turn is activated. Then, the cytosolic Ca^{2+} concentration rises, kinases are activated and synaptic plasticity is induced (for potential mechanisms see Kandel et al. 2014).

The synaptic input of KCs occurs in microcircuits in the small synaptic complexes between PNs and KCs, the microglomeruli (Homberg et al. 1989; Groh et al. 2004). The local Na^{+} and Ca^{2+} dynamics in such a microglomerulus may or may not affect membrane voltage and Ca^{2+} dynamics in the whole KC. Long term potentiation (LTP) leading to local synaptic plasticity in such a microcircuit might then increase the size of a microglomerulus and the effect of local currents on the whole KC and therefore on AP generation. To induce LTP, elevated Ca^{2+} levels in the cell are necessary. However, the ionic currents under standard conditions supported by my study may work against such a mechanism. Once the neuron is activated, it will be hyperpolarized immediately through the transient K^{+} current. Synaptic input leading to strong Ca^{2+} influx would also hyperpolarize the neuron over a longer time through Ca^{2+} dependent K^{+} channels. I will therefore present a potential mechanism showing how activation of a KC through different receptors may overcome the post-activation hyperpolarization. The persistent Ca^{2+} dependent K^{+} channels have been shown to be inhibited by muscarinic acetylcholine receptors (AchR) in vertebrates (Buchanan et al. 2010; Giessel and Sabatini 2010). Furthermore, at least mALT PNs have been shown to employ acetylcholine as a neurotransmitter (Kreissl and Bicker 1989) and various AchR subunits have been identified in

the honeybee MB (Thany et al. 2003). I therefore conclude that the majority of MB input neurons are cholinergic. Additionally, it was shown that activation of muscarinic receptors induces MB volume increase and KC outgrowth in honeybees, although the muscarinic agonists and antagonists were fed to the honeybees in these studies and not directly injected into the MBs (Ismail et al. 2006; Dobrin et al. 2011). Therefore, the effect on KCs might also originate from modulation of the sensory pathways. It was already shown for KCs that they do not contain muscarinic activated ion channels in cell culture (Wüstenberg and Grünewald 2004). Even though the *in vivo* expression of muscarinic AchRs might be different, currents directly activated by muscarinic stimulation are not necessary for a mechanism leading to long term potentiation described in rat and human cells (Buchanan et al. 2010; Giessel and Sabatini 2010). Taken all these points together, a potential mechanism emerges: nicotinic AchR activation leads to KC depolarization via ionic currents, whereas muscarinic AchR activation may prevent the post-activation hyperpolarization of KCs through Ca^{2+} dependent K^+ channels. Normally, KCs are only briefly activated during odor stimulation (Szyszka et al. 2005; Froese et al. 2014) therefore the time window for coincidence detection should be relatively small. By activating the muscarinic AchR and thus blocking of Ca^{2+} dependent K^+ channel activity, the time window for coincidence detection may be increased. In case of coincidental input within this time window, LTP may be promoted. An increased time window cannot be caused by reduced GABAergic feedback as GABA does not affect the temporal pattern of KC responses (Froese et al. 2014). To investigate this hypothesis, the Ca^{2+} dependent K^+ current needs to be recorded under influence of muscarinic agonists/antagonists, to confirm that this current is also muscarinic modulated in honeybee KCs. The effect demonstrated by Dobrin et al. (2011) would then be highly likely caused by muscarinic modulation of KCs. In case of a successful modulation of this current by muscarinic agonists, in a next step one could directly investigate KC outgrowth induced by muscarinic stimulation, for example under a multi-photon laser-scanning microscope setup.

Final conclusions

In the course of this dissertation, it became evident that the coding of olfactory information in the honeybee brain is a complex process. This process does not only involve differential synaptic connectivity between at least two subsystems, but is also influenced by intrinsic neuron properties and neuronal modulation. The investigation of the intrinsic properties of two classes of PNs revealed an impressively sophisticated set of ion channels. A potential cellular mechanism for coincidence detection and long term potentiation in KCs was found, yet the exact mechanism remains to be determined. Regarding the fact that in addition to the variety of ion channels, metabotropic signaling, gene expression metabolism and much more details affect the influences of a single neuron, I will finish my thesis with a quote from David Eagleman:

"Your brain is built of cells called neurons and glia - hundreds of billions of them. Each one of these cells is as complicated as a city."
David Eagleman – Incognito: The Secret Lives of the Brain

General references

Abel R, Rybak J, Menzel R (2001) Structure and response patterns of olfactory interneurons in the honeybee, *Apis mellifera*. J Comp Neurol 437:363–383

Ache BW, Young JM (2005) Olfaction: diverse species, conserved principles. Neuron 48:417–430

Akers RP, and Getz WM (1993) Response of olfactory receptor neurons in honeybees to odorants and their binary mixtures. J Comp Physiol A 173:169–185

Arenas A, Fernández VM, Farina WM (2007) Floral odor learning within the hive affects honeybees' foraging decisions. Naturwissenschaften 94:218–222

Benton R (2006) On the ORigin of smell: odorant receptors in insects. Cell Mol Life Sci 63:1579–1585

Berg BG, Schachtner J, Utz S, Homberg U (2007) Distribution of neuropeptides in the primary olfactory center of the heliothine moth *Heliothis virescens*. Cell Tissue Res 327:385–98

Bhatnagar KP, Meisami E (1998) Vomeronasal organ in bats and primates: extremes of structural variability and its phylogenetic implications. Microsc Res Tech 43:465–475

Bicker G, Kreissl S, Hofbauer A (1993) Monoclonal antibody labels olfactory and visual pathways in *Drosophila* and *Apis* brains. J Comp Neurol 335:413–424

Bicker G, Schäfer S, Kingan TG (1985). Mushroom body feedback interneurones in the honeybee show GABA-like immunoreactivity. Brain Res 360:394–397

Binzer M, Heuer CM, Kollmann M, Kahnt J, Hauser F, Grimmelikhuijzen CJP, Schachtner J (2014) Neuropeptidome of *Tribolium castaneum* antennal lobes and mushroom bodies. J Comp Neurol 522:337–357

Bitterman ME, Menzel R, Fietz A, Schäfer S (1983) Classical conditioning of proboscis extension in honeybees (*Apis mellifera*). J Comp Physiol A 97:107–119

Boch R, Shearer DA, Stone BC (1962) Identification of Iso-Amyl Acetate as an Active Component in the Sting Pheromone of the Honey Bee. Nature 195:1018–1020

Bornhauser BC, Meyer EP (1997) Histamine-like immunoreactivity in the visual system and brain of an orthopteran and a hymenopteran insect. Cell Tissue Res 287:211–221

Brandstaetter AS, Endler A, Kleineidam CJ (2008) Nestmate recognition in ants is possible without tactile interaction. Naturwissenschaften 95:601–608

Breed MD, Guzmán-Novoa E, Hunt GJ (2004) Defensive behavior of honey bees: organization, genetics, and comparisons with other bees. Annu Rev Entomol 49:271–298

Brill MF, Rosenbaum T, Reus I, Kleineidam CJ, Nawrot MP, Rössler W (2013) Parallel Processing via a Dual Olfactory Pathway in the Honeybee. J Neurosci 33:2443–2456

Buchanan KA, Petrovic MM, Chamberlain SEL, Marrion, NV, Mellor, JR (2010) Facilitation of long-term potentiation by muscarinic M(1) receptors is mediated by inhibition of SK channels. Neuron 68:948–963

Buck L, Axel R (1991) A novel multigene family may encode odorant receptors: a molecular basis for odor recognition. Cell 65:175–187

Bushdid C, Magnasco MO, Vosshall LB, Keller A (2014) Humans Can Discriminate More than 1 Trillion Olfactory Stimuli. Science 343:1370–1372

Carcaud J, Hill T, Giurfa M, Sandoz JC (2012) Differential coding by two olfactory subsystems in the honeybee brain. J Neurophysiol 108:1106–1221

Carlin NF, Hölldobler B (1983) Nestmate and kin recognition in interspecific mixed colonies of ants. Science 222:1027–1029

Carlsson, MA, Diesner M, Schachtner J, Nässel DR (2010) Multiple neuropeptides in the Drosophila antennal lobe suggest complex modulatory circuits. J Comp Neurol 518:3359–3380

Chaffiol A, Kropf J, Barrozo RB, Gadenne CG, Rospars JP, Anton S (2012) Plant odour stimuli reshape pheromonal representation in neurons of the antennal lobe macroglomerular complex of a male moth. J Exp Biol 215:1670–1680

Couto A, Alenius M, Dickson BJ (2005) Molecular, anatomical, and functional organization of the *Drosophila* olfactory system. Curr Biol 15:1535–1547

Croy I, Olgun S, Joraschky P (2011) Basic emotions elicited by odors and pictures. Emotion 11:1331–1335

Dacks AM, Reisenman CE, Paulk AC, Nighorn AJ (2010) Histamine-immunoreactive local neurons in the antennal lobes of the hymenoptera. J Comp Neurol 518:2917–2933

Deisig N, Kropf J, Vitecek S, Pevergne D, Rouyar A, Sandoz JC, Lucas P, Gadenne C, Anton S, Barrozo R (2012) Differential Interactions of Sex Pheromone and Plant Odour in the Olfactory Pathway of a Male Moth. PLoS One 7:e33159

De Groot JHB, Smeets MAM, Kaldewaij A, Duijndam MJA, Semin GR (2012) Chemosignals communicate human emotions. Psychol Sci 23:1417–1424

Demattè ML, Osterbauer R, Spence C (2007) Olfactory cues modulate facial attractiveness. Chem Senses 32:603–610

Demmer H, Kloppenburg P (2009) Intrinsic membrane properties and inhibitory synaptic input of kenyon cells as mechanisms for sparse coding? J Neurophysiol 102:1538–1550

Díaz D, Gómez C, Muñoz-Castañeda R, Baltanás F, Alonso JR, Weruaga E (2013) The olfactory system as a puzzle: playing with its pieces. Anat Rec (Hoboken) 296:1383–1400

Díaz PC, Grüter C, Farina WM (2007) Floral scents affect the distribution of hive bees around dancers. Behav Ecol Sociobiol 61:1589–1597

Dobrin SE, Herlihy JD, Robinson GE, Fahrbach SE (2011) Muscarinic regulation of Kenyon cell dendritic arborizations in adult worker honey bees. Arthropod Struct Dev 40:409–419

Downs SG, Ratnieks FLW (2000) Adaptive shifts in honey bee (*Apis mellifera* L .) guarding behavior support predictions of the acceptance threshold model Behav Ecol 11:326–333

Eagleman D (2011) Incognito: The Secret Lives of the Brain. Pantheon U S A

Esslen J, Kaissling K (1976) Zahl und Verteilung antennaler Sensillen bei der Honigbiene *Apis mellifera* L. Zoomorphologie 83:227–251

Farina WM, Grüter C, Díaz PC (2005) Social learning of floral odours inside the honeybee hive. Proc R Soc Lond [Biol] 272:1923–1928

Farkhooi F, Froese A, Muller E, Menzel R, Nawrot MP (2013) Cellular Adaptation Facilitates Sparse and Reliable Coding in Sensory Pathways. PLoS Comput Biol. 9:e1003251

Farris SM (2008) Tritocerebral tract input to the insect mushroom bodies. Arthropod Struct Dev 37:492–503

Fonta C, Sun X, Masson C (1993) Morphology and spatial distribution of bee antennal lobe interneurones responsive to odours. Chem Senses 18:101–119

Forêt S, Maleszka R (2006) Function and evolution of a gene family encoding odorant binding-like proteins in a social insect, the honey bee (*Apis mellifera*). Genome Res 16:1404–1413

Froese A, Szyszka P, Menzel R (2014) Effect of GABAergic inhibition on odorant concentration coding in mushroom body intrinsic neurons of the honeybee. J Comp Physiol A 200:183–195

Galizia CG, Franke T, Menzel R, Sandoz JC (2012) Optical imaging of concealed brain activity using a gold mirror in honeybees. J Insect Physiol 58:743–749

Galizia CG, Kimmerle B (2004) Physiological and morphological characterization of honeybee olfactory neurons combining electrophysiology, calcium imaging and confocal microscopy. J Comp Physiol A 190:21–38

Galizia CG, Kreissl S (2012) Neuropeptides in Honey Bees. In: Galizia CG, Eisenhardt D, Giurfa M (eds) Honeybee neurobiology and behavior— a tribute to Randolf Menzel. Springer, The Netherlands, pp 211–226

Galizia CG, Rössler W (2010) Parallel olfactory systems in insects: anatomy and function. Annu Rev Entomol 55:399–420

Gary NE (1962) Chemical Mating Attractants in the Queen Honey Bee. Science 136:773–774

Gasque G, Labarca P, Reynaud E, Darszon A (2005) Shal and shaker differential contribution to the K+ currents in the *Drosophila* mushroom body neurons. J Neurosci 25:2348–2358

Getz WM, Akers RP (1993) Olfactory response characteristics and tuning structure of placodes in the honey bee Apis mellifera. Apidologie 24:195–217

Giessel AJ, Sabatini BL (2010) M1 muscarinic receptors boost synaptic potentials and calcium influx in dendritic spines by inhibiting postsynaptic SK channels. Neuron 68:936–947

Girardin CC, Kreissl S, Galizia CG (2013) Inhibitory connections in the honeybee antennal lobe are spatially patchy. J Neurophysiol 109:332–343

Giurfa M (2007) Behavioral and neural analysis of associative learning in the honeybee: a taste from the magic well. J Comp Physiol A 193:801–824

Giurfa M, Nuñez JA (1992) Honeybees mark with scent and reject recently visited flowers. Oecologica 89:113–117

Godfrey PA, Malnic B, Buck LB (2004) The mouse olfactory receptor gene family. Proc Natl Acad Sci U S A. 101:2156–2161

Grimm (2006) 1. Allgemeine Unfallversicherungs-Bedingungen (AUB 99)GDV-Musterbedingungen In Grimm (ed) Unfallversicherung: AUB 4th ed. C.H. Beck, Germany

Groh C, Rössler W (2011) Comparison of microglomerular structures in the mushroom body calyx of neopteran insects. Arthropod Struct Dev 40:358–367

Groh C, Tautz J, Rössler W (2004) Synaptic organization in the adult honey bee brain is influenced by brood-temperature control during pupal development. Proc Natl Acad Sci U S A 101:4268–4273

Grünewald B (1999) Morphology of feedback neurons in the mushroom body of the honeybee, *Apis mellifera*. J Comp Neurol 404:114–26

Grünewald B (2003) Differential expression of voltage-sensitive K+ and Ca2+ currents in neurons of the honeybee olfactory pathway. J Exp Biol 206:117–129

Gupta N, Stopfer M (2014) A Temporal Channel for Information in Sparse Sensory Coding. Curr Biol 24:2247–2256

Haddad R, Khan R, Takahashi YK, Mori K, Harel D, Sobel N (2008) A metric for odorant comparison. Nat Methods 5:425–429

Hammer M, Menzel R (1995) Learning and memory in the honeybee. J Neurosci 15:1617–1630

Hansson BS, Stensmyr MC (2011) Evolution of insect olfaction. Neuron 72:698–711

Heinbockel T, Christensen TA, Hildebrand JG (1999) Temporal tuning of odor responses in pheromone-responsive projection neurons in the brain of the sphinx moth *Manduca sexta*. J Comp Neurol 409:1–12

Heisenberg M (2003) Mushroom body memoir: from maps to models. Nat Rev Neurosci 4:266–275

Hildebrand JG, Shepherd GM (1997) Mechanisms of olfactory discrimination: converging evidence for common principles across phyla. Annu Rev Neurosci 20:595–631

Homberg U, Christensen TA, Hildebrand JG (1989) Structure and function of the deutocerebrum in insects. Annu Rev Entomol 34:477–501

Hourcade B, Muenz TS, Sandoz JC, Rössler W, Devaud JM (2010) Long-term memory leads to synaptic reorganization in the mushroom bodies: a memory trace in the insect brain? J Neurosci 30:6461–6465

Howard RW, Blomquist GJ (2005) Ecological, behavioral, and biochemical aspects of insect hydrocarbons. Annu Rev Entomol 50:371–393

Husch A, Paehler M, Fusca D, Paeger L, Kloppenburg P (2009) Distinct electrophysiological properties in subtypes of nonspiking olfactory local interneurons correlate with their cell type-specific Ca2+ current profiles. J Neurophysiol 102:2834–2845

Hussain A, Saraiva LR, Ferrero DM, Ahuja G, Krishna VS, Liberles SD, Korsching S (2013) High-affinity olfactory receptor for the death-associated odor cadaverine. Proc Natl Acad Sci U S A 110:19579–19584

Ibba I, Angioy AM, Hansson BS, Dekker T (2010) Macroglomeruli for fruit odors change blend preference in *Drosophila*. Naturwissenschaften 97:1059–1066

Inoue S, Murata K, Tanaka A, Kakuta E, Tanemura S, Hatakeyama S, Nakamura A, Yamamoto C, Kosakai K, Yoshino M (2014) Ionic channel mechanisms mediating the intrinsic excitability of Kenyon cells in the mushroom body of the cricket brain. J Insect Physiol 68:44-57

Ismail N, Robinson GE, Fahrbach SE (2006) Stimulation of muscarinic receptors mimics experience-dependent plasticity in the honey bee brain. Proc Natl Acad Sci U S A 103:207–211

Ito K, Shinomiya K, Ito M, Armstrong JD, Boyan G, Hartenstein V, Harzsch S, Heisenberg M, Homberg U, Jenett A, Keshishian H, Restifo LL, Rössler W, Simpson JH, Strausfeld NJ, Strauss R, Vosshall LB, Insect Brain Name Working Group (2014) A systematic nomenclature for the insect brain. Neuron 81:755–765

Joerges J, Küttner A, Galizia CG, Menzel R (1997) Representations of odours and odour mixtures visualized in the honeybee brain. Nature 387:285–288

Kaissling KE, Renner M (1968) Antennale Rezeptoren für Queen Substance und Sterzelduft bei der Honigbiene. Z Vgl Physiol 59:357–361

Kandel ER, Dudai Y, Mayford MR (2014) The molecular and systems biology of memory. Cell 157:163–186

Keene AC, Waddell S (2007) *Drosophila* olfactory memory: single genes to complex neural circuits. Nat Rev Neurosci 8:341–354

Kelber C, Rössler W, Kleineidam CJ (2010) Phenotypic plasticity in number of glomeruli and sensory innervation of the antennal lobe in leaf-cutting ant workers (*A. vollenweideri*). Dev Neurobiol 70:222–234

Kelber C, Rössler W, Kleineidam CJ (2006) Multiple olfactory receptor neurons and their axonal projections in the antennal lobe of the honeybee *Apis mellifera*. J Comp Neurol 496:395–405

Kirschner S, Kleineidam CJ, Zube C, Rybak J, Grünewald B, Rössler W (2006) Dual olfactory pathway in the honeybee, *Apis mellifera*. J Comp Neurol 499:933–952

Knaden M, Hansson BS (2013) Neuroscience. Specialized but flexible. Science 339:151–152

Knaden M, Strutz A, Ahsan J, Sachse S, Hansson B (2012) Spatial representation of odorant valence in an insect brain. Cell Rep 1:392–399

Kranz W, Kitts K, Strange N, Cummins J, Lotspeich E, Goodpaster J (2014) On the smell of Composition C-4. Forensic Sci Int 236:157–163

Kreissl S, Bicker G (1989) Histochemistry of acetylcholinesterase and immunocytochemistry of an acetylcholine receptor-like antigen in the brain of the honeybee. J Comp Neurol 286:71–84

Krieger J, Klink O, Mohl C, Raming K, Breer H (2003) A candidate olfactory receptor subtype highly conserved across different insect orders J Comp Physiol A 189:519–526

Krofczik S, Menzel R, Nawrot MP (2008) Rapid odor processing in the honeybee antennal lobe network. Front Comput Neurosci 2:9

Lacher V (1964) Elektrophysiologische Untersuchungen an einzelnen Rezeptoren für Geruch, Kohlendioxyd, Luftfeuchtigkeit und Temperatur auf den Antennen der Arbeitsbiene und der Drohne (*Apis mellifica* L.). Z Vgl Physiol 48:587–623

Lahav S, Soroker V, Hefetz A, Vander Meer RK (1999) Direct Behavioral Evidence for Hydrocarbons as Ant Recognition Discriminators. Naturwissenschaften 86:246–249

Larsson MC, Domingos AI, Jones WD, Chiappe ME, Amrein H, Vosshall LB (2004) Or83b encodes a broadly expressed odorant receptor essential for *Drosophil*a olfaction. Neuron 43:703–714

Lin AC, Bygrave AM, de Calignon A, Lee T, Miesenböck G (2014) Sparse, decorrelated odor coding in the mushroom body enhances learned odor discrimination. Nat Neurosci 17:559–568

Lin DY, Shea SD, Katz LC (2006) Representation of natural stimuli in the rodent main olfactory bulb. Neuron 50:937–949

Majid A, Burenhult N (2014) Odors are expressible in language, as long as you speak the right language. Cognition 130:266–270

Malnic B, Godfrey PA, Buck LB (2004) The human olfactory receptor gene family. Proc Natl Acad Sci U S A 101:2584–2589

Malnic B, Hirono J, Sato T, Buck LB (1999) Combinatorial receptor codes for odors. Cell 96:713–723

Matsui A, Go Y, Niimura Y (2010) Degeneration of olfactory receptor gene repertories in primates: no direct link to full trichromatic vision. Mol Biol Evol 27:1192–1200

Matsumoto Y, Menzel R, Sandoz JC, Giurfa M (2012) Revisiting olfactory classical conditioning of the proboscis extension response in honey bees: a step toward standardized procedures. J Neurosci Methods 211:159–167

Meyer A, Galizia CG (2012) Elemental and configural olfactory coding by antennal lobe neurons of the honeybee (*Apis mellifera*). J Comp Physiol A 198:159–171

Meyer A, Galizia CG, Nawrot MP (2013) Local interneurons and projection neurons in the antennal lobe from a spiking point of view. J Neurophysiol 110:2465–2474

Mobbs PG (1982) The Brain of the Honeybee *Apis Mellifera*. I. The Connections and Spatial Organization of the Mushroom Bodies. Philos Trans R Soc B Biol Sci 298:309–354

Mombaerts P, Wang F, Dulac C, Chao SK, Nemes A, Mendelsohn M, Edmondson J, Axel R (1996) Visualizing an Olfactory Sensory Map. Cell 87:675–686

Muenz TS, Maisonnasse A, Plettner E, et al. (2012) Sensory reception of the primer pheromone ethyl oleate. Naturwissenschaften 99:421–425

Müller D, Abel R, Brandt R Zöckler M, Menzel R (2002) Differential parallel processing of olfactory information in the honeybee, *Apis mellifera* L. J Comp Physiol A 188:359–370

Nakanishi A, Nishino H, Watanabe H, Yokohari F, Nishikawa M (2010) Sex-specific antennal sensory system in the ant *Camponotus japonicus*: glomerular organizations of antennal lobes. J Comp Neurol 518:2186–2201

Neuhaus EM, Gisselmann G, Zhang W, Dooley R, Störtkuhl K, Hatt H (2005) Odorant receptor heterodimerization in the olfactory system of *Drosophila melanogaster*. Nat Neurosci 8:15–17

Nishino H, Nishikawa M, Mizunami M, Yokohari F (2009) Functional and topographic segregation of glomeruli revealed by local staining of antennal sensory neurons in the honeybee *Apis mellifera*. J Comp Neurol 515:161–180

Page RE (2012) The Spirit of the Hive and How a Superorganism Evolves. In: Galizia CG, Eisenhardt D, Giurfa M (eds) Honeybee neurobiology and behavior— a tribute to Randolf Menzel. Springer, The Netherlands, pp 3–16

Palmer MJ, Harvey J (2014) Honeybee Kenyon cells are regulated by a tonic GABA receptor conductance. J Neurophysiol doi: 10.1152/jn.00180.2014

Palmer MJ, Moffat C, Saranzewa N, Harvey J, Wright GA, Connolly CN (2013) Cholinergic pesticides cause mushroom body neuronal inactivation in honeybees. Nat Commun 4:1634

Party V, Hanot C, Said I, Rochat D, Renou M (2009) Plant terpenes affect intensity and temporal parameters of pheromone detection in a moth. Chem Senses 34:763–774

Patterson MA, Lagier S, Carleton A (2013) Odor representations in the olfactory bulb evolve after the first breath and persist as an odor afterimage. Proc Natl Acad Sci U S A 110:E3340–3349

Pelosi P, Zhou JJ, Ban LP, Calvello M (2006) Soluble proteins in insect chemical communication. Cell Mol Life Sci 63:1658–1676

Perez-Orive J, Mazor O, Turner GC, Cassenaer S,Wilson RI, Laurent G (2002) Oscillations and sparsening of odor representations in the mushroom body. Science 297:359–365

Perk CG, Mercer AR (2006) Dopamine modulation of honey bee (*Apis mellifera*) antennal-lobe neurons. J Neurophysiol 95:1147–1157

Petrulis A (2013) Chemosignals, hormones and mammalian reproduction. Horm Behav 63:723–741

Pézier A, Acquistapace A, Renou M, Rospars JP, Lucas, P (2007) Ca2+ stabilizes the membrane potential of moth olfactory receptor neurons at rest and is essential for their fast repolarization. Chem Senses 32:305–317

Pinching AJ, Powell TPS (1971) The Neuropil of the Glomeruli of the Olfactory Bulb. J Cell Sci 9:347–377

Pointer MR, Attridge GG (1997) The Number of Discernible Colours. Color Res Appl 23:52–54

Pollatos O, Kopietz R, Linn J, Albrecht J, Sakar V, Anzinger A, Schandry R, Wiesmann M (2007) Emotional stimulation alters olfactory sensitivity and odor judgment. Chem Senses 32:583–589

Pregitzer P, Schubert M, Breer H, Hansson, BS, Sachse S, Krieger J (2012) Plant odorants interfere with detection of sex pheromone signals by male *Heliothis virescens*. Front Cell Neurosci 6:42.

Prescott J (2012) Chemosensory learning and flavour: perception, preference and intake. Physiol Behav 107:553–559

Ramdya P, Benton R (2010) Evolving olfactory systems on the fly. Trends Genet 26:307–316

Reddy MR, Overgaard HJ, Abaga S, Reddy VP, Caccone A, Kiszewski AE, Slotman MA (2011) Outdoor host seeking behaviour of Anopheles gambiae mosquitoes following initiation of malaria vector control on Bioko Island, Equatorial Guinea. Malar J 10:184

Rein J, Mustard JA, Strauch M, Smith BH, Galizia CG (2013) Octopamine modulates activity of neural networks in the honey bee antennal lobe. J Comp Physiol A 199:947–962

Reinhard J, Srinivasan M V, Zhang S (2004) Olfaction: scent-triggered navigation in honeybees. Nature 427:411

Robertson HM, Wanner KW (2006) The chemoreceptor superfamily in the honey bee, *Apis mellifera*: expansion of the odorant, but not gustatory, receptor family. Genome Res 16:1395–1403

Robinson G (1992) Regulation of Division of Labor in Insect Societies. Annu Rev Entomol 37:637–665

Rössler W, Brill MF (2013) Parallel processing in the honeybee olfactory pathway: structure, function, and evolution J Comp Physiol A 199:981–996

Rössler W, Oland LA, Higgins MR, Hildebrand JG, Tolbert LP (1999a) Development of a glia-rich axon-sorting zone in the olfactory pathway of the moth *Manduca sexta*. J Neurosci 19:9865–9877

Rössler W, Randolph PW, Tolbert LP, Hildebrand JG (1999b) Axons of olfactory receptor cells of transsexually grafted antennae induce development of sexually dimorphic glomeruli in *Manduca sexta*. J Neurobiol 38:521–541

Rössler W, Tolbert LP, Hildebrand JG (1998) Early formation of sexually dimorphic glomeruli in the developing olfactory lobe of the brain of the moth *Manduca sexta*. J Comp Neurol 396:415–428

Rössler W, Zube C (2011) Dual olfactory pathway in Hymenoptera: evolutionary insights from comparative studies. Arthropod Struct Dev 40:349–357

Rouyar A, Party V, Prešern J, Blejec A, Renou M (2011) A General Odorant Background Affects the Coding of Pheromone Stimulus Intermittency in Specialist Olfactory Receptor Neurones. PLoS One 6:e26443

Rybak J, Menzel R (1993) Anatomy of the mushroom bodies in the honey bee brain: the neuronal connections of the alpha-lobe. J Comp Neurol 334:444–465

Sandoz JC (2006) Odour-evoked responses to queen pheromone components and to plant odours using optical imaging in the antennal lobe of the honey bee drone *Apis mellifera* L. J Exp Biol 209:3587–3598

Sandoz JC, Deisig N, de Brito Sanchez MG, Giurfa M (2007) Understanding the logics of pheromone processing in the honeybee brain: from labeled-lines to across-fiber patterns. Front Behav Neurosci 1:5

Sato K, Pellegrino M, Nakagawa T, Nakagawa T, Vosshall LB, Touhara K (2008) Insect olfactory receptors are heteromeric ligand-gated ion channels. Nature 452:1002–1006

Schachtner J, Schmidt M, Homberg U (2005) Organization and evolutionary trends of primary olfactory brain centers in Tetraconata (Crustacea+Hexapoda). Arthropod Struct Dev 34:257–299

Schäfer S, Bicker G (1986) Distribution of GABA-like immunoreactivity in the brain of the honeybee. J Comp Neurol 246:287–300

Schäfer S, Rehder V (1989) Dopamine-like immunoreactivity in the brain and suboesophageal ganglion of the honeybee. J Comp Neurol 280:43–58

Schäfer S, Rosenboom H, Menzel R (1994) Ionic currents of Kenyon cells from the mushroom body of the honeybee. J Neurosci 14:4600–4612

Serizawa S, Ishii T, Nakatani H, Tsuboi A, Nagawa F, Asano M, Sudo K, Sakagami J, Sakano H, Ijiri T, Matsuda Y, Suzuki M, Yamamori T, Iwakura, Y (2000) Mutually exclusive expression of odorant receptor transgenes. Nat Neurosci 3:687–693

Shang Y, Claridge-Chang A, Sjulson L, Pypaert M, Miesenböck G (2007) Excitatory local circuits and their implications for olfactory processing in the fly antennal lobe. Cell 128:601–612

Shearer DA, Boch R (1965) 2-Heptanone in the Mandibular Gland Secretion of the Honey-bee. Nature 206:530–530

Siju KP, Reifenrath A, Scheiblich H, Neupert S, Predel R, Hansson BS, Schachtner J, Ignell R (2014) Neuropeptides in the antennal lobe of the yellow fever mosquito, *Aedes aegypti*. J Comp Neurol A 522:592–608

Silbering AF, Galizia CG (2007) Processing of odor mixtures in the *Drosophila* antennal lobe reveals both global inhibition and glomerulus-specific interactions. J Neurosci 27:11966–11977

Slessor KN, Winston ML, Le Conte Y (2005) Pheromone communication in the honeybee (*Apis mellifera* L.). J Chem Ecol 31:2731–2745

Slifer EH, Sekhon SS (1961) Fine structure of the sense organs on the antennal flagellum of the honey bee, *Apis mellifera* Linnaeus. J Morphol 109:351–381

Smith TD, Garrett EC, Bhatnagar KP, Bonar CJ, Bruening AE, Dennis JC, Kinzнger JH, Johnson EW, Morrison EE (2011) The vomeronasal organ of New World monkeys (platyrrhini). Anat Rec (Hoboken) 294:2158–2178

Stengl M (2010) Pheromone transduction in moths. Front Cell Neurosci 4:133

Stengl M, Funk NW (2013) The role of the coreceptor Orco in insect olfactory transduction. J Comp Physiol A Neuroethol Sens Neural Behav Physiol 199:897–909

Stensmyr MC, Dweck HKM, Farhan A, Ibba I, Strutz A, Mukunda L, Linz J, Grabe V, Steck K, Lavista-Llanos S, Wicher D, Sachse S, Knaden M, Becher PG, Seki Y, Hansson BS (2012) A conserved dedicated olfactory circuit for detecting harmful microbes in *Drosophila*. Cell 151:1345–1357

Strausfeld NJ (2002) Organization of the honey bee mushroom body: representation of the calyx within the vertical and gamma lobes. J Comp Neurol 450:4–33

Strausfeld NJ, Hildebrand JG (1999) Olfactory systems: common design, uncommon origins? Curr Opin Neurobiol 9:634–639

Strube-Bloss MF, Herrera-Valdez MA, Smith BH (2012) Ensemble Response in Mushroom Body Output Neurons of the Honey Bee Outpaces Spatiotemporal Odor Processing Two Synapses Earlier in the Antennal Lobe. PLoS One 7:e50322

Strube-Bloss MF, Nawrot MP, Menzel R (2011) Mushroom body output neurons encode odor-reward associations. J Neurosci 31:3129–3140

Szyszka P, Ditzen M, Galkin A, Galizia CG, Menzel R (2005) Sparsening and temporal sharpening of olfactory representations in the honeybee mushroom bodies. J Neurophysiol 94:3303–3313

Süskind P (1984) Das Parfum. Die Geschichte eines Mörders. Diogenes, Germany

Tabor R, Yaksi E, Weislogel J-M, Friedrich RW (2004) Processing of odor mixtures in the zebrafish olfactory bulb. J Neurosci 24:6611–6620

Tabuchi M, Inoue S, Kanzaki R, Nakatani K (2012) Whole-cell recording from Kenyon cells in silkmoths. Neurosci Lett 6–11

Thany SH, Lenaers G, Crozatier M , Armengaud C, Gauthier M (2003) Identification and localization of the nicotinic acetylcholine receptor alpha3 mRNA in the brain of the honeybee, *Apis mellifera*. Insect Mol Biol 12:255–262

Thom C, Gilley DC, Hooper J, Esch HE (2007) The scent of the waggle dance. PLoS Biol 5:e228

Turner GC, Bazhenov M, Laurent G (2008) Olfactory representations by *Drosophila* mushroom body neurons. J Neurophysiol 99:734–746

Vickers NJ, Baker TC (1994) Reiterative responses to single strands of odor promote sustained upwind flight and odor source location by moths. Proc Natl Acad Sci U S A 91:5756–5760

Vosshall LB, Hansson BS (2011) A unified nomenclature system for the insect olfactory coreceptor. Chem Senses 36:497–498

Vosshall LB, Wong AM, Axel R (2000) An olfactory sensory map in the fly brain. Cell 102:147–159

Wagner D, Tissot M, Cuevas W, Gordon DM (2000) Harvester Ants Utilize Cuticular Hydrocarbons in Nestmate Recognition. J Chem Ecol 26:2245–2257

Wicher D (2013) Sensory receptors-design principles revisited. Front Cell Neurosci 7:1

Wicher D, Berlau J, Walther C, Borst A (2006) Peptidergic counter-regulation of Ca(2+)- and Na(+)-dependent K(+) currents modulates the shape of action potentials in neurosecretory insect neurons. J Neurophysiol 95:311–322

Wicher D, Schäfer R, Bauernfeind R, Stensmyr MC, Heller R, Heinemann SH, Hansson BS (2008) *Drosophila* odorant receptors are both ligand-gated and cyclic-nucleotide-activated cation channels. Nature 452:1007–1011

Williams IH, Pickett JA, Martin AP (1981) The Nasonov Pheromone of the Honeybee *Apis mellifera* L. (Hymenoptera, Apidae) Part II. Bioassay of the Components Using Foragers. J Chem Ecol 7:225–237

Wilson EO, Hölldobler B (2005) Eusociality: origin and consequences. Proc Natl Acad Sci U S A 102:13367–13371

Witthöft W (1967) Absolute Anzahl und Verteilung der Zellen im Hirn der Honigbiene. Zeitschrift für Morphol der Tiere 61:160–184

Wurm Y, Wang J, Riba-Grognuz O, Corona M, Nygaard S, Hunt BG, Ingram KK, Falquet L, Nipitwattanaphon M, Gotzek D, Dijkstra MB, Oettler J, Comtesse F, Shih CJ, Wu WJ, Yang CC, Thomas J, Beaudoing E, Pradervand S, Flegel V, Cook ED, Fabbretti R, Stockinger H, Long L, Farmerie WG, Oakey J, Boomsma JJ, Pamilo P, Yi SV, Heinze J, Goodisman MAD, Farinelli L, Harshman K, Hulo N, Cerutti L, Xenarios I, Shoemaker D, Keller L (2011) The genome of the fire ant *Solenopsis invicta*. Proc Natl Acad Sci U S A 108:5679–5684

Wüstenberg DG, Grünewald B (2004) Pharmacology of the neuronal nicotinic acetylcholine receptor of cultured Kenyon cells of the honeybee, *Apis mellifera*. J Comp Physiol A 190:807–821

Yaksi E, Wilson RI (2010) Electrical Coupling between Olfactory Glomeruli. Neuron 67:1034–1047

Zube C, Kleineidam CJ, Kirschner S, Neef J, Rössler W (2008) Organization of the olfactory pathway and odor processing in the antennal lobe of the ant *Camponotus floridanus*. J Comp Neurol 506:425–441

Zube C, Rössler W (2008) Caste- and sex-specific adaptations within the olfactory pathway in the brain of the ant *Camponotus floridanus*. Arthropod Struct Dev 37:469–479

Abbreviations

OR	odorant recepor	EAG	electro-antennography
OSN	olfactory sensory neuron	mp	melting point
ORN	olfactory receptor neuron	LY	lucifer yellow
S	*Sensilla*	I-V	current-voltage
St	*Sensillum trichoideum*	std	standard
Sb	*Sensillum basiconicum*	TTX	Tetrodotoxin
Sp	*Sensillum placodeum*	4-Ap	4-Aminopyridin
AN	antennal nerve	$I(Na^+,Ca^{2+})$	Na^+/Ca^{2+} current
AL	antennal lobe	$I(K^+)$	K^+ current
T	tract	$I(K^+t)$	transient K^+ current
SZ	sorting zone	$I(K^+p)$	persistent K^+ current
SEG	subesophageal ganglion	K_V	voltage dependent K^+
OL	optic lobe	KV_A	A-type K^+
OB	olfactory bulb	K_{Na}	Na^+ dependent K^+
VNO	vomeronasal organ	K_{Ca}	Ca^{2+} dependent K^+
ACT	antenno-cerebral tract	KNa t	transient Na^+ dependent K^+
APT	antenno-protocerebral tract	KNa p	persistent Na^+ dependent K^+
ALT	antennal-lobe tract	KCa t	transient Ca^{2+} dependent K^+
m	medial	KCa p	persistent Ca^{2+} dependent K^+
l	lateral	BK	big K^+ conductance
ml	mediolateral	SK	big K^+ conductance
PN	projection neurons	HVA	high-voltage activated
CB	cell body	AP	action potential
LN	local interneuron	DUM	dorsal unpaired median
LH	lateral horn	AKH	adipokinetic hormone
MB	mushroom body	DA	dopamine
KC	Kenyon cell	LTP	long term potentiation
EN	extrinsic neuron	Ach	acetylcholine
QMP	queen mandibular pheromone	m	muscarinic
PER	proboscis extension response	n	nicotinic

Curriculum Vitae

Jan Kropf
Dipl. Biol.

Behavioral Physiology and Sociobiology, Zoology II
Biozentrum, University of Würzburg
Am Hubland
97074 Würzburg, Germany
Tel.: +49 931 31 86977
jan.kropf@uni-wuerzburg.de

Education

03/2010- today	PhD-student in the neuroethology group in Würzburg Topic: The dual olfactory pathway of the honeybee. Head of the department: Prof. Dr. Wolfgang Roessler, University of Wuerzburg.
09/2010	Internship in the Kittel laboratory, Groupleader: Dr. Robert J. Kittel, University of Würzburg.
05/2009- 12/2009	Diploma thesis, Groupleader: Prof. Dr. Sylvia Anton Topic: Central processing of a mixture of pheromone and host plant odour in the MGC of Agrotis ipsilon. INRA Versailles, France.
2004-2010	Diploma in Biology, University of Wuerzburg (Neurobiology, Biochemistry, Behavioral Sciences)
12/2007	Student assistant at the Zoology II Department (University of Wuerzburg)
1996-2004	Abitur (university entry diploma) Schiller-Gymnasium Hof

Conferences

05/2014	Frontiers in Insect Behavior, Social Organisation & Evolution, Würzburg, Germany. Contribution (talk): In situ patch-clamp recordings from honeybee projection neurons and Kenyon cells.
09/2013	13th ESITO Villasimius, Sardinia, Italy. Contribution (talk): In situ patch-clamp recordings from honeybee projection neurons.
03/2013	10th Göttingen Meeting of the German Neuroscience Society, Göttingen, Germany Contribution (poster): In situ voltage-clamp recordings from olfactory projection neurons in the honeybee.
08/2012	10th International Congress of Neuroethology, College Park, MD, USA. Contribution (poster): Olfactory subsystems in the honeybee: sensory supply and sex-specificity.
09/2011	12th ESITO St. Petersburg, Russian Federation. Contribution (talk): Sensory supply and sex-specficity of olfactory subsystems in the honeybee.
03/2011	9th Göttingen Meeting of the German Neuroscience Society, Göttingen, Germany Contribution (poster): Projection patterns of Sensilla basiconica and differences in the dual olfactory pathway of honeybee workers and drones.
08/2010	9th International Congress of Neuroethology, Salamanca, Spain. Contribution (poster): Central processing of a mixture of pheromone and plant odor in the MGC of Agrotis ipsilon.

Invited talks

02/2014	Kropf, J., Rössler, W. In situ patch-clamp recordings from honeybee projection neurons and Kenyon cells. MPI for chemical ecology, Jena.
03/2012	Kropf, J., Rössler, W. The dual olfactory pathway in the honeybee. INRA, Versailles.
03/2012	Kropf, J., Rössler, W. The dual olfactory pathway in the honeybee. RCIM, University of Angers.
10/2011	Kropf, J. The dual olfactory pathway in the honeybee. 6th international Symposium organized by the students of the Graduate School of Life sciences, Würzburg, Virchow-Center.

Grants and Fellowships

05/2009- 12/2009 ERASMUS funding for a practical course at the INRA Versailles, France

Teaching Experience

2010- today Mentoring of diploma and bachelor students.

Supervision of the following practical courses for bachelor students:
-Verhaltensphysiologie
-Neurophysiologie
-Integrative Verhaltensbiologie 2

Language skills

German: native speaker
English: fluent
French: proficient

Würzburg, 20.10.2014

Publications

Kropf J, Kelber C, Bieringer K, Rössler W (2014). Olfactory subsystems in the honeybee: sensory supply and sex-specificity. Cell Tissue Res 357:583–95

Chaffiol A*, Dupuy F*, Barrozo RB, **Kropf J**, Renou M, Rospars JP, Anton S (2014). Pheromone modulates plant odour responses in the antennal lobe of a moth. Chem Sens 5:451-463 *These authors contributed equally to this work

Chaffiol A*, **Kropf J***, Barrozo RB, Gadenne C, Rospars JP, Anton S (2012). Plant odour stimuli reshape pheromonal representation in neurons of the antennal lobe macroglomerular complex of a male moth. J Exp Biol 215:1670-1680 *These authors contributed equally to this work

Deisig N, **Kropf J**, Vitecek S, Pevergne D, Rouyar A, Sandoz JC, Lucas P, Gadenne C, Anton S, Barrozo RB (2012). Differential interactions of sex pheromone and plant odour in the olfactory pathway of a male moth. PLoS ONE 7: e33159

Acknowledgments

Hiermit möchte ich mich bei allen Menschen bedanken, die mir in den letzten Jahren mit Rat, Tat, Sinn und Unsinn beistanden!

In erster Linie gilt mein Dank meinem Doktorvater **Wolfgang**, der es mir in den letzten Jahren ermöglicht hat mein Setup aufzubauen und meine Versuche durchzuführen. Auf die Frage nach einem weiteren nötigen Setup-Bestandteil, habe ich nie ein Nein zu hören bekommen, obwohl die endgültigen Ergebnisse doch auf sich warten ließen. Die Erfahrungen, die ich im Rahmen der Entwicklung meines elektrophysiologischen Versuchsaufbaus machen konnte sind immens und ich möchte sie nicht missen. Die Diskussionen mit Wolfgang und seine lobende Art haben mir sehr geholfen, mich für meine Versuche und die Schreibarbeiten zu motivieren. Außerdem bin ich sehr dankbar dafür, dass ich auf viele verschiedene Konferenzen in aller Welt fahren durfte. Dies hat mir ermöglicht sehr viele neue, berufliche und private Kontakte zu knüpfen. Schlussendlich bin ich sehr froh, dass die Prügelstrafe am Mikroskop nur im Raum stand und hoffe auf eine baldige Verbreiterung aller Türen der Zoologie II.

Robert hat mir im ersten Jahr meiner Doktorarbeit ein Setup zur Verfügung gestellt, obwohl er nicht wissen konnte, auf was er sich mit mir und dem Projekt einlässt. Die Vorversuche in seinem Labor zeigten mir, dass die damals geplanten Experimente durchführbar waren und was ich dafür benötigte. Außerdem habe ich dort sehr viel über elektrophysiologische Techniken gelernt und wurde sowohl beruflich als auch privat herzlich empfangen. Besonders danken möchte ich Robert noch dafür, dass er mich auf meinen gelungen Auftritt auf der Mainpost-Homepage hingewiesen hat.

Sylvia hat mich bereits in meiner Diplomarbeit betreut und stand mir schon damals stets super zur Seite. Dies hat sich bis heute nicht geändert. Die herzliche Atmosphäre, die Sylvia auch schon in kurzen emails schafft, genieße ich immer. Im Laufe meiner Doktorarbeit hatte ich einmal die Freude, Sylvia in Frankreich besuchen zu können und hatte dort eine super Zeit, unter anderem auch, weil ich einer meiner Lieblingsbeschäftigungen nachgehen durfte und eine Wand mit der Hilfe eines Vorschlaghammers zertümmert habe…

Für die erfolgreiche Fertigstellung meines ersten Doktorarbeitspapers möchte ich mich bei **Christina**, **Kathrin** und **Conny** bedanken. Christinas konsequente Diskussionskultur gepaart mit Feierabendbier hat das Manuskript dabei hervorragend vorangebracht. Kathrin hat super Färbungen von Sensillen gemacht, mich dabei bei Laune gehalten und mich ab und zu mit höchsten Elektrodenvibrationsfrequenzen in den Wahnsinn getrieben. Conny danke ich für die perfekte Ausführung von Traktfärbungen, in der Hinsicht ist sie unschlagbar! Und zwei, drei Tricks habe ich mir auch abgeschaut.

Da ich in der Auswertung von voltage-clamp Daten, wie sie im zweiten Manuskript vorliegen, wenig Erfahrung hatte, habe ich mich bei jeder sich bietenden Möglichkeit, meist auf Konferenzen, mit den Fachleuten des Gebiets unterhalten. Vor allem **Dieter Wicher**, **Philippe Lucas** und **Peter Kloppenburg** haben mir in diesem Sinne viel geholfen. Herzlichen Dank!
Bei generellen elektrophysiologischen Fragen konnte ich mich auch immer an meinen lieben Gangnachbarn **Martin** Fritz **Brill** wenden, der stets guten Rat parat hat.

Generell war die Arbeitsatmosphäre im Rössler-lab stets sehr, sehr angenehm, dafür möchte ich in erster Linie meinen aktuellen und ehemaligen Mitdoktoranden **Martin**, dem Mädelszimmer **Tina**, **Fritzi** und **Anne**, **ToM**, **Maren, Andi**, **Sara**, **Markus**, **Nils**, **Pauline**, **Martin Streinzer, Linde, Leonie**, **Karl**, **Flo, Johannes, Danny, Steffi** und **Nicole** danken. Außerdem waren natürlich auch die Postdocs/PIs **Claudi, Johannes, Martin** blau-passiv, **Oli,** A**gus** und **Ayse** immer für einen Spass zu haben. Wärend meiner kurzen Zeit im Kittel-lab, war die Zusammenarbeit mir **Nadine** und **Dmitrij** sehr angenehm. Im speziellen möchte ich mich noch bei **Fritzi** für das Korrekturlesen meiner Arbeit und bei **Nihil** für das fast-Korrekturlesen meiner Arbeit bedanken!

Die stets gute Versorgung mit Versuchstieren, Honig und Grillfeiern verdanke ich unserem Imker **Dirk**. **Conny**, die gute Seele unseres Labors, kümmert sich immer um alle Kleinigkeiten und auch größere Probleme! Unsere Sekretärin **Susanne** hat mir jederzeit geholfen, im Bürokratiezirkus die Übersicht zu behalten. Allen dafür herzlichen Dank!

Bei **Flavio** möchte ich mich für die stets interessanten Diskussionen und netten Gespräche bedanken. Dank seiner Arbeitsgruppe habe auch ich einen etwas besseren Einblick in die Ameisenwelt bekommen. Eine herzliche Begrüßung am Gang, die gute Laune verschafft, findet

man stets bei **Annette, Karin s**owie **Adrienne**, bei der man unter Umständen dazu noch etwas einstecken muss…

Herzlichen Dank auch an das underfrängische Draumduo **Oli** und **Oli** für beeindruggende Fussballdibbsbiele und Fussballsbiele! Da sollde man besser nicht die Augen zusammengneifen… Sonst gibd's noch was auf die Nase...

Meinen beiden Masterstudenten **Frank** und **Daniel** möchte ich für die Weiterentwicklung der Patch-Clamp-Versuche danken. Meinen Bachelorstudenten **Martin**, **Sven** und **Schmalz** danke ich für ihre hervorragenden Arbeiten an ihren Projekten, der Mithilfe bei der Studentenbetreuung und dem jugendlichen Flair, den sie in das Labor brachten.

Besonders bedanken möchte ich beim SPP Integrative Analysis of Olfaction, welches mir den Großteil der finanziellen Mittel zur Verfügung gestellt hat und außerdem für viele neue Freundschaften gesorgt hat. In diesem Kontext möchte ich noch **Mihaela** ausdrücklich hervorheben. Sie hat für eine reibungslose und durchaus angenehme Abwicklung von allem SPP-Aktivitäten gesorgt.

Außerdem danke ich all meinen Freunden, mit denen ich privat viel Spass hatte! Um mich dabei kurz zu fassen: **Tischler, Handballer, Rest:** danke!

Schlussendlich bedanke ich mich bei meinen **Eltern**, die mich schon mein komplettes Leben unterstützen, wo sie nur können. Ihr wart und seid immer für mich da! Vielen, vielen Dank!!!!